Nanoscale Advances

ROYAL SOCIETY OF CHEMISTRY

REVIEW

View Article Online
View Journal | View Issue

Open Access Article. Published on 08 July 2021. Downloaded on 10/31/2025 2:11:41 AM.
This article is licensed under a Creative Commons Attribution-NonCommercial 3.0 Unported Licence.

Check for updates

Cite this: *Nanoscale Adv.*, 2021, **3**, 5183

Carbon dots for cancer nanomedicine: a bright future

Samer Bayda,[a] Emanuele Amadio,[b] Simone Cailotto,[b] Yahima Frión-Herrera,[b] Alvise Perosa *[b] and Flavio Rizzolio *[bc]

Cancer remains one of the main causes of death in the world. Early diagnosis and effective cancer therapies are required to treat this pathology. Traditional therapeutic approaches are limited by lack of specificity and systemic toxicity. In this scenario, nanomaterials could overcome many limitations of conventional approaches by reducing side effects, increasing tumor accumulation and improving the efficacy of drugs. In the past few decades, carbon nanomaterials (*i.e.*, fullerenes, carbon nanotubes, and carbon dots) have attracted significant attention of researchers in various scientific fields including biomedicine due to their unique physical/chemical properties and biological compatibility and are among the most promising materials that have already changed and will keep changing human life. Recently, because of their functionalization and stability, carbon nanomaterials have been explored as a novel tool for the delivery of therapeutic cancer drugs. In this review, we present an overview of the development of carbon dot nanomaterials in the nanomedicine field by focusing on their synthesis, and structural and optical properties as well as their imaging, therapy and cargo delivery applications.

Received 14th January 2021
Accepted 14th June 2021

DOI: 10.1039/d1na00036e

rsc.li/nanoscale-advances

1. Introduction

Nanomedicine as a new branch of science is of interest for many investigators due to important advances for cancer treatment. Early diagnosis and effective cancer therapies are required to treat cancer, with approximately 18.1 million new cases and 9.6 million deaths yearly worldwide.[1] Nanomedicine has been defined by the European Science Foundation (ESF) as follows: "*Nanomedicine uses nano-sized tools for the diagnosis, prevention and treatment of disease and to gain increased understanding of the complex underlying pathophysiology of disease. The ultimate goal is improved quality of life*".[2] It involves diagnosis, imaging and drug delivery with nanoparticles in the 1–1000 nm range.[3,4] Nanotechnology could overcome many limitations of conventional approaches by reducing side effects, increasing tumor accumulation and improving the efficacy of drugs.[5–9] Early pioneers in the modern era of nanomedicine can be traced back to Ilya Metchnikov and Paul Ehrlich, who jointly received the Nobel Prize for medicine in 1908, for their work on phagocytosis[10] and cell-specific diagnostics and cell-targeted therapies.[11] They coined the phrase "magic bullet" and gave us immunotherapeutics and the first synthetic low molecular weight chemical entities. In the last 30 years, research on nanoparticles for nanomedicine has been increasing and includes studies with polymer–drug conjugates,[12–14] polymer–protein conjugates,[15] polymer nanocapsules,[16–18] liposomes,[19–23] block-copolymer micelles,[24–27] antibody–drug conjugates,[28] DNA–drug complexes[29–31] and albumin–drug conjugates.[32] Nanotechnology has developed rapidly allowing the incorporation of multiple therapeutics, and sensing and targeting agents into nanoparticles providing new devices with the ability to detect, prevent and treat complex disease such as cancer.[22,27,30,33] Nanotechnology represents a complementary strategy to be integrated with the information derived from the genetic and epigenetic characteristics of tumors.[34,35] It is well known that chemotherapeutic agents present severe side effects including bone marrow suppression, cardiac and kidney toxicity, hair loss and mucositis. In addition, these drugs are poorly soluble in biological fluids and quickly cleared from the body.[36] The important properties for a drug delivery system with nanoparticles are biocompatibility and biodegradability, prevention of degradation and clearance of the drug by minimizing protein binding and escaping the immune system, and increasing tumor accumulation by passive or active targeting.[37]

With the advancements in nanotechnology, the size, structure, composition, and surface properties of nanoparticles can be controlled during synthesis. In fact, these properties play important roles in the design of nanoparticle-based drug carriers with a high-level of efficacy.[38–41] Potential for surface functionalization to prevent agglomeration is considered as one of the most important factors of nanoparticle synthesis. For example, inorganic nanoparticles, such as gold or silver

[a]*Faculty of Sciences, Jinan University, Tripoli, Lebanon*
[b]*Department of Molecular Science and Nanosystems, University Ca' Foscari of Venice, Italy. E-mail: alvise@unive.it; flavio.rizzolio@unive.it*
[c]*Department of Pathology, IRCCS CRO Aviano National Cancer Institute, 33081 Aviano, Italy*

© 2021 The Author(s). Published by the Royal Society of Chemistry

Open Access Article. Published on 08 July 2021. Downloaded on 10/31/2025 2:11:41 AM. This article is licensed under a Creative Commons Attribution-NonCommercial 3.0 Unported Licence.

nanoparticles, can easily aggregate together in water due to their hydrophobic properties.[27] Furthermore, when they are injected into the blood flow, the surfaces of inorganic nanoparticles generally bind with serum proteins through electrostatic interactions. Therefore, these particles can be recognized by the immune cells and eventually scavenged by phagocytosis. To overcome these problems, hydrophilic and biocompatible polyethylene glycol (PEG) polymers have been widely used to decorate the surface of inorganic nanoparticles. With a high grafting density, tethered PEG polymers form a brush on the surface of these nanoparticles, and thus, they can be well-dispersed in water,[42,43] reduce the absorption of serum proteins,[44,45] and increase the circulation time and the accumulation in tumor sites *in vivo* due to the enhanced permeability and retention (EPR) effect.[42,46–48]

Among numerous types of nanomaterials developed in the past years, carbon nanomaterials have attracted particular interest in a large variety of fields including biomedicine,[49–56] owing to their distinctive physical and chemical properties. Based on their covalent bonds linking their carbon atoms, carbon nanomaterials may be classified into sp^2- and sp^3-carbon nanomaterials (Fig. 1). Typical sp^2-carbon nanomaterials include zero-dimensional (0D) fullerenes, one-dimensional (1D) carbon nanotubes (CNTs), and two-dimensional (2D) graphene, all with well-defined structures. Carbon nanoparticles (CNPs) or carbon dots (CDs) are nanoclusters of amorphous carbon (or composed of small crystalline structures) with sizes smaller than 10 nm and can also be considered as a type of 0D sp^2-carbon nanomaterial.

Many carbon nanomaterials, including CNTs, graphene derivatives and CDs, show interesting inherent optical properties such as fluorescence, making them useful as contrast agents in optical imaging and sensing.[57–60] The excellent electrical properties of CNTs and graphene allow them to be extensively used in a wide range of biosensing platforms.[61–63] sp^2-carbon nanomaterials, especially single-walled carbon nanotubes (SWCNTs) and graphene with all carbon atoms exposed on their surfaces, exhibit ultra-high surface areas available for efficient drug loading and bioconjugation.[49,63–67] For fullerenes and CNTs with hollow structures, the inside space may be utilized to load other functional species for theragnostic purposes.[68,69] CNTs and graphene derivatives with strong optical absorbance in the near-infrared (NIR) region are also useful for photothermal ablation of cancer.[67,70–73] Moreover, compared with many other inorganic nanomaterials such as quantum dots (QDs), which usually contain heavy metals, carbon nanomaterials simply composed of carbon are relatively safe at least in terms of elementary composition. This article reviews the progress in the research and development of carbon dots (CDs) in nanomedicine. Compared to other reviews on this topic,[74–76] this article focuses its attention on synthetic strategies that could be employed for fabricating CDs and endowing them with particular characteristics that are essential for the design of efficient biological applications. The optical properties of these materials will be discussed as well as their biological applications with particular attention towards nanomedicine applications such as bioimaging, drug carriers, gene therapy, thermal treatments, cancer diagnosis and receptor-mediated therapy.

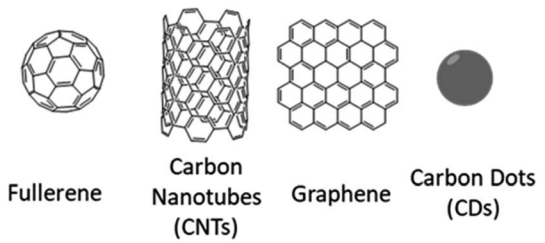

Fig. 1 Different types of carbon nanomaterials explored for biomedical applications.

2. Carbon dots

Carbon dots are a new class of carbon nanomaterials which have been acknowledged as quasi-spherical particles with sizes below 10 nm.[77,78] The accidental discovery of these nanoparticles during the separation and purification of SWCNTs by Xu *et al.* in 2004 triggered subsequent studies to exploit their fluorescence properties to create a new class of viable fluorescent nanomaterials.[77] Fluorescent CNPs were named carbon quantum dots (CQDs), or carbon dots (CDs), or carbon nanodots (CNDs) in 2006 by Sun *et al.* who proposed a synthetic route to produce CDs with enhanced fluorescence emissions *via* surface passivation.[58] Over the past decade, a variety of additional terms have emerged in the literature describing different structures of the nanoparticles, such as graphene quantum dots (GQDs) or carbon nanoclusters. For more discussion about this topic, we recommend to the readers the recent contribution of Valcàrcel and co-workers.[79] In this review, the term carbon dots (CDs) will be generically used to describe such nanoparticles without consideration of their actual morphologies.

Resulting from their tunable structure and diverse composition, CDs can have advantageous characteristics such as excellent chemical stability, ease of modification, high water solubility, tunable fluorescence with high quantum yield, good biocompatibility and low toxicity. Particularly, CDs have wide application including bioimaging,[75,80–85] drug delivery,[52,53,75,84,86–88] photodynamic therapy,[89–95] sensors,[96–103] optoelectronics[104–107] and photocatalysis.[108–115] Furthermore, it has recently been found that CDs exhibit strong luminescence upon two-photon excitation in the NIR region, further expanding their applications in bioimaging.[116,117] In fact, the colorful photoluminescence, high photostability, and low toxicity of CDs enable them as strong competitors and potential alternatives to heavy metal-based semiconductor quantum dots (QDs) currently in use.[118]

2.1. Synthetic methods

In recent years, much progress has been made in terms of the synthesis, properties and applications of CDs.[100,118,119] Many methods have been proposed to prepare CDs, which can be

 © 2021 The Author(s). Published by the Royal Society of Chemistry

Open Access Article. Published on 08 July 2021. Downloaded on 10/31/2025 2:11:41 AM.
This article is licensed under a Creative Commons Attribution-NonCommercial 3.0 Unported Licence.

roughly classified into "top-down" and "bottom-up" approaches. Top-down methods consist of arc discharge,[77] laser ablation,[58,81,116,120–122] and electrochemical oxidations,[123–126] where the CDs are formed or "broken off" from a larger carbon structure. Bottom-up approaches consist of, for example, combustion/thermal/hydrothermal,[127–132] microwave,[133] or ultrasonication methods[117,134] during which the CDs are formed from smaller molecular precursors. Typically, their surfaces are oxidized by nitric acid (HNO_3) and further purified by centrifugation, dialysis, electrophoresis, or other separation techniques. Three potential issues related to the fabrication of the CDs should be taken into account: (1) aggregation in larger clusters can occur preventing the formation of the nanomaterials; this can be avoided by using electrochemical synthesis, confined pyrolysis or solution chemistry, (2) excessive heterogeneity of their dimensions should be avoided since the size strongly influences the luminescence and chemical properties; this can be performed by post-treatments such as gel electrophoresis, centrifugation, and dialysis (3) control of the surface composition and derivatization leads to materials with different properties such as solubility, photoluminescence and QY; this can be tuned by varying the synthetic conditions and the post treatment protocols.

2.1.1. Top-down approaches

Arc-discharge methods. In 2004, Xu *et al.* isolated a fluorescent carbon nanomaterial while purifying SWCNTs derived from arc-discharge soot (Fig. 2). To improve the hydrophilicity of the material, the authors oxidized the arc soot with 3.3 M HNO_3 to introduce carboxyl functional groups, and then extracted the sediment with a NaOH solution (pH 8.4) to produce a stable black suspension. The suspension was separated by gel electrophoresis into SWCNTs, short tubular carbons, and a fast moving band of highly fluorescent material, which was composed of CDs.[77]

Laser-ablation methods. Sun *et al.* produced CDs *via* laser ablation of a carbon target in the presence of water vapor with argon as a carrier gas at 900 °C and 75 kPa.[58] Upon post surface passivation with PEG_{1500N}, the final CDs emitted strong and tunable photoluminescence in both solution and solid states, depending on the excitation wavelength progressively changing from 400 nm to 600 nm. Hu *et al.*[120] reported the synthesis and the passivation of fluorescent CDs by laser irradiation of a suspension of carbon materials in organic solvent. By selecting organic solvents, the surface states of CDs could be modified to achieve tunable light emission. Based on control experiments, the origin of the luminescence was attributed to the surface states related to the ligands on the surface of CDs. In this approach, a pulsed Nd:YAG laser was used to irradiate graphite or carbon black dispersed in diamine hydrate, diethanolamine, or PEG_{200N} for 2 h while under ultrasonication to aid in particle dispersion.

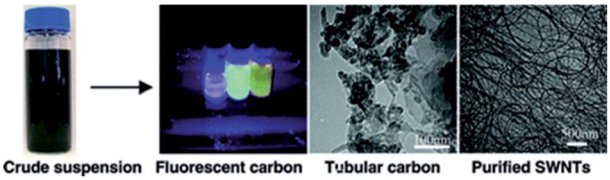

Fig. 2 Picture of different fractions of fluorescent carbon under 365 nm UV irradiation and TEM images of short tubule carbon and purified SWNTs. Figure adapted from ref. 77 with permission from American Chemical Society, copyright 2004.

After laser irradiation, centrifugation was used to precipitate residual carbon powder fragments while CDs remained suspended in the supernatant. These CDs averaged 3 nm in size, with lattice spacings varying from 0.20–0.23 nm, similar to that of diamond.[120] Kim *et al.* reported the synthesis of nitrogen doped CDs, starting from graphite flakes and employing EDTA as a doping agent. Laser ablation of ethanol solution of graphite and EDTA produced CDs with a relatively good QY (4.2–9.1%) and presented a N/C ratio of (7–15%) depending on the sonication power and a dimension around 2 nm.[135]

Electrochemical synthesis. Electrochemical synthesis of CDs was first demonstrated by Zhou *et al.* when they grew MWCNTs from scrolled graphene layers on carbon paper by chemical vapor deposition (CVD). These nanotubes were designed to serve as the working electrode in an electrochemical cell consisting of a platinum (Pt) wire counter electrode and a Ag/$AgClO_4$ reference electrode with degassed acetonitrile solution containing 0.1 M tetrabutylammonium perchlorate (TBA + ClO_4^-) as the electrolyte. This solution changed from colorless to yellow to dark brown, which indicated the formation of CDs with good solubility in various solvents.[126]

Li *et al.* reported an alkali-assisted electrochemical method to prepare 1–4 nm CDs with controlled sizes. They were able to cut a graphite honeycomb layer into ultra-small particles, obtaining CDs with a narrow size range and thereby offering a straightforward and facile strategy to prepare high-quality CDs. Using graphite rods as both the anode and cathode and NaOH/EtOH as the electrolyte, they synthesized CDs with a current intensity of 10–200 mA cm^{-2}. The alkaline medium is the key factor, and OH– groups are essential for the formation of CDs by this electrochemical oxidation process since the same procedure performed in an acidic environment did not yield any CDs.[136] Another facile electrochemical approach was reported by Ming *et al.* for the large-scale synthesis of high-quality CDs using only pure water as an electrolyte. The obtained CDs featured a highly crystalline nature, excellent water solubility, and remarkable down- and up-converted photoluminescence (PL) properties without extra purification. Moreover, they demonstrated that CDs possessed high photocatalytic activity under visible irradiation.[137] The use of a microbial fuel cell (MFC) to produce CDs was exploited by Liu *et al.* who used a graphite rod as the cathode and carbon source. Such CDs contained a high amount of oxygen on the surface, improving their PL properties, and were exploited to prepare a photocatalytic ink to target pollutant degradation and for H_2 generation. The CDs adhered to normal paper and efficiently degraded Rhodamine B under visible light. When the CDs were instead employed in a MFC for hydrogen production they showed good performance under visible light irradiation.[138]

2.1.2. Bottom-up approaches

Combustion/acidic oxidation methods. Liu *et al.* first reported that fluorescent CDs can be obtained from the combustion soot

Open Access Article. Published on 08 July 2021. Downloaded on 10/31/2025 2:11:41 AM. This article is licensed under a Creative Commons Attribution-NonCommercial 3.0 Unported Licence.

of candles after refluxing with oxidative acid.[139] A glass plate placed over a burning candle was used to collect the hydrophobic soot, which could be turned hydrophilic by means of HNO_3 treatment. The suspension was purified by electrophoresis, revealing the presence of three bands, the first one consisting of nine fast-moving fluorescent smaller bands with different emission spectra. This study indicated that the fluorescence emission of CDs is size-dependent and/or charge-dependent.

This candle-burning approach was also followed by Ray *et al.* The candle soot was similarly collected and refluxed with 5 M HNO_3 for 12 h. The particle suspension was then precipitated by adding acetone and centrifuging at 14 000 rpm for 10 minutes. Size separation was achieved by fast centrifugation; the particles were centrifuged at different speeds and the solids were collected every time. At 8000 rpm precipitate was no longer observed and the supernatant contained CDs with particle sizes in the 2–6 nm range. Precipitates at lower centrifugation speeds contained large carbon nanoparticles of 201–350 nm in size. The 2–6 nm CDs were found to be graphitic, according to the lattice spacing in HRTEM images, and exhibited high PL quantum yields in comparison with the larger particles.[130]

In a further study, Tian *et al.* purified CDs from the combustion soot of natural gas. By inverting a glass beaker above the flame of a natural gas burner, they were able to collect around 100 mg of soot, which was then refluxed in 5 M HNO_3 for 12 h, followed by centrifugation and dialysis to afford purified CDs. The purified CDs exhibited PL with a λ_{ex} maximum of 310 nm and an emission wavelength (λ_{em}) maximum of 420 nm. High-resolution transmission electron microscopy (HRTEM) showed CDs with an average diameter of (4.8 ± 0.6) nm and with crystalline lattices consistent with graphitic carbon.[131] ^{13}C NMR and FT-IR measurements also revealed the presence of sp^2 carbon and carboxylic/carbonyl moieties, thus leading the authors to conclude that the CDs consist of a nanocrystalline core featuring graphitic sp^2 carbon atoms and a surface functionalized with carboxylic/carbonyl moieties.[131]

Acidic oxidation is another popular method to prepare CDs. Typically, in this process strong acid treatment of carbon precursors is conducted at high temperature. Leblanc's group reported an acidic oxidation route for converting carbon powder into CDs, in which a mixture of sulfuric acid, nitric acid and carbon powder was refluxed at 110 °C for 15 h.[140] After cooling, CDs were successfully obtained as a black powder. Qian *et al.* reported a mild and facile synthesis of CDs from the mixed acid treatment of activated carbon.[141] In their synthesis, a reaction temperature of 80 °C was used and the purified product could be obtained by dialysis.

More recently, our group synthesized CDs from black tea using acidic oxidation. This synthesis is simple and economical because of the selection of an inexpensive carbon source. CDs are synthesized with a narrow size distribution, tunable optical properties covering visible to deep red absorption, non-toxicity and easy synthesis for large-scale production. These CDs are utilized to label subcellular structures such as exosomes. More importantly, these new CDs can escape lysosomal sequestration and rapidly distribute in the cytoplasm to release doxorubicin (DOX) with better efficacy than the free drug at low pH, similar to the tumor microenvironment.[53]

Park *et al.* employed a different acidic treatment for tuning the PL of the CDs employing tomatoes as the precursor. The biomass was first lyophilized and then treated with H_2SO_4, or H_3PO_4 at room temperature or at 80°. The syntheses yielded CDs with a blue, green and yellow emission and a high biocompatibility towards HeLa cells. Furthermore, all the samples were employed as sensors for Fe^{3+}, with the blue CDs demonstrating the best performances with a detection limit of 0.016 μM.[142]

Thermal/hydrothermal/solvothermal methods. For the synthesis of CDs, thermal/hydrothermal or solvothermal treatments are the most employed bottom-up procedures due to their low cost, easy feasibility, environmental friendliness and applicability with various renewables carbon sources.[118,119,143–146]

In general, with the thermal method organic precursors are first pyrolyzed at high temperature (*i.e.* 200–400 °C) without solvent for hours or days under air or inert gas yielding a carbonized solid. Next the CDs are recovered using water or other suitable solvents and purified by filtration or dialysis. However, this thermal method can only be applied for organic precursors having a melting point lower than the working temperature. Compared with this pyrolytic decomposition method, both the hydrothermal or solvothermal procedures are typically carried out in the presence of water or organic solvent in a pressure reactor at lower temperatures (*i.e.* 50–300 °C) and shorter reaction times (minutes or hours). In the solvothermal carbonization the CDs are recovered by extraction with an organic solvent followed by a concentration/evaporation step.[82] By using the solvothermal method, Bhunia *et al.* synthesized two kinds of CDs, hydrophobic and hydrophilic with diameters <10 nm from the carbonization of carbohydrates.[82] The hydrophobic ones were produced by mixing the carbohydrate with octadecylamine and octadecene before heating to 70–300 °C for 10–30 minutes. The hydrophilic ones instead were produced in water in a wide range of pH after heating at 80 °C for 1 hour, with the final materials presenting interesting yellow and red emissions. Generally, hydrothermal or solvothermal methods are simple and the obtained CD suspension can be used without further purification.

Despite the difficulties to accurately rationalize the morphology and the photoluminescence properties of the CDs made by thermal or solvothermal methods, generally large carbogenic structures with low luminescence are obtained by pyrolysis while nanoscopic particles with strong photoluminescence are obtained with the hydrothermal or solvothermal methods. These differences can be ascribed mainly to the degree of carbonization reached during the synthesis and, therefore, to their different molecular-, amorphous- or graphitic-like nature (see chapter below).

One of the first examples of the thermal synthesis of CDs was reported by Giannelis' group in 2008.[127,128] The authors demonstrated the applicability of the pyrolytic procedure by heating different ammonium citrate salts or 4-aminoantipyrine at 300 °C for 2 h in air leading to the formation of both

 © 2021 The Author(s). Published by the Royal Society of Chemistry

Open Access Article. Published on 08 July 2021. Downloaded on 10/31/2025 2:11:41 AM.
This article is licensed under a Creative Commons Attribution-NonCommercial 3.0 Unported Licence.

hydrophilic and lipophilic surface-functionalized carbogenic nanoparticles. These nanoparticles possessed an average size <10 nm, were highly dispersible in organic or aqueous solvents (depending on their surface functionalization) and emitted light in the visible when excited at different wavelengths. By extending the procedure to neat citric acid a completely insoluble carbogenic solid was obtained. Recently, Guo *et al.* developed a simple and low-cost approach to synthesize highly fluorescent CDs, by a one-step hydrothermal treatment of sodium citrate and ammonium bicarbonate in water. Experimental investigation confirmed that NH_4HCO_3 decomposed to CO_2 and NH_3 that conferred high pressure into the reaction medium, and thus facilitated the decomposition of sodium citrate into small nanoparticles that produced the CDs. These CDs had an average size of 1.59 nm and exhibited a high PL quantum yield (68%) as well as good photostability. XPS confirmed the presence of carboxyl and hydroxyl groups on the surface of the CDs and they were found to be very stable at a high concentration of ionic solution, and could be used to detect mercury ions in aqueous solution with good selectivity and sensitivity.[147] Generally, in all the preceding cases the synthesis involves the carbonization of the reagents (*via* dehydrogenation, decarboxylation and further polymerization reactions) leading to a complex carbonaceous material formed by amorphous aggregates and carbogenic structures having sp^2/sp^3 carbon domains decorated with –OH, –COOH, –COOR, and amino derived functional groups.[104] Nowadays, citric acid is effectively considered the most common starting material for the thermal or hydrothermal synthesis of highly luminescent CDs, especially in combination with other heteroatom-doping reagents, such as nitrogen- or sulfur-containing compounds.[148–150]

In 2014, Guo's group demonstrated the possibility of producing water soluble CDs using only citric acid (treatment at 180 °C for 2.5 h) as an organic precursor by suspending the resulting insoluble carbogenic solid in water, adjusting the pH to 7.0 using NaOH and thus forming Na^+-functionalized CDs (Fig. 3).[151]

Following these preliminary investigations, further improvements of this methodology have been carried out in Reisner's group by increasing the heating time up to 40 h at 180 °C, thus avoiding the purification step to remove the residual citric acid.[152] These amorphous CDs (a-CDs) had an average diameter of 6.8 ± 2.3 nm and low crystallinity, consisting predominantly of an amorphous carbon core with regions of graphitic carbon and carboxylate functionalities on the surface. Graphitic CDs (g-CDs) with an average size of 3.6 ± 1.0 nm were also prepared *via* a higher temperature pyrolysis of citric acid.[152] In brief, the precursor was heated in air at 180 °C for 40 h and then at 320 °C for 100 h during which full graphitization occurs. Furthermore, they extended this thermal procedure to produce graphitic nitrogen doped CDs (g-N-CDs) with a narrow size distribution and a small average diameter of 3.1 ± 1.1 nm by using aspartic acid in air at 320 °C (required for the decomposition of the reagent) for 100 h.[148] The resulting "nitrogen-doped" carbon dots are quasi-spherical with a nanocrystalline graphitic N doped core with carboxylates as the primary surface functionality (Fig. 4).

Very recently, Perosa's group synthesized amorphous and graphitic non-doped or N-doped CDs by two different preparation methods – hydrothermal and pyrolytic – and from two sets of reagents – neat citric acid and citric acid doped with diethylenetriamine (Fig. 5).[153]

They demonstrated that the hydrothermal syntheses yielded amorphous CDs, either non-doped (a-CDs) or nitrogen-doped (a-N-CDs) while the pyrolytic treatment afforded graphitic CDs, either non-doped (g-CDs) or nitrogen-doped (g-N-CDs). The morphology, structure and optical properties of the four different types of CDs were also determined, revealing significant differences depending on the synthetic pathway. The CDs were then employed as photosensitizers in an organic reaction, demonstrating excellent performance depending on their structure and synthetic pathway.[154,155]

Zhu *et al.* fabricated nitrogen-doped citric acid derived CDs by a hydrothermal method. Citric acid and ethylene diamine were dissolved in deionized-water and heated at 200 °C for 5 h in a Teflon-lined autoclave. The reaction occurred by first condensing citric acid and ethylene diamine, whereupon they formed polymer-like aggregates, which were then carbonized to form the CDs. The quantum yield of these N-doped CDs reached 80.6% at an excitation wavelength of 360 nm, nearly equal to that of most semiconductor QDs and fluorescent dyes.[156]

More recently, Lu *et al.* synthesized N-CDs with an average size of 2.6 nm using a one-pot hydrothermal treatment with

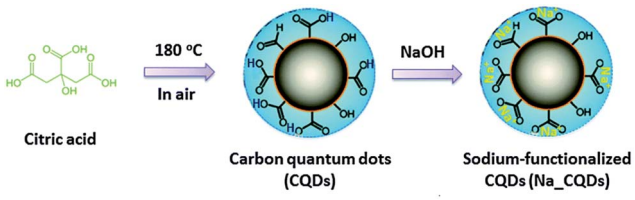

Fig. 3 Schematic illustration for the fabrication of Na^+-functionalized carbon quantum dots (Na-CQDs). Figure reproduced from ref. 151 with permission from Royal Society of Chemistry, copyright 2014.

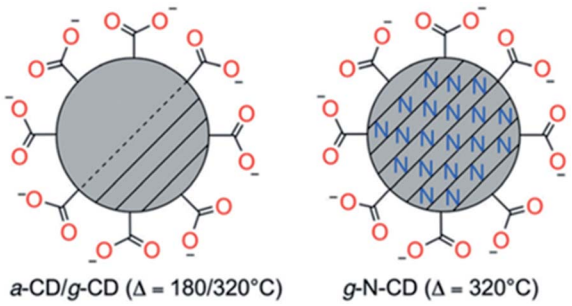

Fig. 4 Schematic representation of amorphous or graphitic CD structures obtained by the thermal decomposition of citric (a-CDs and g-CDs) or aspartic (g-N-CDs) acids. Picture of different fractions of fluorescent carbon under 365 nm UV irradiation and TEM images of short tubule carbon and purified SWNTs. Figure reproduced from ref. 148 with permission from Wiley, copyright 2017.

Open Access Article. Published on 08 July 2021. Downloaded on 10/31/2025 2:11:41 AM.
This article is licensed under a Creative Commons Attribution-NonCommercial 3.0 Unported Licence.

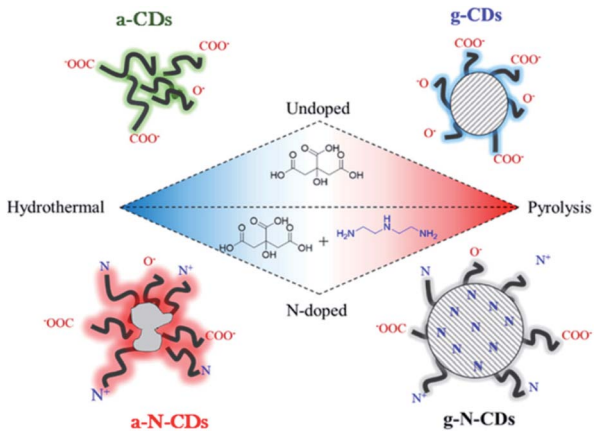

Fig. 5 Schematic representations of the four CDs studied in this work: purely carbogenic (a-CDs, g-CDs) or N-doped (a-N-CDs, g-N-CDs) obtained by a hydrothermal method (180 °C, hours, water) or thermolysis (220 °C, days, neat) of citric acid with or without diethylenetriamine as a doping agent. Figure reproduced from ref. 153 with permission from American Chemical Society, copyright 2018.

citric acid as the carbon source in the presence of polyethylenimine (PEI) as a simultaneous nitrogen dopant and surface passivation agent. N-CDs synthesized emitted a strong blue luminescence with a QY of 51%. The N-CDs exhibited excellent photostability and low cytotoxicity making the N-CDs promising optical nanoprobes for real-time live-cell imaging. Moreover, their small size and the surface positive charge rendered by the polyethylenimine (PEI) endow them with the ability to cross the blood-brain barrier (BBB), making them potentially useful in traceable drug delivery in brain disorders.[132]

The second prominent heteroatom which is included into the structure of CDs is sulfur. Aside from limited examples, where only sulfur was reported to be doped into CDs,[157,158] most studies focus on their co-doping with nitrogen, in order to improve the optical properties of the CDs, in particular their PL QY.[159] Dong *et al.* synthesized nitrogen-sulfur co-doped CDs *via* a one-pot hydrothermal treatment of citric acid and L-cysteine at 200 °C (PL QY of 73%).[159]

Aside from citric acid, another approach towards the synthesis of N-doped CDs was recently reported by Jiang *et al.*, who synthesized color-tunable CDs by heating phenyl-diamines in ethanol at 180 °C for 12 h (Fig. 6). The difference in functional group configuration from ortho, to meta and para changed the emission color of the resulting CDs from green, to blue to red.[160]

In recent years, more work has been carried out to find other bio-based precursors (glucose,[155,161,162] sucrose,[163] fructose,[155] ascorbic acid,[155] polyols,[164] polymers,[165,166] amino acids,[167,168] proteins,[169,170] natural products,[100,103,171–174] and some wastes[175–178]) to synthesize CDs. In this context, Zhang *et al.* reported a high-yield synthesis of hydrophilic CDs by controlled carbonization of sucrose. Green luminescent CDs and non-luminous CDs were effectively separated by dialysis. After surface functionalization with PEG_{2000N}, the non-luminous CDs

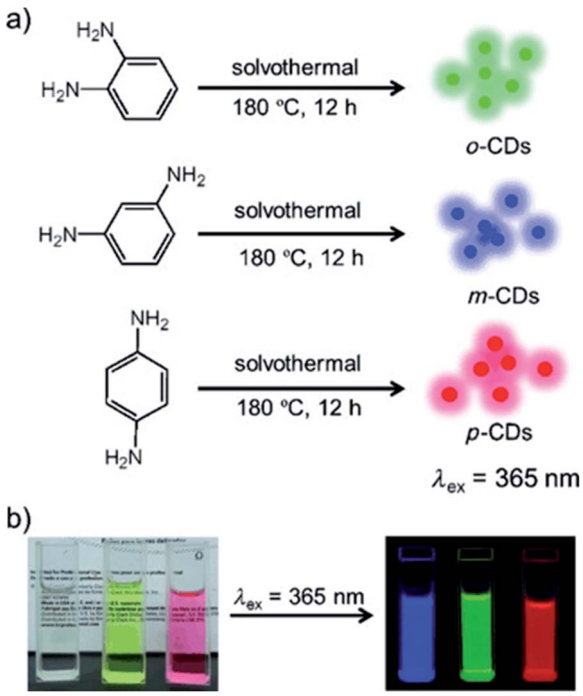

Fig. 6 (a) Preparation of the red, green and blue (RGB) PL CDs (CDs) from three different phenylenediamine isomers (*i.e.*, *o*PD, *m*PD and *p*PD); (b) photographs of *m*-CDs, *o*-CDs, and *p*-CDs dispersed in ethanol in daylight (left), and under $\lambda = 365$ nm UV irradiation (right). Figure adapted from ref. 160 with permission from Wiley, copyright 2015.

emitted blue fluorescence.[179] Another one-step synthetic route in which the CDs were synthesized from the hydrothermal oxidation of carbohydrates (glucose/sucrose/starch) with acid/alkali additives, was reported. Addition of HCl enhanced emission of the CDs at longer wavelengths while NaOH enhanced the emission of CDs at shorter wavelengths. The authors proposed that these additives induce different defects on the surface of the CDs which act as surface energy traps that result into the different PL behaviors. These CDs exhibited NIR emission excited by NIR excitation as well as up-conversion PL properties. The elemental analysis showed that they contained predominantly elemental carbon and oxygen. It was also revealed that the functional carboxyl and hydroxyl groups on the surface of these CDs made them dispersible in water.[180]

Fluorescent CDs with a diameter of about 2.0 nm were prepared directly *via* a simple hydrothermal method by using L-ascorbic acid as a carbon source. The solvent used in the dissolution of the acid was investigated and proved to have a strong link with the CD PL. Ethanol proved to be the best as it provided a reaction medium for the uniform growth of the nanoparticles due to its ability to cap and inhibit the aggregation of the nanoparticles. In contrast to the previous methods, no strong acid or further surface modification was needed for the preparation. The CDs had uniform shapes and sizes in the range 2.0–2.5 nm and were water soluble and exhibited λ_{ex} dependent emission. Experiments revealed that the emission of these CDs exhibited good stability in reaction media of high

 © 2021 The Author(s). Published by the Royal Society of Chemistry

Open Access Article. Published on 08 July 2021. Downloaded on 10/31/2025 2:11:41 AM. This article is licensed under a Creative Commons Attribution-NonCommercial 3.0 Unported Licence.

ionic concentrations that could be tuned by adjusting the pH.[181] Water-soluble and well-crystallized CDs with a lateral size of about 3.0 nm were also fabricated by a hydrothermal cutting method.[182] The atomic force microscopy (AFM) observation of the CDs deposited on a mica substrate shows a narrow height distribution from 1.5 to 1.9 nm, suggesting that the CDs typically consist of 2–3 graphene layers.

In order to favor the formation of biocompatible nanostructures suitable for medical applications and to avoid the formation of harmful chemical compounds, Cailotto *et al.* hydrothermally synthesized monosaccharide-derived CDs starting from fructose, glucose and ascorbic acid, without any passivating or doping additives.[155] These CDs were characterized from a morphological, chemical and toxicological point of view and their potential application as drug nanocarriers was tested using doxorubicin as a model drug. Interestingly, the cytotoxicity of the CDs was affected by the choice of the starting materials; CDs synthesized from fructose were found to be toxic while high biocompatibility was observed starting from glucose or ascorbic acid. Their drug loading capabilities were evaluated indicating the crucial role of the CD morphologies, rather than the surface functional groups, in controlling the doxorubicin uptake. With the more suitable glucose derived CDs, the authors found up to $28\%_{w/w}$ of drug loading.

Zhou *et al.* reported large-scale CD preparation starting from watermelon peel. The fresh peel was carbonized at 220 °C for 2 h under an air atmosphere, filtered, centrifuged and dialyzed yielding highly luminescent CDs with a blue fluorescence, good water-solubility, small particle size, and good stability in a wide range of pH values and at a high salt concentration.[183] Passivation enabled their use in biological applications, such as *in vivo* bioimaging and as bioprobes, as it introduced specific function on the surface of the nanomaterial.[184]

Sahu *et al.* prepared highly photoluminescent CDs with a quantum yield (QY) of 26% in a one-step hydrothermal treatment of orange juice followed by centrifugation.[185] These CDs with sizes of 1.5–4.5 nm were applied in bioimaging due to their high photostability and low toxicity. Yang *et al.* reported a one-step synthesis of amino-functionalized fluorescent CDs by hydrothermal carbonization of chitosan at 180 °C for 12 hours.[80] These CDs are demonstrated as excellent probes as bioimaging agents.

Microwave methods. Microwave heating has become important in synthetic chemistry. Compared with other methods it is more convenient and rapid to heat the carbon precursors and it simplifies the synthesis yielding CDs readily within a few minutes and with higher yield. Multicolor luminescence has been achieved by microwave synthesis of CDs using dextrin as a starting material in the presence of sulfuric acid. This solution was microwave heated for 2.5 min at 800 W and a light brown supernatant was obtained along with a black precipitate. The solution containing the CDs was centrifuged to obtain a clear solution. The obtained CDs were characterized using different techniques and the luminescence spectra showed that the particles attained multicolor luminescence without any requirement for surface-passivating agents. The quantum yield was between 5 and 9%.[186] This multicolor luminescence might be very helpful in the field of bioimaging. Wang *et al.* presented a facile one-step microwave assisted approach to prepare water-soluble phosphorus-containing CDs with strong green fluorescence. In this synthesis, 2 mL of 70% phytic acid and 1 mL ethylene diamine were mixed in 25 mL ultrapure water, and then heated for about 8 min in a domestic 700 W microwave oven. Notably, these CDs present two-peak emissions when excited at low wavelengths; however at high excitation wavelengths (360–460 nm), only one emission peak at 525 nm was observed. The highest quantum yield of the resulting phosphorus-containing CDs was about 21.65%.[187]

Qu and co-workers reported a one-step microwave heat treatment of carbohydrates to synthesize multicolored photoluminescence CDs without any surface passivation reagents. Glycerol was mixed with phosphate solution and subjected to microwave heating for 14 min to generate the CDs. The PL showed that the emission spectra were broad and ranged from blue to yellow depending on the excitation wavelength. The CDs possessed carboxyl and hydroxyl moieties that enhanced their hydrophilicity and stability in aqueous systems, shown by their ability to maintain PL intensity even with increased ionic strength. The obtained CDs were biocompatible and were found to be promising in biolabelling and bioimaging. This work has also demonstrated that inorganic ions were able to effectively promote the carbonization of carbohydrates.[188]

Ding *et al.* reported the synthesis of N and S co-doped CDs by employing 1,6-hexanediamine dihydrochloride dissolved in DMSO as the only precursor. After 30 min of microwave irradiation the CDs were obtained and purified by dialysis and freeze drying. The nanomaterial exhibited a respectable QY of 24% and presented an emission ranging from blue to orange. The N,S-CDs were successfully employed in the detection of MnO_4^- and $Cr_2O_7^{2-}$ and showed excellent biocompatibility.[189]

Jaiswal *et al.* developed a simple one step microwave mediated synthesis of CDs using biocompatible PEG as a sole source of carbon and a passivating agent.[190] An aqueous PEG solution was irradiated for 10 min to generate the amorphous CDs with an estimated average size of 3.6–5.4 nm. The obtained CDs were compliant to size separation by gel electrophoresis, and possessed high photostability, which was confirmed by their ability to maintain luminescence under extended irradiation. Zhu *et al.* synthesize CDs by combining PEG_{200} and a saccharide (for example, glucose, and fructose) in water to form a transparent solution, followed by heating in a 500 W microwave oven for 2–10 min. The solution turned from colorless to dark brown over the course of the reaction. The reaction time plays a crucial role in determining the properties and size of the CDs, in fact longer heating times result in CDs enlarging slightly and emitting at longer wavelengths. For example, the average CD diameters were (2.75 ± 0.45) nm and (3.65 ± 0.6) nm for heating times of 5 and 10 minutes, respectively. Without the addition of PEG, besides the same color change, the nanomaterial obtained presents a weak and irregular PL.[133]

In order to enhance the PL properties of the CDs, their doping with boron and nitrogen was achieved by employing urea and boric acid in combination with citric acid. The microwave irradiation of this mixture led to CDs with a mean

Open Access Article. Published on 08 July 2021. Downloaded on 10/31/2025 2:11:41 AM.
This article is licensed under a Creative Commons Attribution-NonCommercial 3.0 Unported Licence.

diameter of 2 nm and a QY between 15 and 30%. Their strong luminescence was exploited for the investigation of energy transfer with photosynthetic pigments. The experiments reveal that the emission of the CDs was quenched by the pigments, meaning that an energy transfer process between the two species was involved. This phenomenon allows the increase of the spectrum range in which the photosynthetic pigment can absorb light, enhancing their photocatalytic activity.[191]

Very recently, Prato and co-workers prepared and characterized a redox library of amino doped CDs with tunable oxidation/reduction properties starting from commercially available quinones, arginine and ethylene diamine highlighting their potential applicability as photocatalysts.[192] These CDs were prepared by microwave irradiation (240 °C, 26 bar and 200 W for 180 seconds) of an aqueous solution of the precursors, followed by dialysis. In all cases, after the hydrothermal treatment, the colour of the reaction mixture turned dark brown as a result of the formation of CDs. Benzoquinone, naphthoquinone-, and anthraquinone-based carbon nanodots exhibited interesting electrochemistry with oxidation potentials between +1.48 V and +0.98 V *vs.* SCE and reducing potentials in the range −1.52 V and −2.05 V *vs.* SCE (Fig. 7).

By extending this microwave assisted multi-component synthetic approach, the Prato group prepared the first example of chiral CDs (CNDs-*R* or CNDs-*S*) by using arginine, as the core precursor, and (*R*,*R*)- or (*S*,*S*)-1,2-cyclohexanediamine (CHDA) as the chiral surface precursors (Fig. 8).[193] These particles, with a mean particle size around 3 nm, are highly soluble in water and display a mirror-image profile both in the UV-Vis and in the infrared regions, as detected by electronic and vibrational circular dichroism, respectively. The origin of chirality was ascribed to the presence of numerous cyclohexanediamine moieties around the carbon-based amorphous core. The authors used the chiral nanodots as templates for the preparation of porphyrin based supramolecular assemblies thus opening the way for developing a variety of new chiral composite materials and applications.

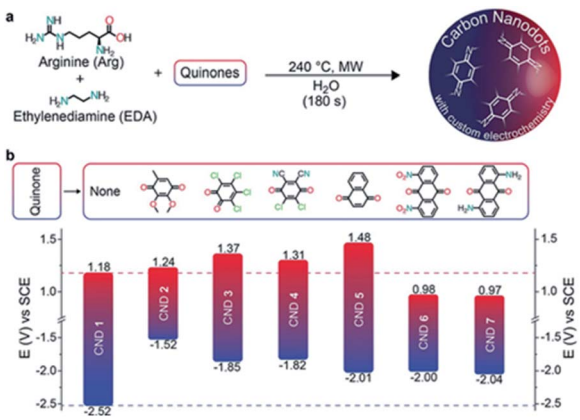

Fig. 7 (a) Bottom-up synthesis of the quinone derived amino doped CDs. (b) Redox potentials of the CDs (with the structures of the corresponding starting quinones employed as precursors). Figure adapted from ref. 192 with permission from Wiley, copyright 2018.

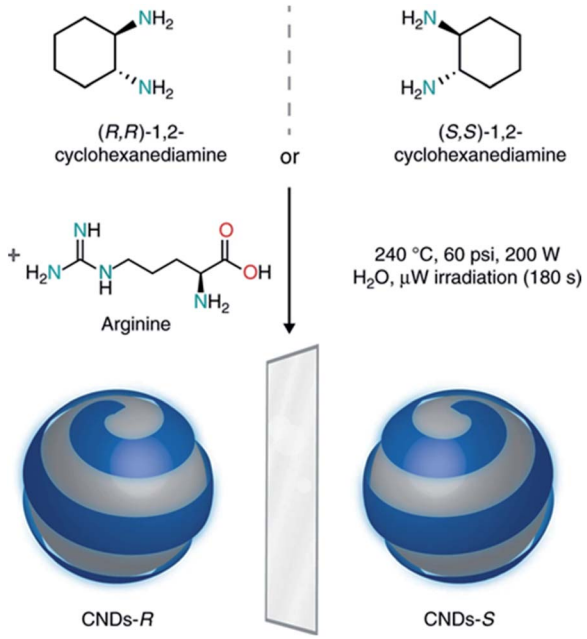

Fig. 8 Design and synthesis of chiral carbon nanodots. Chiral CNDs were synthesized starting from (*R*,*R*)- or (*S*,*S*)-1,2-cyclohexanediamine and arginine, under hydrothermal microwave-assisted conditions (240 °C, 70–110 psi, 200 W for 180 s). Figure adapted from ref. 193 with permission from Nature Publishing Group, copyright 2018.

Ultrasonication methods. The ultrasonication method is a process in which the ultrasonic waves produce alternating expansion and compression in a reaction solution, resulting in the growth and implosive collapse of bubbles irradiated with the waves. The mechanism causes high speed interparticle collisions, which can change the morphology, composition, and reactivity of the particles. When integrated with carbonization, the energy of the ultrasonic waves generates intermediates that can be further carbonized to generate very small CDs. Li *et al.* described a simple synthesis of CDs from glucose or active carbon by using an ultrasonic treatment method.[117,134] Such monodispersed water-soluble fluorescent CDs could emit bright and colorful PL covering the entire visible-to-NIR spectral range. Notably, the NIR emission of CDs could be obtained by NIR excitation. Furthermore, the CDs had excellent up-conversion fluorescence properties.[117]

2.2. Chemical composition and structure

C, H, and O are the three main elements present in CDs, in varying ratios. The introduction of heteroatoms has been studied to tune the conduction/valence band position, which confers additional functions.[123,127,194] For example, the quantum yield (QY) of CDs could be significantly improved by incorporating nitrogen while CDs with a wide band gap could be synthesized by incorporating sulfur.[158,159,195–197] Furthermore, P-doped CDs showed green fluorescence, which could be utilized as an imaging signal with a low background.[187,198,199] Other heteroatoms such as Cl and B could also be incorporated into CDs by changing the synthetic methods or starting materials.[200,201]

 © 2021 The Author(s). Published by the Royal Society of Chemistry

Open Access Article. Published on 08 July 2021. Downloaded on 10/31/2025 2:11:41 AM. This article is licensed under a Creative Commons Attribution-NonCommercial 3.0 Unported Licence.

Along with the elemental composition, the morphology of CDs may also be affected by both the preparation methods and the nature of the precursors. For instance, the CDs prepared by "top-down" approaches are composed of nanocrystalline cores with predominantly graphitic or turbostratic carbon (sp^2 carbon) or graphene, and graphene oxide sheets fused by diamond-like sp^3 hybridized insertions. Hu *et al.* reported that the selected-area electron-diffraction (SAED) experiments on CDs with a size of about 3 nm prepared by laser ablation with surface modification revealed a ring pattern, with the ratio of the squares of the ring radius of 3 : 8:11 : 16 : 19. This implies a diamond-like structure, with the rings respectively corresponding to the (111), (220), (311), (400), and (331) planes of diamond.[120] This feature is retained also in the case where PEG_{200N} is not employed as the passivating ligand. The lattice spacing observed was 0.2–0.23 nm and is, in fact, quite close to the (100) facet of graphite. The lattice fringes of the diffraction planes of diamond-like and graphitic carbon lie very close to one another, thus rendering unambiguous assignment difficult without other corroborating evidence. Additionally, Ray *et al.* found that the CDs prepared from oxidizing candle soot had 0.208 nm lattice spacing, which suggests sp^3 diamond-like carbon or sp^2 graphitic carbon.[130] By ^{13}C NMR analysis, Tian *et al.* confirmed the presence of sp^2 carbon with signals in the $\delta = 90$–180 ppm range, while the absence of signals in the $\delta = 8$–80 ppm confirms the absence of any detectable aliphatic moieties. Furthermore, FTIR measurements also confirmed the presence of C=C aromatic ring stretches. Therefore, the authors concluded that these CDs consisted of a nanocrystalline core of graphitic sp^2 carbon atoms functionalized with peripheral carboxylic/carbonyl moieties.[131] One-step thermal decomposition reactions of citrate salts produced CDs with a size of 7 nm, whose XRD patterns were indicative of disordered carbon alongside the respective passivation agent.[128] The XRD pattern of CDs made from octadecylammonium citrate shows two superimposed broad reflections: one centered at 4.3 Å and a sharper peak at 4.14 Å, which are indicative of disordered carbon and densely packed alkyl groups arising from the octadecyl chains, respectively. The XRD pattern of CDs prepared by the supported method displayed a sharp, low-intensity reflection centered at $d_{002} = 3.3$ Å, which was very close to the graphite (002) lattice spacing.[127] However, the XRD pattern of the hydrophilic CDs (prepared by controlled carbonization of sucrose) showed an (002) interlayer spacing of 4.2 Å, which is larger than that of bulk graphite (3.3 Å), indicating poor crystallization.[179] The nanocrystalline core may also contain superficial carboxyl moieties, which impart excellent water solubility and suitable chemically reactive groups for further functionalization and surface passivation with various organic, polymeric, inorganic or biological materials to CDs.[202] Upon surface passivation, the fluorescence properties of CDs are enhanced. Surface functionalization also modifies their physical properties, like their solubility in aqueous and non-aqueous solvents.[81,202]

Unless otherwise modified, oxidized CDs generally feature carboxylic moieties on the surface, with overall oxygen contents ranging from 5–50 weight (wt) %, depending upon the experimental conditions used.[118]

Over the last few years, comprehensive research has been carried out to clarify the exact structures of the CDs prepared by "bottom-up" methods. In general, the morphology of such CDs consists of a complex mixture of crystalline or graphitic-like carbogenic cores, amorphous polymeric-like compounds, and even small molecular-like fluorophores.[203–208] Moreover, the actual degrees of carbonization, size and morphology of the CDs depend on the kind of bottom-up method (thermal/hydrothermal/solvothermal, microwave or ultrasonication), and on the reaction conditions (*i.e.* the nature of the precursors, solvents, the time, the temperature and the presence of doping heteroatoms). Currently, citric acid (CA) is the most common source for the synthesis of highly luminescent CDs, especially in combination with other doping reagents, such as nitrogen-containing compounds.[149,150] Overall, while the harsh pyrolytic conditions result in the production of CDs with a graphene-like sub-structure, the mild hydro-solvo-thermal procedures often lead to the synthesis of molecular fluorophores and amorphous CDs.

In 2012 Dong *et al.* demonstrated that a moderate or harsh thermal decomposition of citric acid resulted in the production of two different CDs with either an incomplete or a complete graphene-like structure respectively. In brief, after moderate pyrolysis (30 min, 200 °C), the citric acid can be partially carbonized to form nanosheets (graphene quantum dot (GQDs)) containing abundant, small but uniform sp^2 clusters. The GQDs show a strong and excitation-independent photoluminescence. By heating the same reaction mixture for a longer time (120 min at 200 °C) full pyrolysis occurred forming larger nanosheets (*i.e.* graphene oxide (GO)). The GO contained abundant small sp^2 clusters isolated within the sp^3 C–O matrix. These sp^2 clusters should be non-uniform in size and poorly passivated, resulting in a weak and excitation-dependent PL activity.[209]

A similar study conducted by Wang *et al.* on the decomposition of citric acid confirms that by increasing the pyrolysis temperature and time, larger particles will be constructed which possess low luminescence. Only at relatively lower temperatures (180 and 200 °C) and shorter times, sufficient quantities of highly luminescent uniformly sized CDs were formed which therefore exhibit a strong excitation-independent photo-luminescence. The authors suggest that in the first instance, the reaction proceeds towards the nucleation of some molecules of citric acid producing highly fluorescent materials, which further evolve through crosslinking and stacking forming extend amorphous and crystalline carbon domains.[210]

Mild pyrolysis (180 °C, 30 min) has been applied also to the synthesis of heteroatom doped CDs revealing the presence of molecular fluorophores; under more severe conditions (up to 400 °C for 1 h or 320 °C for 100 h) a carbogenic-heteroatom doped core was observed.[211] Specifically, the reaction between citric acid and ethanol amine was carried out at different temperatures of 180, 230, 300 and 400 °C. Under mild conditions, no CNPs were detected notwithstanding the highly fluorescent nature of the final solution. NMR and ESI-MS analyses reveal the molecular nature of the solution and some molecular

Open Access Article. Published on 08 July 2021. Downloaded on 10/31/2025 2:11:41 AM.
This article is licensed under a Creative Commons Attribution-NonCommercial 3.0 Unported Licence.

fluorophores were also identified. By increasing the reaction temperature, the formation of small spherical nanoparticles and progressive decrease of the QY (Fig. 9) were observed. The data suggest that the fluorophores produced at a low temperature are used as building blocks for the synthesis of CDs at a higher temperature.

Besides pyrolysis, also mild hydrothermal/microwave procedures have been used for the synthesis of heteroatom doped CDs. For example, Song *et al.* demonstrated that the hydrothermal treatment of citric acid and ethylene diamine at low temperatures produces a mixture containing carbon cores, oligomers and molecular fluorophores.[204] The authors identified 1,2,3,5-tetrahydro-5-oxo imidazo[1,2-*a*]pyridine-7-carboxylic acid (IPCA), a bright blue fluorophore (Scheme 1a), which was found to exist individually or bonded to the carbon core and thus to strongly affect the luminescence properties of the nanoparticles. IPCA was then used in hydrothermal synthesis at two different temperatures, confirming how the temperature influences the degree of graphitization. From these experimental findings, the authors hypothesised the presence of a chemical equilibrium between IPCA and carbon cores with polymer clusters acting as a transition state. Accordingly, the synthetic outcomes could be affected by many factors such as the reagent ratio, initial pH and temperature. For the latter they demonstrated that molecules/oligomers were dominant in the CDs prepared at lower temperatures while the carbon cores prevailed in the CDs prepared at high temperatures.

Since then, many molecular fluorophores have been detected in solution during the synthesis of CA-derived CDs. TPCA and TPDCA organic fluorophores (Scheme 1b) were the main ingredients and the fluorescence origins of N,S-CDs synthesized by hydrothermal treatment of CA with L-cysteine or cysteamine at low temperatures (200 °C) for 3 h.[205]

Fluorescent derivatives of citrazinic acid (Scheme 1c) were also identified, which are likely to constitute molecular species

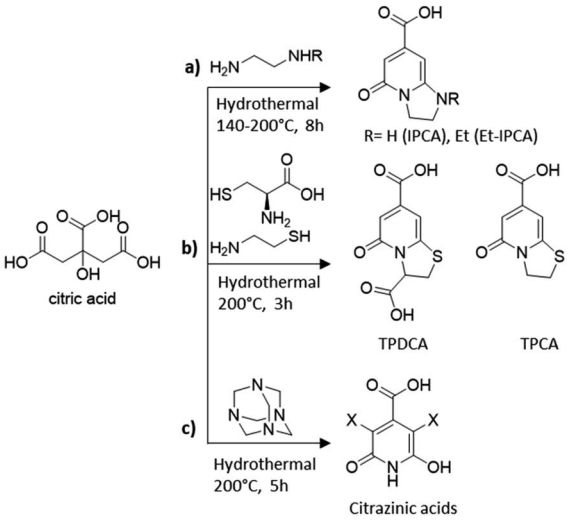

Scheme 1 Molecular fluorophores identified in the synthesis of CA-based CDs using different amino-containing precursors: (a) ethylene diamine,[204] (b) cysteine and cysteamine,[205] and (c) hexamethylenetetramine.[207]

either free or bonded to the carbonized nanoparticles, in the CD material formed by hydrothermal treatments of CA with hexamethylenetetramine at 200 °C for 5 h.[206] The authors further compared the optical properties of different CD species demonstrating the significant differences between samples predominantly composed of the carbon core and those containing molecular derivatives of citrazinic acids.

Many other recent contributions further describe the separation and characterization of different fluorophore molecules, arising from the synthesis of CDs, leading to a deeper understanding of the existing relationship between the structural composition and the optical properties of the CDs as clearly described in the following section.

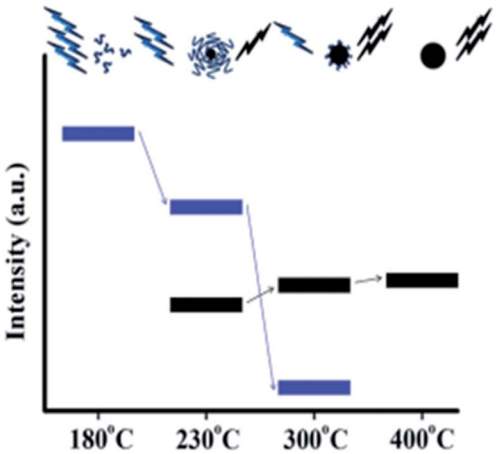

Fig. 9 Schematic representation of the emission characteristics of the photoactive species produced from the thermal treatment of mixture of CA and EA. The organic fluorophores (blue groups) and the carbogenic core (black sphere). Figure adapted from ref. 211 with permission from American Chemical Society, copyright 2012.

2.3. Optical properties

2.3.1. Absorbance. CDs typically show strong optical absorption in the UV region, with a tail extending out into the visible range (Fig. 10).[58]

Most of the CDs, such as those prepared by laser-passivation,[120] electrochemical oxidation,[126] or microwave/ultrasonic method,[133,134] have an absorption band around 260–320 nm. The several shoulder peaks in UV absorption spectra are generally attributed to the π–π* transitions of aromatic rings and C=C double bonds or to the n–π* transitions of C=O bonds or other sub-fluorophore groups.[212] However, the absorbance of CDs was found to increase to a longer wavelength (350–550 nm) after surface passivation with 4,7,10-trioxa-1,13-tridecanediamine (TTDDA).[213]

2.3.2. Photoluminescence

Origin of photoluminescence. One of the most fascinating behaviors of CDs, from a fundamental viewpoint of application, is their photoluminescence (PL). Although the exact mechanism which generates the light absorption and emission for CDs is still an open issue, the more reasonable hypotheses attribute it

 © 2021 The Author(s). Published by the Royal Society of Chemistry

Open Access Article. Published on 08 July 2021. Downloaded on 10/31/2025 2:11:41 AM.
This article is licensed under a Creative Commons Attribution-NonCommercial 3.0 Unported Licence.

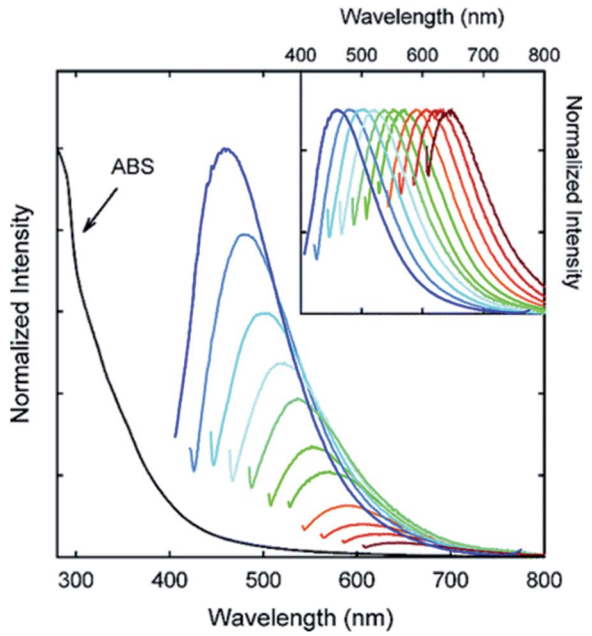

Fig. 10 Absorption and emission spectra of PPEI-EI passivated CDs in water with increasing λ_{ex} from 400 nm on the left with 20 nm increments. Inset: emission intensities normalized to quantum yields. Figure adapted from ref. 58 with permission from American Chemical Society, copyright 2006.

to the morphology and to the chemical/physical properties of the CDs. In summary, these are the three possible origins of PL:

(i) The first is the quantum confinement effect, which is determined by the degree of π conjugation and by the size of the carbon core. This type of PL, which arises from a band-edge recombination, is commonly observed in the homologous "metal based" quantum dots and confers to the carbon-based nanoparticles a size-dependent, excitation-independent, and a very narrow emission band.

(ii) The second type of emission is generated by the surface states, which are determined by surface defects, functional groups, and surface passivation of the carbogenic core. In this case the superficial defects trap the photoexcited electrons and/or holes in the band gap thus generating PL with lower energy. The resulting PL is a combination of the first two types of mechanisms leading to a luminescence with an ill-defined behavior and strongly dependent on the synthetic procedure used.

(iii) The third is the molecule state type which is associated with the presence of fluorophores in the CDs. In this case, neither quantum confinement nor surface defect effects exist, and the luminescence is solely a consequence of the superposition of several "molecular" type emissions. PL is therefore size-independent, and excitation-dependent and exhibits a very broad emission band.

The photoluminescence properties of the carbon dots are therefore strictly correlated with their intrinsic structure and consequently to the synthetic procedure used. Despite the difficulties to determine the actual origin of luminescence and to further classify the CDs based on their exact morphology, in general the first two PL mechanisms are invoked for "graphitic-like" CDs synthetized *via* both top-down or harsh bottom-up approaches (*i.e.* pyrolysis) while the third for "amorphous-like" CDs prepared through soft hydro/solvothermal bottom-up treatments. Herein, recent studies on the PL properties of CDs will be discussed.

Based on the origin of PL described above, the PL activity of graphitic-like CDs can be easily tuned by modifying both the core size and the nature of the functional groups.

In 2010, Li *et al.* presented clear evidence for luminescence arising from quantum-confinement effects and size-dependent optical properties of CDs prepared by an alkali-assisted electrochemical method starting from a graphite honeycomb.[136] Fig. 11a shows the optical images of CDs of four sizes, illuminated by white and UV light. The bright blue, green, yellow, and red PL of CDs is strong enough to be seen with the naked eye and the respective PL spectra are shown in Fig. 11b. The dimensions of the CDs increase the PL range from UV to NIR emission as shown in Fig. 11c.

The PL behavior was also retained after the plasma treatment for the removal of surface oxygen. Theoretical calculations performed on the CDs reveals that the HOMO–LUMO gap depends on the size of the graphene fragments. As the size increases, the gap energy decreases gradually, reaching the visible spectral range with CDs of 14–22 Å diameter, which agrees well with the visible emission of CDs with diameters of <3 nm (Fig. 11d). Thus, they deduced that the strong emission of CDs comes from the quantum-sized graphite structure instead of the carbon–oxygen surface.[136]

Few years later, in 2012, by comparing carbon nanoparticles with different dimensions obtained by one step hydrothermal treatment of orange juice followed by size separation *via*

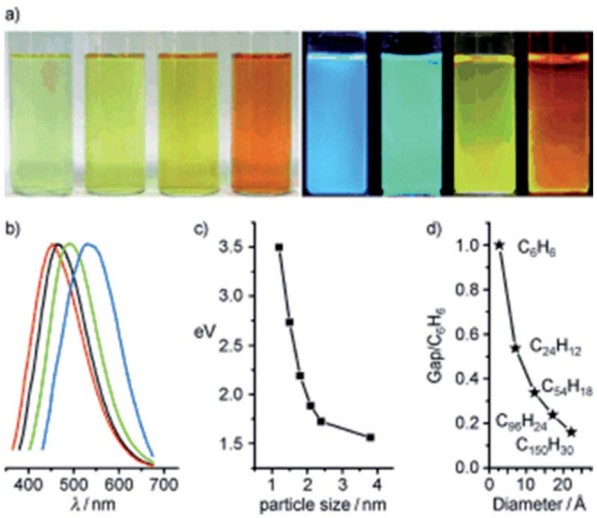

Fig. 11 (a) Typical sized CD optical images illuminated under white (left) and UV light (right); (b) PL spectra of typical sized CDs: the red, black, green, and blue lines are the PL spectra for blue-, green-, yellow-, and red-emission CDs, respectively; (c) relationship between the CD size and the PL properties; (d) HOMO–LUMO gap dependence on the size of the graphene fragments. Figure adapted from ref. 136 with permission from Wiley, copyright 2010.

Open Access Article. Published on 08 July 2021. Downloaded on 10/31/2025 2:11:41 AM.
This article is licensed under a Creative Commons Attribution-NonCommercial 3.0 Unported Licence.

centrifugation, Mohapatra *et al.* confirmed the red shift in the emission wavelength of CDs with increasing size.[185] As the size of CDs increases, the nature and content of sp^2 hybridized sites and the band gap from the quantum confinement effect would be affected. In particular, the authors pointed out that excitation dependent photoluminescence could be caused by surface states, excitons of carbon, emissive traps, aromatic conjugation structures and free zig-zag sites.

Zhang and co-workers in 2016 prepared different sized CDs *via* gel electrophoresis of the crude nanoparticles prepared through a photo-Fenton reaction of graphene oxide.[214] They demonstrate that the PL of CDs depends on both the nanoparticle size, according to the quantum confinement effect, and the peripheral carboxylic groups. More importantly, it was revealed that for small sized CDs the surface status effect prevails on the PL with the contribution of the carbon skeleton which appears only when exciting the nanomaterial at longer wavelengths. However for the large sized CDs the effect of the graphitic core is dominant over their PL leading to an emission wavelength which increases with size (minor energy gap). The latter phenomenon can only be explained with the quantum confinement effect.

An additional extensive analysis of the contribution on the PL of the carbon core of the CDs was reported by Zhu *et al.* who demonstrated the role of the aromatic carbon domain in achieving the blue fluorescence of the carbon nanoparticles. In more detail, in a perfect graphene core with few surface groups the band gap between the conjugated π-domains is the intrinsic PL center. Other important contributions to the photoluminescence of the carbon nanoparticles may derive from their surface states: the surface chemical groups and the hybridization structure of the edge groups. Carboxyl and amide groups are responsible for the green emission of the carbon nanoparticles, while the hydroxyl groups guarantee a blue photoluminescence. These results were proved by different factors; first of all, long exposure to the UV light results in an enhanced PL due to the oxidation of the hydroxyl groups to carboxyl groups. Converting the hydroxyl groups in amide groups results in an enhanced PL and if these CDs are reduced a strong blue luminescence is observed.[215] These results confirmed the great complexity of the photoluminescence origin of the CDs and that different factors may contribute to it.

Considering the effect on the PL of the superficial CD decorations, many other studies have appeared in the last few years. As reported by Sun *et al.*, the PEG_{1500N} passivation of CDs formed by laser ablation of graphite powder and cement led to an emission spectrum spanning from purple to red which further spreads to the NIR region with the excitation wavelength progressively increasing from 400 nm on the left in 20 nm increments (Fig. 10).[58] Upon surface passivation with organic or polymeric materials, such as poly(propionyl ethyleneimine-*co*-ethyleneimine) (PPEI-EI) attached to the CD surface, surface defects are stabilized and strong fluorescence emissions both in a solution-like suspension and in solid state were detected. The emissions of such passivated CDs covered a broad range of the visible region and extended into the NIR region as shown in Fig. 10. It should be noted that the surface passivation agents used were not emissive in the visible and NIR regions, and thus any fluorescence emissions observed must have originated from the surface passivated CDs. The tunable emission properties of CDs are clearly demonstrated in Fig. 10. From the fluorescence spectra of PPEI-EI-passivated CDs, it is evident that the emissions are broad and excitation wavelength-dependent.[58,216] The tunable emissions of the surface-passivated CDs could be a result of varied fluorescence characteristics of particles of different sizes of the CDs and the distribution of different emissive sites on the surface of the CDs.

More recently, Ding and co-worker using urea and *p*-phenylenediamines as precursors prepared equal-sized CDs from blue to red with an excitation-independent luminescence emission spectra.[217] The observed colour changes were found to depend on the degree of superficial oxidation structures rather than the particle size. In more detail, the observed red shift in their emission peaks from 440 to 625 nm was ascribed to a gradual reduction in their band gaps with the increasing incorporation of oxygen species into their surface structures (Fig. 12).

Moreover, pH-dependent PL emission was also reported and this phenomenon can be reasonably explained by surface states, as Qu *et al.* have discussed.[218] Functional groups such as N–H and O–H on the surface of CDs can form intramolecular and intermolecular hydrogen bonds, which endow the CDs with different surface states. pH changes could cause deprotonation or protonation of functional groups inducing variation of surface states and fluorescence. Jia *et al.* reported that CDs prepared from direct heating of ascorbic acid solution show a practically linear dependence on the pH of the solution in the range of 4.0 to 8.0. The fluorescence intensity decreased by as much as 90% from acidic to alkaline pH. The shift in the pH caused the deprotonation of the carboxyl groups on the surface of the CDs, leading to electrostatic doping/charging of the CDs and Fermi level shift.[219] A similar effect could also be triggered by solvent polarity as Gao *et al.* observed by changing the solvent from water to ethylene glycol. This may be due to the change of surface states and the decrease of non-irradiative transitions.[164] It is worth noting that some CDs exhibit fluorescence that is independent of the excitation wavelength and pH.[220,221]

Regarding the third molecular state effect of the PL on the CDs, an unequivocal demonstration was given by Song *et al.* in 2015 who were able to isolate and characterize the molecular fluorophore IPCA (5-oxo-1,2,3,5-tetrahydro-imidazo[1,2-*a*]

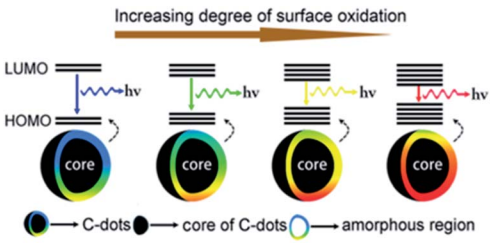

Fig. 12 Model for the tunable PL of CDs with different degrees of oxidation. Figure adapted from ref. 217 with permission from Wiley, copyright 2015.

 © 2021 The Author(s). Published by the Royal Society of Chemistry

Open Access Article. Published on 08 July 2021. Downloaded on 10/31/2025 2:11:41 AM.
This article is licensed under a Creative Commons Attribution-NonCommercial 3.0 Unported Licence.

pyridine-7-carboxylic acid) demonstrating that its absorption and emission spectra were identical to the one of the synthetized CDs (Fig. 13).[204] The resulting fluorophore was found to be the main emitting species in these CDs.

Other recent research studies describe a great variety of organic fluorophores responsible for the optical properties of CDs. Worthy of mention is the study conducted by Schneider *et al.* on CDs derived from the soft hydrothermal treatment of citric acid in the presence of three different amino compounds (Fig. 14, reactions (a)–(c)).[206] In the solutions of CDs obtained from the reactions (a) and (b) schematized in Fig. 14, molecular fluorophores were detected, and their PL and absorption spectra resemble the ones of a pure solution of the fluorophore. A further demonstration of the key role of the molecular fluorophores comes from the reaction (Fig. 14c) that did not produce any detectable fluorescent compounds; here the CDs have a different PL spectrum with redshifted emission peaks and a significantly lower PL lifetime and QY.

Other important considerations regarding the role of molecular fluorophores in determining the final PL properties of the nanomaterials have been pointed out by Zhang *et al.* They demonstrated that the optical properties of CDs synthesized from citric acid and cysteine are regulated by the presence of the fluorophores TPDCA (5-oxo-3,5-dihydro-2*H*-thiazolo [3,2-*a*] pyridine-3,7-dicarboxylic acid) and TPCA (5-oxo-3,5-dihydro-2*H*-thiazolo [3,2-*a*] pyridine-7-carboxylic acid).[205] Both, the molecular fluorophores and the CDs show the same UV-Vis absorption, excitation and emission, QY, fluorescent lifetime, excitation-independent-emission, pH dependent fluorescence and photobleaching. In addition, the authors were able to isolate and characterize TPCA and TPDCA from the CD solution confirming that the PL mechanism is governed by the molecular state.

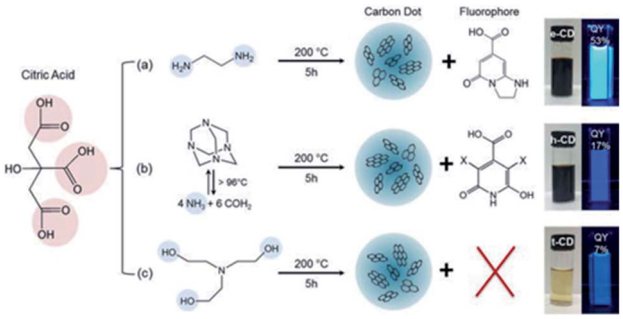

Fig. 14 Synthesis conditions of citric acid-based CDs using three different nitrogen-containing precursors. Figure reproduced from ref. 206 with permission from American Chemical Society, copyright 2017.

Fu *et al.* further investigated the origin of the luminescence of CDs obtained from citric acid and ethylene diamine.[208] The authors were able to reproduce the optical behavior of such CDs by employing simple polyaromatic hydrocarbons (PAHs) like pyrene, anthracene and perylene. Tuning the concentration of these three compounds, they were able to reproduce most of the optical properties of the CDs (Fig. 15). From these results they assert that CDs likewise predominantly comprise small PAHs embedded in a matrix consisting of sp^3-hybridized carbon. Defects states and surface chemical functionalities also participate in defining the optical properties of the materials but will only play a minor role.

Based on this topic Hinterberger *et al.* produced CDs from citric acid and cysteine under different hydrothermal conditions, and then they purified the mixture by silica gel chromatography. This system allowed the separation of three different fractions, the first one rich in fluorophore molecules (5-oxo-3,5-

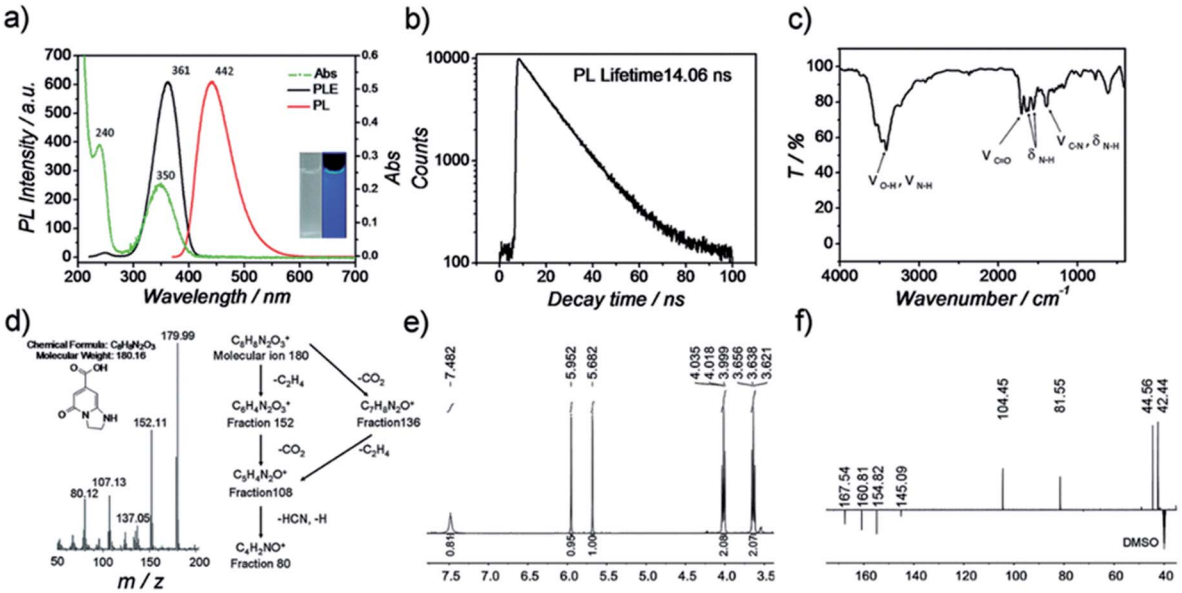

Fig. 13 Characterization of IPCA (a) PL and Abs spectra of IPCA; inset photographs of IPCA solution under visible and UV light, (b) PL lifetime measurements of IPCA, (c) IR spectra of IPCA, (d) mass spectra of IPCA, (e) 1H-NMR of IPCA and (f) DEPTQ ^{13}C-NMR of IPCA. Figure reproduced from ref. 204 with permission from Royal Society of Chemistry, copyright 2015.

Open Access Article. Published on 08 July 2021. Downloaded on 10/31/2025 2:11:41 AM.
This article is licensed under a Creative Commons Attribution-NonCommercial 3.0 Unported Licence.

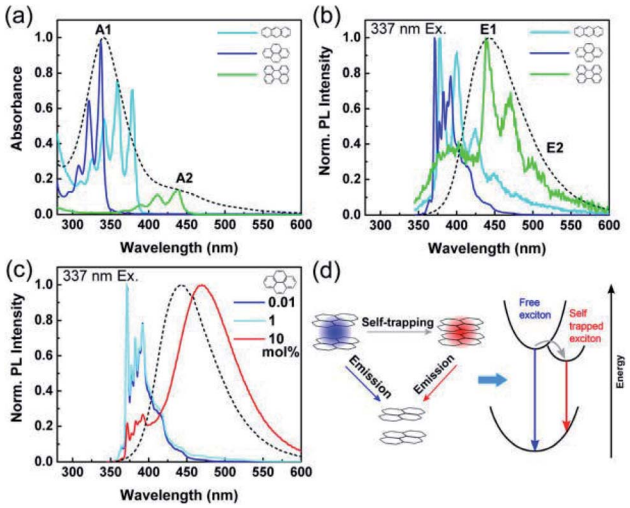

Fig. 15 (a) Absorption spectra of anthracene (light blue), pyrene (dark blue), and perylene (green) dispersed in a PMMA matrix with a concentration of 0.01 mol% as well as of CDs in aqueous solution (black dashed line). (b) Normalized PL spectra of the same samples as in (a) excited at 337 nm. (c) Normalized PL spectra of pyrene in PMMA films excited at 337 nm, as a function of pyrene concentration with the CD PL spectrum (black dashed line) for comparison. (d) Scheme of the exciton self-trapping process in a pyrene molecule pair: a free exciton (blue spot) may be self-trapped on a molecule pair as a self-trapped exciton (red spot), causing the reduction of energy and mobility. Figure reproduced from ref. 208 with permission from American Chemical Society, copyright 2015.

dihydro-2*H*-thiazolo [3,2-*a*] pyridine-7-carboxylic acid) (TPDCA), the second one less photoluminescent composed of fluorophores bound on the CDs surface and the last one composed of CDs without fluorophores. The analyses revealed that under mild condition the solution is mainly composed of fluorophores and possesses a high QY (72%). With harsher conditions, a drop in the QY was observed as the fluorophores were destroyed and embodied in the structure of the CDs. This study demonstrated the complexity and the heterogeneity of the solutions of CDs, and how their luminescence properties could be tuned by employing different synthetic protocols.[222]

An additional very recent hypothesis on the origin of the PL behavior of the CDs and the specific role played by the different components was made by Fang *et al.*[207] They suggested that the PL of CDs is the result of a cooperative effect between the graphitic carbon core, the defect states and the molecular fluorophore. The authors used citric acid and amino group-containing molecules as precursors to prepare CDs having luminescent pyridine-derivatives along with a carbogenic core which were separated by a dialysis treatment. The PL behavior of the molecules agreed with the one of the original CD solution with, however, a higher QY and a less evident excitation-dependent behavior.

Combining these outcomes with an accurate optical study the authors proposed a hypothetical PL mechanism in which fluorophores, defect states and the carbon core play a different role. UV irradiation of the fluorophores generates excited electrons from the π orbitals to the π* orbitals. Some of the excited electrons in the π* orbitals may recombine with the holes in the π orbitals directly, emitting the PL signal centred at 420–440 nm, which can be referred as the intrinsic emission like the band-edge emission observed in QDs. The other excited electrons in the π orbitals may be trapped by the defect states of energies lower than in the π* orbitals before they are finally recombining with the holes in the π orbitals. Meanwhile, some electrons may be excited and trapped directly by the defect states and relax through either radiative or non-radiative ways. Therefore, when the excitation wavelength is in the range of 280–380 nm, the CD produced both intrinsic and defect PL signals. When the excitation wavelength is longer than 380 nm, *i.e.* at a lower energy which is less than needed for the π–π* transition, the electrons can only be excited to the defect states. The graphitic core, in this hypothesis, acts as a quencher of the radiative relaxation pathway of both defect and intrinsic states through a fluorescence resonance energy transfer (FRET) effect thus lowering the QY.[207]

In conclusion, while the PL spectra depend on both molecular fluorophores and defect states, the magnitude of QY is mainly affected by the graphitic core of the CDs.

Overall, even if this latter PL mechanism is satisfactory from an intuitive level, many other issues (such as the role of the carbon core size and the structural morphologies of the CD, *i.e.* amorphous or crystalline) were not effectively addressed. Therefore, there is a lack of a real understanding of the mechanisms of fluorescence of these nano-systems remain to date.

Photostability. The ability to maintain a stable fluorescence emission intensity after a long continuous excitation is called photostability. Wei *et al.* demonstrated that CDs have an excellent photostability when synthesized from glucose and various amino acids. After 60 min of excitation, the PL intensity of all the CDs preserved 90% of the initial intensity. PL of the CDs was much more stable than that of fluorescein isothiocyanate (FITC) dye, CdTe QDs and previously reported polymer nanoparticles or dye-doped silica (Fig. 16).[195]

Ge *et al.* prepared red-emissive CDs using polythiophene phenylpropionic acid as a precursor, and their photostability was investigated. Fixed-cell images of the CDs labeled HeLa cells showed intense red fluorescence, after 120 min of irradiation. By contrast, the ones of FITC, decay very rapidly after 10 min, confirming the higher photostability of the CDs *in vitro*.[223]

The diversity and uncontrollable nature of the surface defects on the CDs reduce the radiative recombination, limiting their QY and their application in several fields.[224] In order to improve the luminescence of CDs, great effort has been made through physical and chemical methods. Wang *et al.* reported CDs with a PL QY of 55–60% after column chromatography purification of the CD mixture with 16–20% PL QY.[225] To enhance the QY of CDs, diverse designs have been developed including surface passivation, element doping, and inorganic salt doping. Passivation is the common strategy to improve the QY of CDs due to its facile processability and high efficiency. Most of the time it implies oxidation or reduction of the CD surface and subsequent capping with organic polymers or diamine compounds. Zheng *et al.* reported that original CDs prepared with graphite oxide as a precursor were reduced by

 © 2021 The Author(s). Published by the Royal Society of Chemistry

Open Access Article. Published on 08 July 2021. Downloaded on 10/31/2025 2:11:41 AM.
This article is licensed under a Creative Commons Attribution-NonCommercial 3.0 Unported Licence.

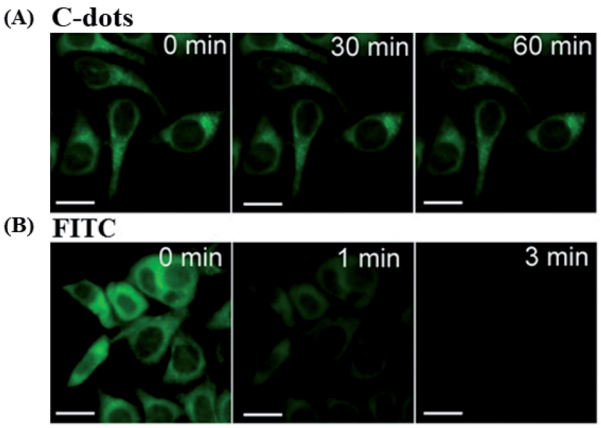

Fig. 16 Stability comparison of the fluorescence signals of HeLa cells labeled by CDs (A), and FITC (B). Scale bar = 10 μm, figure reproduced from ref. 195 with permission from Nature Publishing Group, copyright 2014.

$NaBH_4$, and the QY of the reduced-state CDs increased greatly from 2 to 24%; meanwhile, the maximum emission wavelength shifted from 520 to 450 nm at an excitation wavelength of 360 nm (Fig. 17).[226]

To stabilize and maximize fluorescence, CDs are usually doped with inorganic salts or with organic precursors containing different elements. Nitrogen is the most widely used doping element leading, in most of the cases, to higher QY.[195,227,228] Jiang *et al.* prepared CDs with high QY (44.9%) from amino acids *via* a microwave method.[229] Li *et al.* prepared nitrogen and sulfur co-doped CDs *via* a hydrothermal method with extremely high QY (73%).[159] In this method, L-cysteine was used as a precursor for doping of the CDs. Sulfur is also employed as a doping agent to increase the PL properties of the CDs; based on this topic Xu *et al.* synthesized S-doped CDs with significant fluorescence QY (67%) *via* a hydrothermal method.[230] Moreover, some other methods have been developed to improve the QY of CDs. For example, Sun *et al.* developed CDs doped with Zn to achieve high QY. An aqueous suspension of CDs and $Zn(CH_3COO)_2$ was hydrolyzed with NaOH, and then $Zn(OH)_2$ was converted to ZnO by thermal annealing; the QY of the ZnO-doped CDs in aqueous solution was around 45%. After precipitation with Na_2S, the QY of the ZnS-doped CDs were consistently higher than 50%. Sun *et al.* speculated that the combination of organic and inorganic passivation agents, might provide another form of surface passivation or enhance the surface passivation effect. Under the two-photon excitation at 800 nm, these doped CDs emitted bright luminescence in the visible region, suggesting promising potential for imaging applications.[231]

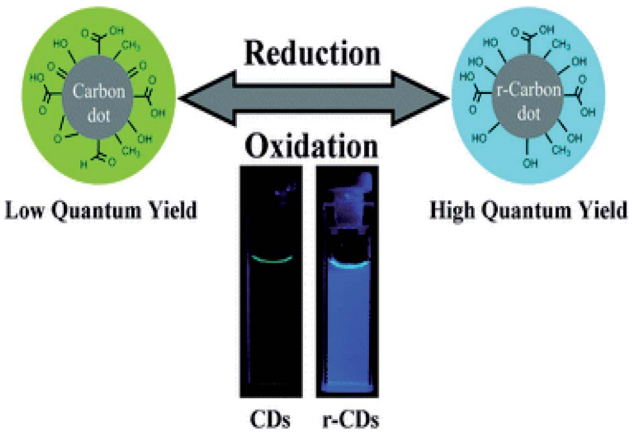

Fig. 17 Graphical representation of the synthesis of reduced state CDs (r-CDs) with blue luminescence from original CDs. Inset: photographs of aqueous solutions of the CDs (CDs) (left) and the r-CDs (right) obtained under UV light (360 nm). Figure reproduced from ref. 226 with permission from Royal Society of Chemistry, copyright 2011.

Up-conversion photoluminescence. In addition to normal fluorescence, a new and interesting phenomenon has been discovered recently: up-conversion fluorescence emission. Up-conversion fluorescence is anti-Stokes behavior, in that a longer excitation wavelength produces a shorter emission wavelength. As shown by Sun *et al.*, CDs were strongly emissive in the visible region under irradiation by an argon-ion laser (458 nm) or a femtosecond pulsed laser for two-photon excitation in the NIR range (800 nm).[116] The authors show that the one- and two-photon luminescence images for the same scanning area of CDs are well matched. The representative two-photon luminescence spectrum shows that such CDs have up-conversion photoluminescence (UCPL) properties. The results from further bio-imaging experiments *in vitro* also showed the UCPL properties of CDs.

Recently, Jiang *et al.* reported that CDs emitted strong UCPL under excitation with a femtosecond pulsed laser ($\lambda = 800$ nm) and this has been demonstrated to be a two-photon excitation process.[160]

Stan *et al.* studied the up-conversion fluorescence of N-doped CDs in the wavelength range of 750–960 nm.[232] Interestingly, distinct from the down-conversion case, up-conversion fluorescence showed excitation wavelength independent and solvent polarity dependent emission. Moreover, such up-conversion fluorescence can be easily observed by the naked eye. Shen *et al.* fabricated CDs surface-passivated with PEG by a one-pot hydrothermal reaction. The PL quantum yield of the CDs at an excitation wavelength of 360 nm was about 28%. The CDs possessed the up-conversion PL properties, and emitted blue PL in the fluorescence microscopy images both under the ultraviolet and 808 nm laser.[233]

As shown in Fig. 18a, when the excitation wavelength changed from 700 to 980 nm, the up-converted emission peaks shifted from 431 to 544 nm, respectively. The shifting between the energy of up-converted emission light (E_m) and excitation light (E_x) was almost unchanged, about 1.1 eV. Fig. 18b shows the linear relationship between E_m and E_x, and the function of the fit line is $E_m = 1.00E_x + \delta_E$ ($R^2 = 0.9747$) with $\delta_E = 1.1$ eV. The authors speculate on the UCPL due to the anti-Stokes PL, where δ_E between the π and σ orbitals is near 1.1 eV.[216]

To further confirm this and explain how UCPL comes from the CDs, an energy level structural model was established, in which the UCPL spectrum could be regarded as an anti-Stokes

Open Access Article. Published on 08 July 2021. Downloaded on 10/31/2025 2:11:41 AM.
This article is licensed under a Creative Commons Attribution-NonCommercial 3.0 Unported Licence.

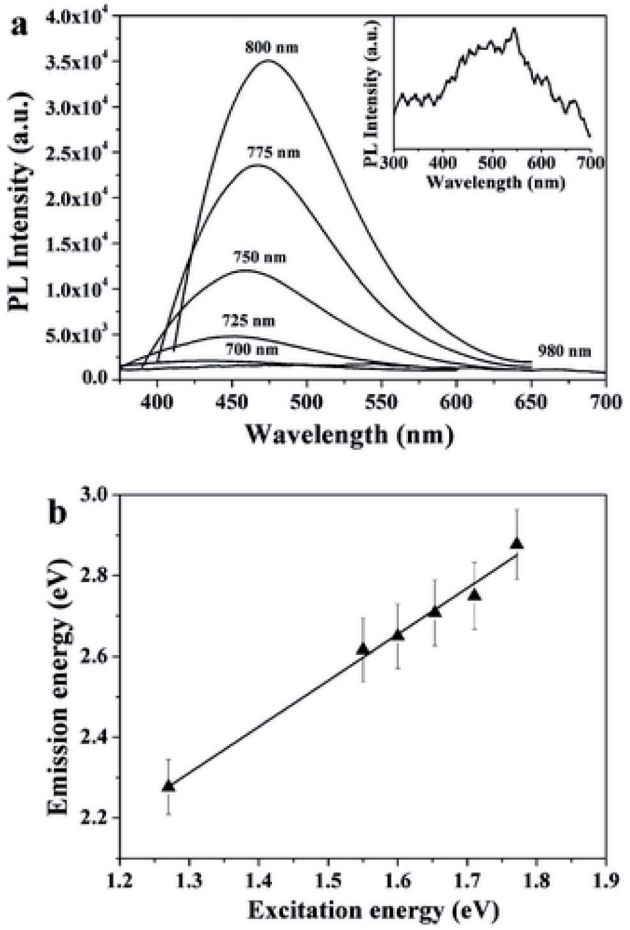

Fig. 18 (a) Upconverted PL properties of the CDs-PEG; the inset shows the enlarged image of the PL spectrum excited using a 980 nm laser. (b) The energy of the excitation light as a function of the emission. Figure reproduced from ref. 216 with permission from Royal Society of Chemistry, copyright 2011.

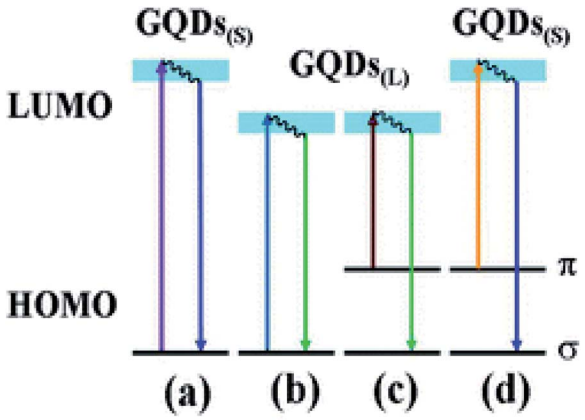

Fig. 19 A schematic illustration of various typical electronic transitions processes of CDs. Normal PL mechanisms in CDs of small sizes (a) and large sizes (b); UCPL mechanisms in CDs of large sizes (c) and small sizes (d). Figure reproduced from ref. 216 with permission from Royal Society of Chemistry, copyright 2011.

transition (Fig. 19). The energy levels of π and σ orbitals were provided by the carbene ground-state multiplicity, which is related to the energy difference (δ_E) between the π and σ orbitals. The energy between the excitation light and the emission light in the up-conversion process was close to 1.1 eV (Hoffmann determined δ_E should be below 1.5 eV). When a bunch of low-energy photons excite the electrons in the π orbital, the π electrons would be excited to a high-energy state such as the LUMO, and then fall back to a low-energy state. Thus, an UCPL is emitted if the electrons transition back to the σ orbital. The electrons in the σ orbital can also be excited and they only can emit normal PL (Fig. 19). This explains why the difference between up-conversion excitation and emission light is a constant energy related to the energy difference of the π and σ orbitals.[216]

The UCPL of CDs opens new opportunities for cell imaging with two-photon luminescence microscopy, as well as highly efficient catalyst design, for application in bioscience and energy technology.

Chemiluminescence. Chemiluminescence (CL) refers to a phenomenon whereby during a chemical reaction, a substance can absorb chemical energy to turn into an excited state and then go back to the ground state by light irradiation. The CL properties of CDs were first discovered when the CDs coexisted with some oxidants, such as potassium permanganate ($KMnO_4$) and cerium(IV).[234] During this process, the CDs with surface energy traps serve as electron acceptors for the electron donator $O_2^{\bullet-}$ and strong CL emitter. The electron paramagnetic resonance (EPR) reveals that oxidants, such as $KMnO_4$ and cerium(IV), can inject holes into the CDs. This process increases the population of the holes in the CDs and accelerates the electron–hole annihilation, resulting in energy release in the form of CL emission. This is the first CL route accounting for the CL (CL1). The other important route (CL2) is the Mn(II)* excited state, which returns to the ground state with CL emission at 650 nm (Fig. 20). Moreover, the CL intensity was dependent on the concentration of the CDs in a certain range. It was also found that increasing the temperature had a positive effect on the CL due to the thermal equilibrium of the electron distribution in the CDs (Fig. 20). It is interesting to note that for this system the CL properties can be designed by changing their surface groups.[235]

Recently CDs obtained from citric acid and melamine were employed to enhance the CL reaction of $K_2Cr_2O_7$ with $NaHSO_3$. The nanomaterial acts as both an energy acceptor and luminophore in the CL reaction inducing an amplification of the signal. This effect was exploited for the determination of iodide since this ion can interact strongly with the potassium species leading to an enhancement of the signal.[236]

A novel CL phenomenon was also observed for the CDs in a strong alkaline solution (NaOH or KOH). The CDs exhibited excellent electron donor ability towards dissolved oxygen to form the superoxide anion radical ($O_2^{\bullet-}$) in a solution of NaOH. These results provided direct evidence for the excellent electron-donating ability of CDs.[237] Radiative recombination of the injected electrons by "chemical reduction" of the CDs and thermally excited generated holes was suggested to account for

 © 2021 The Author(s). Published by the Royal Society of Chemistry

Open Access Article. Published on 08 July 2021. Downloaded on 10/31/2025 2:11:41 AM.
This article is licensed under a Creative Commons Attribution-NonCommercial 3.0 Unported Licence.

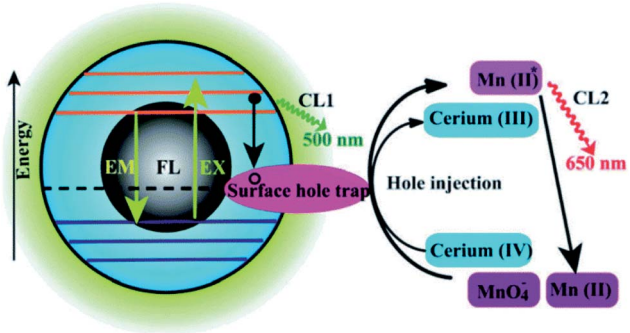

Fig. 20 Schematic illustration of the FL and CL mechanisms in the CDs-$KMnO_4$ and CDs-cerium(IV) systems. CL1 and CL2 represent two CL routes in the system. Figure reproduced from ref. 234 with permission from Royal Society of Chemistry, copyright 2012.

the CL behavior in strong alkaline solutions.[237] The dual role of CDs as an electron donor and acceptor offers great potential in optronics and catalysis.

Electrochemiluminescence. Differently from fluorescence and CL, electrochemiluminescence (ECL) happens when the substances produced in an electrochemical reaction are excited *via* electron injection and then emit light to return back to the ground state. The ECL emission of CDs (2.0 nm) produced by Zheng *et al.* from the electrochemical oxidation of graphite was observed as the potential was cycled between +1.8 and −1.5 V.[125] The suggested ECL mechanism involves the formation of excited-state CDs (R*) by electron-transfer annihilation of negatively charged ($R^{\bullet-}$) and positively charged ($R^{\bullet+}$) species (the ET1 route in Fig. 21). $R^{\bullet+}$ is the more stable of the two species, as indicated by the greater intensity of the cathodic ECL (Fig. 21A). Interestingly, when produced by microwave synthesis, 3 nm PEG_{200}-functionalized CDs also exhibited ECL behavior, but the $R^{\bullet-}$ species was found to be more stable in this case.[133] The presence of peroxydisulfate ($S_2O_8^{2-}$) enhanced the ECL (the ET2 route in Fig. 21B) in the cathodic potential range and produced a stable and sensitive (as no other co-reactants tested elicited an ECL enhancement) ECL response, thus suggesting the application of CDs for ECL sensing.[125] More recently Kumar *et al.* employed P doped CDs in the fabrication of a solid-state ECL platform, for the detection of Cu^{2+}. They observed that the ECL intensity of the phosphorous doped CDs is way higher compared to that of the undoped ones. Moreover, if Cu^{2+} is added to the solution the intensity could be further enhanced, thus increasing the detection limit for this particular ion.[238]

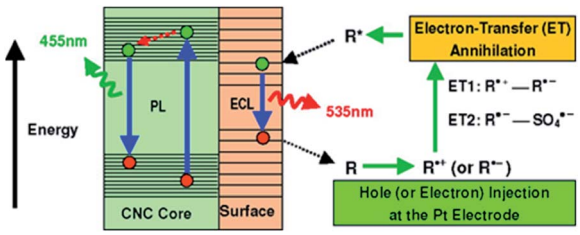

Fig. 21 The ECL and PL mechanisms in CDs. Figure reproduced from ref. 125 with permission from American Chemical Society, copyright 2009.

2.4. Biological properties and applications

Carbon dots exhibit many biological applications due to their low toxicity, biocompatibility and bio-degradation.[53,239,240] Recent advancements of CDs in the medical or pharmaceutical field include their application in bioimaging-detection, drug-carrier development, gene transfer, diagnosis, cancer therapy, and so on.[241,242] However, some studies have reported that many factors including CD synthesis methods, the size, the shape and functional groups on the surface of CDs could affect the efficiency of CDs causing hazardous effects on human health. Therefore, *in vitro* and *in vivo* toxicity studies of CDs are the new challenge to understand the mechanism of these nanoparticles and confirm their safety.[243–245]

2.4.1. *In vitro* and *in vivo* toxicity studies. Although *in vivo* toxicity studies of CDs remain a critical issue, the low cytotoxicity of these nanoparticles could be the main reason for scarcity of studies in animal models. Wang *et al.* evaluated the genotoxicity, the acute toxicity and subacute toxicity of CDs fabricated from raw soot by nitric acid treatment and PEG passivation. The results showed no genotoxic or toxic effects in the mice model used.[246] In another study, Tao *et al.* investigated the *in vivo* toxicity effect of CDs following intravenous administration (20 mg kg^{-1}) in mice. The experiments were carried out for 3 months without showing toxic effects in the treated mice.[247]

In recent years, zebrafish embryos have attracted widespread attention as strategies for the toxicological evaluation of CDs due to their homology to the human genome, their short generation time and optical transparency, which allows in real-time the bioimaging-detection of CDs.[248–252] In a study by Tathagata *et al.*, the authors reported the nontoxic effects of CDs from curcumin using the zebrafish model. The nonaqueous curcumin was transformed into a highly hydrophilic CD after hydrothermal synthesis. Multicolor fluorescence, high photostability, and low cytotoxicity were reported in fibroblast cells NIH-3T3, human lung adenocarcinoma cells A549 and human colorectal adenocarcinoma HCT-15. Meanwhile, bioimaging, biocompatibility and toxicity studies were performed using zebrafish embryo toxicity (ZET) tests.[251] Further experiments demonstrated that fruit-based CDs from kiwi and avocado did not show sub-lethal signs of toxicity in a zebrafish model, demonstrating the low toxicity of this type of CD produced from natural sources.[252]

On the other hand, many recent reviews have described several studies on the cytotoxic effect of CDs against different cell line models including, breast adenocarcinoma SKBR3, mouse embryonic fibroblast NIH-3T3,[253] human renal epithelial cells 293T, normal breast epithelial cells MCF-10A, normal human liver cells HL-7702 (L-02), normal human skin fibroblasts NSFbs,[241] human lung adenocarcinoma cells A549, human colorectal adenocarcinoma HCT-15 and others.[251] To date, several of these cytotoxic studies have shown that CDs did

Open Access Article. Published on 08 July 2021. Downloaded on 10/31/2025 2:11:41 AM.
This article is licensed under a Creative Commons Attribution-NonCommercial 3.0 Unported Licence.

not alter cell viability.[74,254] Therefore, according to various researchers, the immense variety of synthesized CDs with different physicochemical properties is the next challenge in exploring the *in vitro* and *in vivo* toxicity of CDs. In fact, CD toxicity can be reduced by surface-engineering techniques that use surface passivation molecules or biocompatible polymers at a minimum concentration.[74] This approach could guarantee the combination of CDs with therapeutic agents resulting in an excellent biological effect.

2.4.2. Bioimaging-detection. Real-time observation is one of the main topics of CD study, which allows the elucidation of the translocation of molecules, the interaction with targets and the response to extracellular signals.[255] Based on structural diversities, CDs have multiple advantages over semiconductor quantum dots (QDs), including comparable optical properties and photochemical stability. In addition, CDs are known for their tunable photoluminescence (PL) and multicolor PL properties. Indeed, these properties make CDs very desirable as alternatives to semiconductor QDs for application in bioimaging both *in vitro* and *in vivo*.[53,256]

It has already been reported that CDs mainly enter into the cells by endocytosis and are concentrated in the cytoplasm. In fact, there are few reports which show that CDs enter into the cell nucleus.[257] Fluorescent CDs were used for cellular imaging for the first time by Cao *et al.* The authors used PPEI-EI passivated CDs for two-photon luminescence microscopy in human breast cancer MCF-7 cells.[116] The cells incubated with CDs exhibited a bright luminescence in both the cell membrane and cytoplasm regions. The results indicate that the ability of the cells to take up CDs depends on the temperature.

Synthesis methods of CDs are an essential way to prepare multifunctional CDs with imaging ability. Bhunia *et al.* synthesized a series of fluorescent CDs from several carbohydrates including sucrose, glucosamine, glucose, and dextrans of different molecular weights, ascorbic acid and cellulose. The synthesized nanoparticles were then incubated with HeLa cells for 3–6 hours. The CDs showed very low binding properties to the cells due to their low surface charge and small size. Moreover, the particles emitted different fluorescence spectra based on their size,[82] suggesting that few CDs are capable of penetrating into the cell membrane and a few just help in staining the cells and cell nuclei. Thus, the surface functionalization and size of CDs play a major role for applications in bioimaging.

Several studies have indicated that surface modification of CDs is another crucial factor related to the multicolor PL properties of these nanoparticles.[257] Bhunia *et al.* conducted an *in vitro* study synthesizing various CDs with different fluorescence. The target recognition was realized by surface modification of CDs with folic acid, which indicated that the fluorescence properties of these nanoparticles are stable to chemical modification.[82] In another study by Tang *et al.*, the authors modified CDs with doxorubicin and folic acid for specific cancer cell recognition, drug transport, and fluorescence imaging analysis.[258]

On the other hand, some research groups discovered that CDs are able to exhibit multicolor emissions. Our research group synthesized fluorescent CDs that are biocompatible and suitable for bioimaging of exosomes.[53] CD loaded exosomes emitted blue, green, red and violet fluorescence upon excitation at 350, 490, 550, and 630 nm, respectively. A clearly noticeable dotted appearance of CD loaded exosomes can be observed suggesting that these CDs can be utilized to probe exosomes for biological applications (Fig. 22).

Other evidence indicates that changes in solvents and the adjustment of raw material proportions used in the preparation of CDs have allowed modifications in the emission wavelength of these nanoparticles.[259] In fact, Xiong *et al.* acquired various colors (λ_{em} ranged from 443 to 745 nm) emitted by CDs adjusting the type of solvent (ethanol, sulfuric acid, formamide and *N*,*N*-dimethylformamide) and the proportions of raw materials (*o*-phenylenediamine and L-glutamic) used in the CD synthesis.[260]

The fluorescence of CDs could be preserved for 60 hours. Therefore, these nanoparticles could be suitable for long-term observation when performing *in vivo* bioimaging studies.[257] Although the emission in the NIR region is relatively weak, CDs have great potential for *in vivo* fluorescence tracking studies because of the biological transparency window in the NIR region, which affords maximum penetration *in vivo*.[261] Indeed, developing CDs with effective emissions in the visible and NIR regions has been described.[217,262–264]

Yang *et al.* were the first to explore the utility of CDs as contrast agents in live mice. They obtained CDs and ZnS-doped CDs from chemical processing of raw nanomaterials by laser ablation. After PEG_{1500N} modifications, they were used for *in vivo* optical imaging of mice. CDs or ZnS-doped CDs solutions

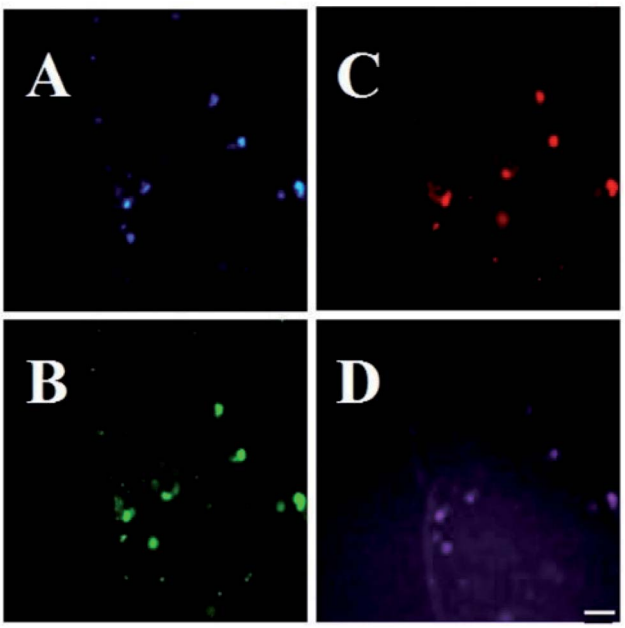

Fig. 22 Exosomes isolated from the cell culture medium of MDA-MB-231 cells treated with CNPs (2 mg mL^{-1}) for 2 h and collected after 48 h. Images were acquired with different excitation filter sets: (A) 350 nm, (B) 490 nm, (C) 550 nm and (D) 630 nm. Scale bar: 20 μm, figure reproduced from ref. 53 with permission from Elsevier, copyright 2017.

 © 2021 The Author(s). Published by the Royal Society of Chemistry

Open Access Article. Published on 08 July 2021. Downloaded on 10/31/2025 2:11:41 AM.
This article is licensed under a Creative Commons Attribution-NonCommercial 3.0 Unported Licence.

were injected into the mice body with various injection methods. The injected carbon dots in mice diffused relatively slowly, and the fluorescence faded at 24 h postinjection.[81]

As seen in Fig. 23, CDs were intravenously injected into mice for whole-body circulation. The abdomen was shaved for fluorescence detection of the dots trapped in organs during the circulation, but only emissions from the bladder area were observed. The images also show fluorescence of the dissected kidneys and liver. It was also observed that the injected CDs were removed from the body *via* the urine excretion pathway.

Furthermore, it has been noticed that blue and green emitting CDs are not suitable for *in vivo* imaging because the short-light excitation wavelength could harm living cells and biological systems.[265,266] Hence, one of the great challenges of *in vivo* bioimaging studies is to achieve efficient and safe red-light emitting CDs.[267] In studies by Liu *et al.*, the authors obtained efficient red emissive nitrogen-CDs with a good excitation-independent emission, high quantum yield (QY) (10.83% – in water and 31.54% – in ethanol), good biocompatibility and water dispersibility. Nitrogen-doped conjugated CDs were injected into nude mice and the fluorescence images were observed after 0.5, 1.0, 1.5, 3.0, and 20 h. As seen in Fig. 24, the images indicate that red-emitting CDs exhibit strong penetrability and rapid excretion from the body of mice.[263]

More recently, other studies by Li *et al.* reported the development of new CD-based materials with a second near-infrared emission (NIR-II). The designed watermelon-derived CDs exhibited high QY, great photothermal efficiency and biocompatibility. The CDs were administrated by hypodermic injection in BALB/c mice and the *in vivo* bioimaging was conducted using a NIR-II imaging apparatus (Fig. 25). Interestingly, fluorescence signals indicated the rapid renal excretion of CDs, which was associated with the particle size.[267]

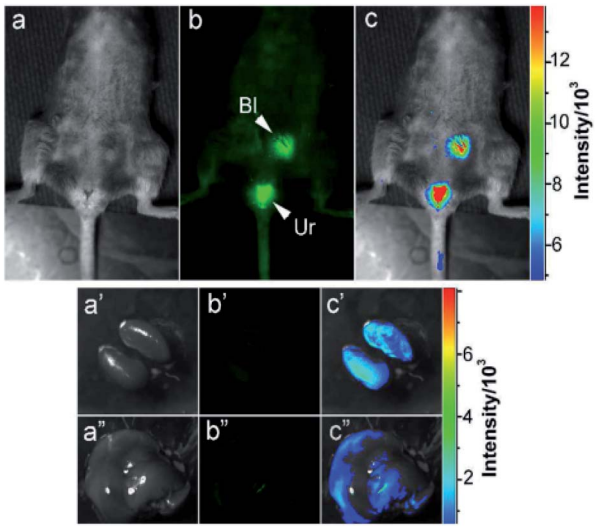

Fig. 23 Intravenous injection: (a) bright field, (b) as-detected fluorescence (Bl: bladder and Ur: urine), and (c) color-coded images. The same order for the images of the dissected kidneys (a′–c′) and liver (a″–c″). Figure reproduced from ref. 81 with permission from American Chemical Society, copyright 2009.

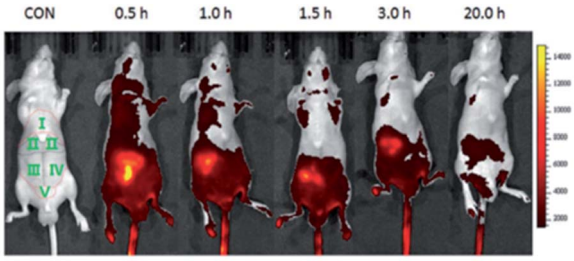

Fig. 24 Real time *in vivo* imaging of nude mice with intravenous injection of 100 μL of PBS solution of CDs-50 at different time points. (I: Thoracic region, II: area of liver, III: area of small intestine, IV: area of large intestine, V: bladder region). Figure reproduced from ref. 263 with permission from Wiley, copyright 2018.

In another *in vivo* bioimaging study, Kang *et al.* validated the use of zebrafish embryos as a model for bioimaging studies. The distribution of designed CDs from glucose was successfully observed in zebrafish embryos, indicating the selective accumulation of these nanoparticles in the eye and yolk sac (Fig. 26). Furthermore, these CDs showed low toxicity and high biocompatibility in the zebrafish model.[268]

Tathagata *et al.* obtained similar results evaluating the biolabeling potential of surface-passivated CDs from curcumin in zebrafish embryos. This biological model showed fluorescence in green, blue and in red indicating the uptake of CDs through the chorionic membrane (Fig. 27).[251]

2.4.3. Biosensing. In addition to their superior biocompatibility, CDs possess the ability to serve as either excellent electron donors or electron acceptors. By monitoring the changes in their fluorescence intensity under external physical or chemical stimuli, CDs were used to detect substances such as DNA,[269] PO_4^{3-},[270] thrombin,[271] nitrite,[272] glucose,[273] biothiol,[97] Cr^{3+},[274] Fe^{3+},[218,275] Ag^{+},[276] Hg^{2+},[97,277,278] Cu^{2+},[98,173] Cd^{2+},[275] and pH.[279] The surface functional groups on CDs indicate distinctive affinities to different target ions, which results in the quenching of PL intensity through an electron or energy transfer process and high selectivity to other ions.

The detection of heavy metals is of importance because of their hazardous effect on the environment and human health.

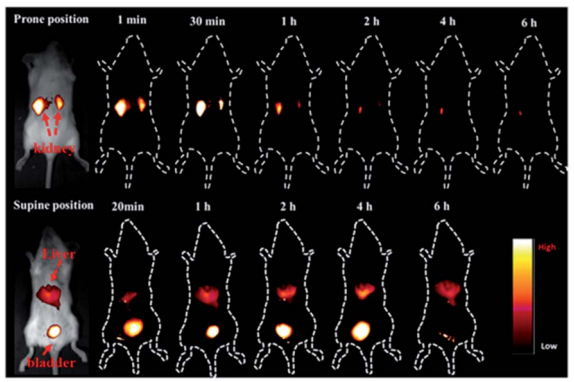

Fig. 25 Time-dependent bioimaging of mouse treated with CDs (20 μg g^{-1}) through the tail vein. Figure reproduced from ref. 267 with permission from American Chemical Society, copyright 2019.

Open Access Article. Published on 08 July 2021. Downloaded on 10/31/2025 2:11:41 AM.
This article is licensed under a Creative Commons Attribution-NonCommercial 3.0 Unported Licence.

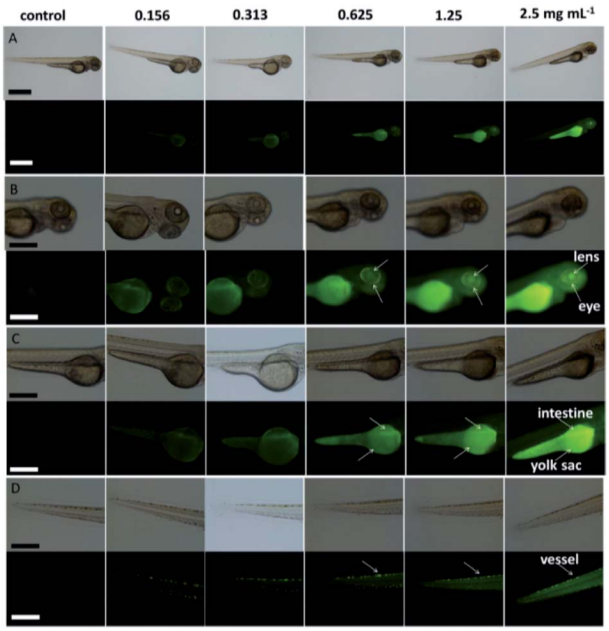

Fig. 26 Bright field (upper) and fluorescence (lower) images of (A) whole bodies, the (B) head, the (C) yolk sac, and the (D) tail of zebrafish larvae at 84 h after soaking for 10 h in CD solution of different concentrations. Enlarged images showing the (B) eye and lens, and (C) yolk sac and intestine, as well as the (D) vessel in the tail, with fluorescence images. Scale bars, 1.0 mm for (A) and 500 μm for (B), (C) and (D). Figure reproduced from ref. 268 with permission from Nature Publishing Group, copyright 2015.

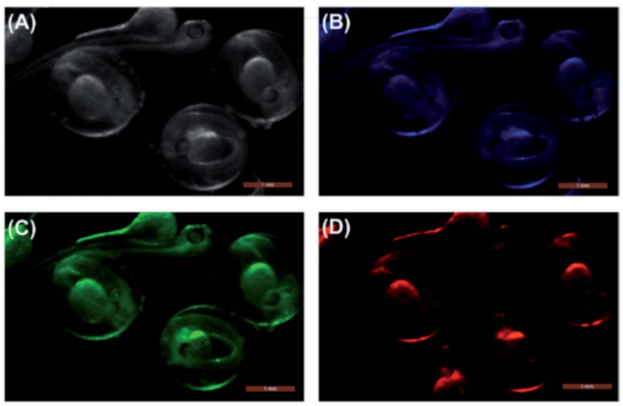

Fig. 27 Bright field (A) and multicolor fluorescence with blue (B), green (C), and red (D) images of zebrafish embryos after soaking for 24 h in 0.4 mg mL^{-1} concentration of CD solutions. Figure reproduced from ref. 251 with permission from American Chemical Society, copyright 2018.

One of the first attempts of utilizing CDs in sensing is the selective detection of Hg^{2+} in aqueous solutions[147,280] and live cells.[281]

Based on the quenching effect of Hg^{2+} on the fluorescence of CDs, Yan *et al.* adopted the Hg^{2+}-CDs system for selective detection of Hg^{2+} in aqueous solution as well as in live cells.[282] The authors reported the synthesis of two types of CDs using citric acid with *N*-(*b*-aminoethyl)-*g*-aminopropyl (CDs-1) and 1,2-ethyldiamine (CDs-2) that possess a high QY of 55.4% and 65.5 respectively. The study of the effective and selective quenching of fluorescence emissions of CDs-1 and CDs-2 by Hg^{2+}, demonstrated that both CDs acted as selective and sensitive fluorescent probes for the detection of traces of Hg^{2+} in both aqueous solutions and live cells. Upon the addition of 20 mM of Hg^{2+}, the fluorescence intensity of CDs-1 was rapidly quenched by 55%, while that of CDs-2 was quenched by 80%, and both remained stable after 1 h of observation. This confirms the feasibility of using CDs-1 and CDs-2 as chemical sensing probes for Hg^{2+}. The selectivity of CDs-1 and CDs-2 toward Hg^{2+} was then assessed by comparing the extent of fluorescence quenching of CDs-1 and CDs-2 through the addition of 20 mM of different metal ions. Among all metal ions tested, Hg^{2+} quenched the fluorescence of both CDs-1 and CDs-2 to the largest extent. However, the fluorescence was reversible and recovered by adding ethylene diamine tetraacetic acid (EDTA). Furthermore, successful attempts were made in detecting Hg^{2+} in cultured cells.[282]

Qu *et al.* reported a preparative route toward distinctive fluorescent CDs from dopamine (DA). The CDs exhibited excellent PL properties, and they were used for multicolor bioimaging and as a new kind of sensor for label-free detection of dopamine (DA) and Fe^{3+} with high sensitivity and selectivity. The method depends on Fe^{3+}-induced oxidation of the hydroquinone groups on the surfaces of CDs to the quinone species, which can quench the fluorescence of the CDs and DA due to their competition with CDs to react with Fe^{3+}. It offers a favorable protocol for rapid detection of Fe^{3+} and DA. Moreover, this sensing platform exhibits high sensitivity and selectivity toward Fe^{3+} and DA *versus* other metal ions and the other DA analogues and offers the advantages of cost efficiency, simplicity and environmentally friendliness.

Dong *et al.* designed branched poly(ethylenimine)-functionalized CDs (BPEI-CDs) as a fluorescence sensor for copper ion (Cu^{2+}) detection. On account of the inner filter effect, in that the excitation and emission wavelengths of the CDs were absorbed by the cupric amine complex formed on the surface, a quenching phenomenon would happen. Under the optimum experimental conditions, the CDs show good sensitivity and selectivity towards Cu^{2+} and the limit of detection and linear response range were determined to be 6 nM and 10–1100 nM, respectively.[280]

More interestingly, a tunable ratiometric pH sensor was developed for the quantitative measurements of the intracellular pH of cells based on CDs.[281] The amino-coated CDs were functionalized with pH-sensitive fluorescein isothiocyanate (FITC) and pH-insensitive rhodamine B isothiocyanate (RBITC), resulting in the dual-emission probe upon single excitation. The pH sensor exhibited low cytotoxicity, good cell-permeability, and excellent reversibility between pH 5–9. Thus, real-time quantitative determination of intracellular pH of intact HeLa cells and the pH fluctuations associated with oxidative stress was successfully performed.[281]

On the other hand, the π–π stacking interactions between CDs and DNA can also be used as a binding strategy for the detection of DNA.[269] The fluorescence from the dye-labeled

 © 2021 The Author(s). Published by the Royal Society of Chemistry

Open Access Article. Published on 08 July 2021. Downloaded on 10/31/2025 2:11:41 AM.
This article is licensed under a Creative Commons Attribution-NonCommercial 3.0 Unported Licence.

single-stranded DNA probe is quenched after adsorption onto the CD surface *via* π–π interactions. When the target DNA matches the dye-labeled DNA to form double-stranded DNA, the fluorescence is recovered. This strategy is also employed for the determination of metal ions such as Hg^{2+} and Ag^{+} through T–Hg^{2+}–T and C–Ag^{+}–C base pairs, respectively.[276,277]

Apart from utilizing the fluorescence of CDs as an analytical signal, recent studies have revealed that CDs exhibit good chemiluminescence (CL)[283] and electrochemiluminescence (ECL).[284] For example, Wang *et al.* developed a paper-based DNA biosensor by using CDs as CL signals and nanoporous gold (NPG) as a signal amplification agent. First, they constructed microfluidic paper-based analytical devices (μPADs). Then, the capture DNA (S1) with thiol groups was immobilized onto the μPADs. Besides, in the presence of target DNA (S2), the signal DNA (S3) could fix on the surface of μPADs by hybridization with S2. Finally, by injecting with $KMnO_4$, the CL reaction was triggered and the concentration of target DNA S2 could be easily measured in the luminescence analyzer (Fig. 28).[283]

Wu *et al.* constructed an assay for cancer cell detection by using modified CDs as ECL sensors and graphene as a signal amplification agent (Fig. 29).[284] The sensors were developed as follows: first, the electrode was modified with amino-functionalized graphene that was covalently grafting poly(allyl amine hydrochloride) (PAH) onto graphene. Then the CDs@Ag composite was introduced onto the surface of the electrode. After the thiol containing amino acid, cysteine, was linked to the C-dot@Ag surface, folic acid was further conjugated with cysteine *via* a carbodiimide-mediated wet-chemistry approach between the carboxylic acid end groups on folic acid and the amine groups on cysteine. Each modifying process played a unique and important role in the sensitivity/selectivity of the sensor: (1) the metal shell on CDs accelerated the electron transfer between CDs@Ag and graphene. (2) Folic acid could specifically target folate receptors with high affinity, which enabled them to act as a bridge between the electrode and cancer cells. (3) The graphene conjugation could facilitate electron transfer due to its good conductivity and large surface area. Due to the specificity and affinity of folic acid, the fabricated electrode could selectively recognize the surface of human cervical cancer cells (HeLa) and human breast cancer cells

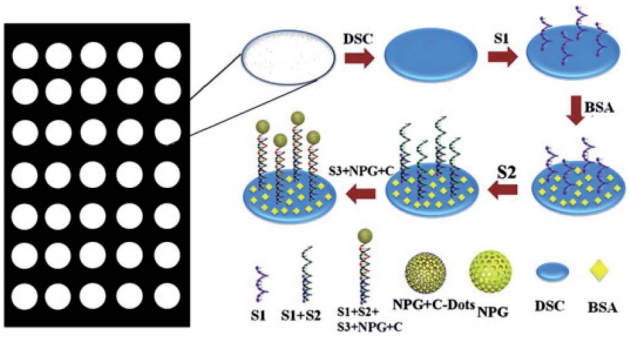

Fig. 28 The CD-based CL sensor for the detection of DNA. Figure reproduced from ref. 283 with permission from Royal Society of Chemistry, copyright 2013.

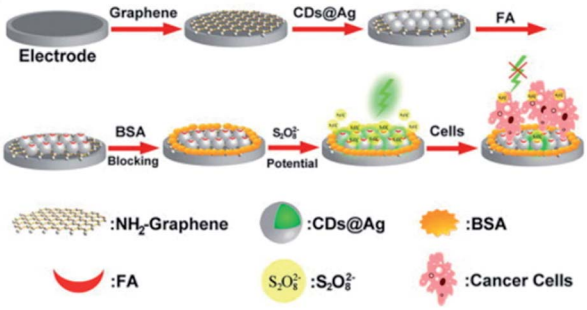

Fig. 29 The CD-based ECL platform for the detection of cancer cells. Figure reproduced from ref. 284 with permission from Royal Society of Chemistry, copyright 2013.

(MCF-7) by targeting the folate receptor (FR). The presence of cancer cells caused a remarkable decrease in the ECL signal which originated from the blocking of the CDs@Ag nanocomposite surface and preventing them from coming into contact with the ECL coreactant $N_2S_2O_8$. The detection limit was calculated to be 10 cells per mL at 3σ.

On the other hand, it is known that plant part-derived CDs can be used as biosensors to detect various bioactive molecules, including proteins, nucleic acids, enzymes, amino acids, vitamins, bacteria, thiols group, drugs, metal ions and biological samples.[285] Based on Chromium (Cr) toxicity, Roshni *et al.* used CDs from ground nuts (N-CDs) to detect Cr^{6+}. N-CDs showed a selective activity towards Cr^{6+} with a detection limit (LOD) of 0.1 mg L^{-1}. The methodology was carried out in the presence of Cr^{3+} and glutathione as a reducing medium for the conversion of Cr^{4+} to Cr^{3+},[286] which is considered one of the least toxic micronutrients for humans.[287]

In another study, Monte-Filho *et al.* used CDs derived from onion juice and lemon for the detection of riboflavin (vitamin B2). The selectivity of the CDs for the detection of riboflavin was tested with diverse substances, indicating that CDs were selective for riboflavin. Moreover, the CDs exhibited a good linear relationship between the fluorescence resonance energy transfer and the riboflavin concentration, suggesting the development of an analytical method for the determination of riboflavin in multivitamin and mineral supplements.[288]

Ahmadian-Fard-Fini *et al.* were able to detect *E. coli* by using a fluorescence sensor of CDs derived from grapefruit extracts and lemon. Fluorescence signals from various concentrations of *E. coli*-labeled CDs were observed. Furthermore, the authors were able to measure unknown concentrations of *E. coli*.[289]

2.4.4. Drug-carrier development. CDs are excellent drug delivery systems (DDSs) due to their simple fabrication techniques, particle size, biocompatibility, lower cytotoxicity and sustained drug release.[74] CDs overcome the problems of conventional drug carriers; in fact, multicolor fluorescence CDs are considered excellent drug carriers because of their modified functional groups, maximum drug-loading capacity and low cytotoxicity.[76,290]

The most widely investigated DDSs are based on AuNPs, but their toxicity limits their applications in clinical therapy.[291]

Open Access Article. Published on 08 July 2021. Downloaded on 10/31/2025 2:11:41 AM.
This article is licensed under a Creative Commons Attribution-NonCommercial 3.0 Unported Licence.

Therefore, CDs serve as good alternatives to AuNPs since different functionalizations could result in many possibilities for conjugation with drug molecules in combination with targeting agents, expanding the drug choices for delivery.[292] Tang *et al.* reported a Förster resonance energy transfer (FRET)-based CD drug delivery system that could perform real-time monitoring of drug release (Fig. 30).[258] The authors used the fluorescent drug molecule doxorubicin (DOX). The DOX adsorbed onto the surface of CDs *via* π–π stacking. Then FRET occurred between the CDs and DOX, which resulted in a decrease of the FL of CDs and an increase of the FL of DOX. With the release of DOX from the surface of CDs, FRET between CDs and DOX was weakened while the FL of CDs increased, which could be used to monitor the release of DOX.[258]

The obtained system showed excellent targeted delivery and drug release efficiency towards cancer cells in acidic pH environments. At pH 7.4, the fluorescence barely increases over the course of 72 h, exhibiting a very low value of total release (<10% fluorescence intensity of the original CDs-FA-DOX conjugates); this indicates a negligible DOX release under the neutral conditions. A substantial increase of the drug release rate is observed for acidic solutions, in which the release rate in pH 5.0 solution is higher than that in pH 6.0 solution. In addition, compared with those of free DOX molecules, which complete release within ≈10 h, the release accumulation profiles for both pH 5.0 and 6.0 solutions show sustained release over a long period (>72 h). The percentages of accumulated release in the pH 5.0 solution are 55%, 72%, and 78% after 24, 48, and 72 h, respectively.[258]

This enhanced drug release rate at low pHs is particularly advantageous for cancer treatment. The slow DOX release in neutral environments can minimize the extracellular loss of drug molecules before reaching the tumor targets, as well as potential damage to normal cells. However, most of the DOX can persistently be released when the drug delivery capsules are internalized by tumor cells at low pHs (4.5–6.0), leading to enhanced cancer therapy.

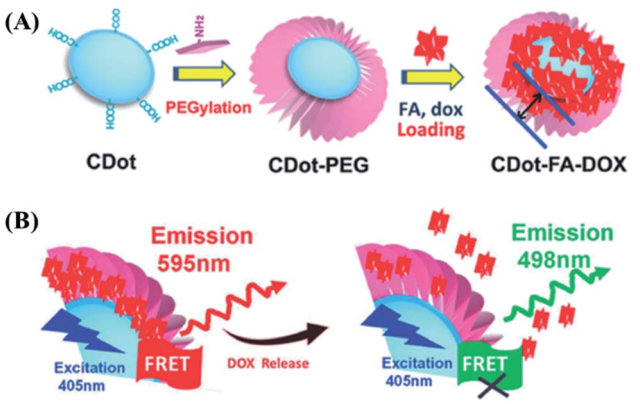

Fig. 30 (A) The drug delivery system that could perform real-time monitoring of drug release based on PEG-functionalized CDs. Doxorubicin (DOX) was used as a drug molecule, which was adsorbed onto the surface of CDs through π–π stacking; (B) proposed mechanism of real-time monitoring of DOX release based on the FRET process between DOX and CDs. Figure reproduced from ref. 258 with permission from Wiley, copyright 2013.

More recently, our group developed CDs with a carboxyl-rich surface which can be utilized as a trackable drug delivery.[53] The CDs are conjugated with doxo, *via* electrostatic interactions between the carboxyl groups of CDs and the amine group of DOXO molecules. The pH difference between cancer and normal cells was exploited as the triggering mechanism for DOXO release. The CDs maintained a stable interaction with doxo at alkaline pH with a slow-release profile, compared to a fast release profile when the medium was acidified to levels of the extracellular space of the tumor and in subcellular compartments (Fig. 31A). Subsequently, the cell viability of breast (MDA-MB-231), and colon (LoVo and DLD-1) cancer cell lines treated with CD loaded doxo (Cdoxo) exhibited better cytotoxicity than free doxo in MDA-MB-231 and DLD-1 cells. An *in vivo* study followed over a period of approximately 2 months did not show any symptoms of stress or clinical illness. The body weight of the mice increased during the observational period (Fig. 31B). Cdoxo-treated mice demonstrate that the tumor volume was reduced compared to the tumors of mice treated with free doxo (Fig. 31C).[53]

In view of the future use of a fully biocompatible drug delivery nano-system, we further optimize the hydrothermal synthesis of CDs to avoid the formation of harmful chemical compounds starting from fructose (F-CDs), glucose (G-CDs) and ascorbic acid (A-CDs), without any passivating or doping additives.[155] Interestingly, the cytotoxicity of the CDs was affected by the choice of the starting materials: CDs synthesized from fructose were found to be toxic (due to the presence of toxic furanic compounds/frameworks formed during the hydrothermal degradation of the fructose precursor) while high biocompatibility was observed starting from glucose or ascorbic acid. Finally, the CD drug loading capabilities were evaluated by studying their interactions with DOX as a model. The study revealed the importance of the graphitic core domains, rather than the surface functional groups, in achieving high CDs-DOX affinities F-CDs > G-CDs ≫ A-CDs (Fig. 32A). With the more suitable glucose derived CDs, up to 28% w/w of DOX loading was observed (Fig. 32B).

Similarly, a theragnostic nanomedicine (CDs-oxa) was synthesized by a condensation reaction between the amino groups on the surface of fluorescent CDs and the carboxyl group of the oxaliplatin derivative oxa(IV)–COOH. The CDs-oxa was taken up by cancer cells through endocytosis and the drug was released upon the reduction of oxa(IV)–COOH to oxaliplatin(II) because of the highly reducing environment in cancer cells. It was also demonstrated that the distribution of the CDs-oxa can be closely tracked by monitoring the fluorescence signal of the CDs, thereby offering great help in the customization of the injection time and dosage of the medicine (Fig. 33).[293]

In an attempt to enhance the loading capacity of CDs, Mewada *et al.* tested the drug carrying and folic acid-mediated delivering capacities of highly fluorescent swarming CDs. Folic acid on the CD surface was used as a navigational molecule due to its association with different types of cancer cells. The drug loading capacity for DOX was estimated to be 86% and the

 © 2021 The Author(s). Published by the Royal Society of Chemistry

Open Access Article. Published on 08 July 2021. Downloaded on 10/31/2025 2:11:41 AM.
This article is licensed under a Creative Commons Attribution-NonCommercial 3.0 Unported Licence.

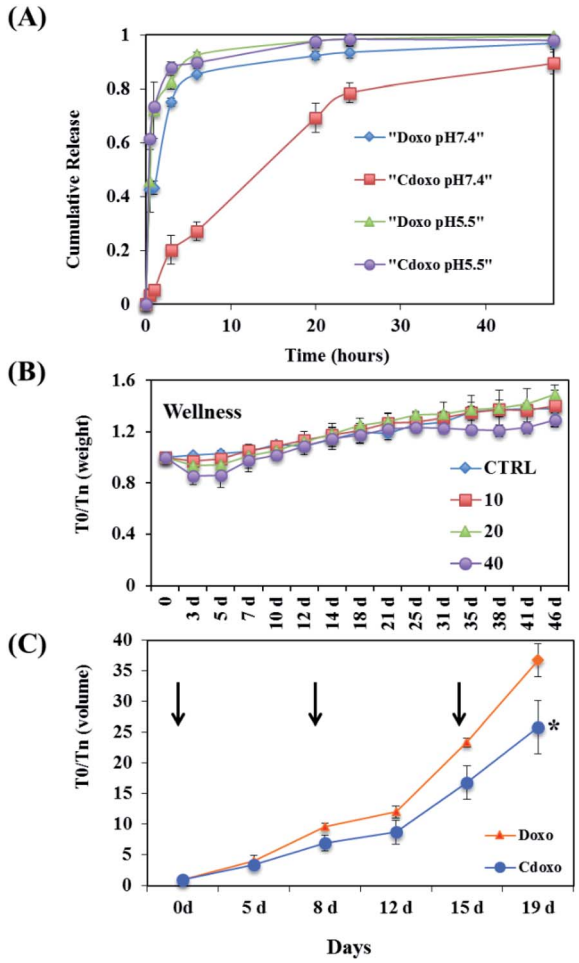

Fig. 31 (A) Release of doxo from CDs. The cumulative release of doxo was evaluated by measuring the fluorescence of doxo, which resides inside the dialysis membrane at each time point at pH 5.5 and 7.4; (B) weight of mice treated with different concentrations (mg kg^{-1}) of CNPs as indicated; (C) mice were treated 3 times (arrows) at 3 mg kg^{-1} Cdoxo or free doxo, and the tumor volume was measured (*y*-axis) **p* value < 0.05. Figure reproduced from ref. 53 with permission from Elsevier, copyright 2017.

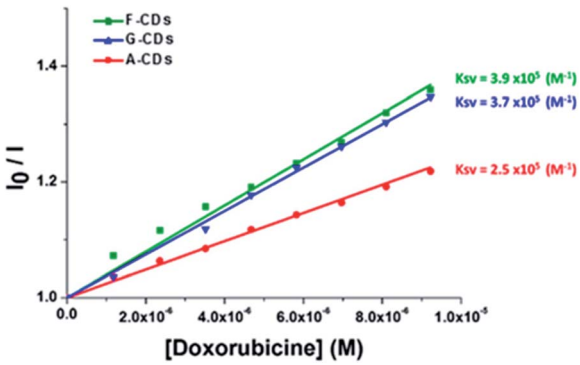

Fig. 32 Stern–Volmer plots of the relative emission intensities (λ_{ex} = 340 nm, λ_{em} = 441 nm) of CDs (0.25 mg mL^{-1}) as a function of the DOX concentration. Figure reproduced from ref. 155 with permission from American Chemical Society, copyright 2018.

release of DOX from the DOX-loaded CDs followed first order release kinetics. Furthermore, due to the targeting ability of the folic acid molecule, CDs loaded with DOX showed greater cytotoxicity to cancer cells than free DOX.[294]

Similarly, other researchers have also used CDs loaded with DOX. Wang *et al.* reported that DOX-conjugated beer CDs (DOX-BCDs) exerted a prolonged drug release profile towards MCF-7 cells. The analysis of the results confirmed the internalization of DOX-BCDs by cells and showed that DOX-BCD induced a greater cytotoxic effect than single DOX treatment.[295] On the other hand, Zeng *et al.* developed green-emitting CDs by conjugating the amine moiety of DOX and native carboxyl groups present on the surface of CDs *via* non-covalent bonding. *In vitro* and *in vivo* studies indicated that these CDs are stable cancer drug delivery systems. Furthermore, DOX-CD conjugates showed low toxicity and selectivity towards cancer cells.[52]

According to the different studies reported, functional groups on the surface of the CDs render them potential non-toxic candidates in targeted drug delivery. Furthermore, their fluorescence properties allow a simultaneous analysis of drug distribution and their therapeutic functions.[74,258,294–296]

2.4.5. Gene transfer. Gene therapy is a promising alternative for the treatment of many pathological disorders. This experimental technique requires an efficient and safe carrier for the delivery of biocompatible therapeutic loads with fluorescence properties.[74] In this context, the properties of CDs make them efficient emerging carriers for cellular uptake monitoring and gene delivery. Gene therapy includes the use of pDNA, mRNA, and noncoding RNAs, which can be internalized by endocytosis[297] (Fig. 34).[298]

In a study by Liu *et al.*, the authors utilized polyethylenimine (PEI) passivated CDs as transfection agents. Fluorescence properties of CDs allowed the observation of the plasmid DNA distribution during transfection, providing detailed information on the physiological function of plasmid DNA.[261] Kim *et al.* also performed a DNA transfection and monitored the trafficking of cellular plasmids. The authors compared the gene delivery ability of plasmid DNA (pDNA), PEI-functionalized CDs (PEI-CDs) and PEI-functionalized gold colloids (PEI-AU). Quantitative analysis of the cellular uptake and dissociation of pDNA from the nanoassembly indicated that the fluorescence intensity of PEI-CD remained stronger compared to that of PEI-AU at the onset of cellular uptake. However, the authors reported that both the carrier systems could provide a highly

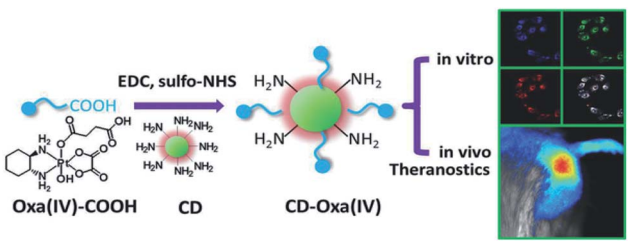

Fig. 33 Synthetic scheme for CDs-oxa (CD-oxa) and its applications in bioimaging and theranostics. Figure reproduced from ref. 293 with permission from Wiley, copyright 2014.

Open Access Article. Published on 08 July 2021. Downloaded on 10/31/2025 2:11:41 AM.
This article is licensed under a Creative Commons Attribution-NonCommercial 3.0 Unported Licence.

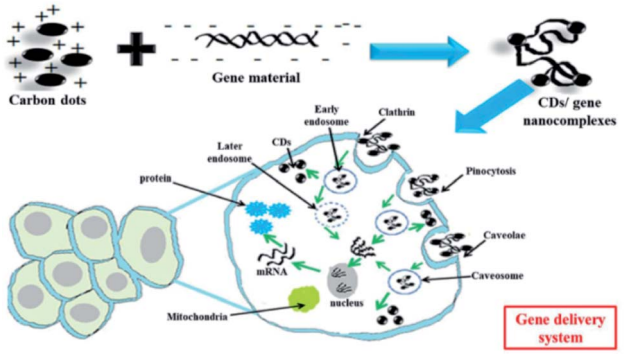

Fig. 34 General mechanisms of gene delivery *via* CDs: here, CDs bind gene materials *via* electrostatic interactions, enter the cells *via* endocytosis and release the payloads into the nucleus. Figure reproduced from ref. 298 with permission from BMC, copyright 2019.

intriguing method to monitor the dissociation of polyplex inside of the cytoplasm.[299]

Recently, Zhang *et al.* developed hyaluronic acid (HA)/PEI functionalized CDs (HP-CDs) for gene therapy in cancer cells. The HP-CDs showed an excellent gene condensation capacity, low toxicity and biocompatibility. The HP-CDs were internalized into cancer cells *via* HA-receptor-mediated endocytosis indicating a high transfection efficiency.[300]

Additionally, Chen *et al.* studied the impact of gene therapy on mesenchymal stem cells (EMSCs) using different CDs derived from porphyra polysaccharide. The CDs were loaded with a combination of transcription factors Ascl1 and Brn2 (CDs-pDNA NPs). The results revealed an efficient neuronal differentiation of the EMSCs with CDs-pDNA NPs compared with the retinoic acid-containing induction medium.[301] Another study by Ghafary *et al.* synthesized a nano-carrier using CDs conjugated with a chimeric peptide MPG-2H1 and DNA loading (CDs-MPG-2H1) to obtain two different color emissions (red and green). The nanocomplexes increased the gene internalization in the cells, showing that this carrier has a high potential for increasing nuclear internalization.[302]

It is known that the siRNA delivery is one of the best strategies for treating incurable diseases due to its efficiency of intracellular delivery.[303] In this context, Dong *et al.* studied poly(L-lactide)-polyethylene glycol (PLA)-CDs and PEG-CDs as nanocomplexes for simultaneous gene delivery and intracellular miRNA bioimaging. The results showed that CDs conjugated with PLA or PEG provide a nanocomposite with low cytotoxicity and stable photoluminescence. Furthermore, using the HeLa cell line as a model, the authors reported that carriers exhibited an effective miRNA delivery.[304] Moreover, Wu *et al.* investigated the effect of folate-conjugated reducible PEI-passivated CD for lung cancer treatment. The nanocomplexes were loaded with two types of siRNA (EGFR and cyclin B1). The results indicated that the carriers were accumulated into cancer cells and induced the silencing of the targeted gene.[305]

2.4.6. Diagnosis and clinical prognosis. Imaging analysis has an important role in diagnosis and prognosis of certain pathologies. In this sense, the use of fluorescent nanoparticles as imaging probes is one of the best strategies. Notably, studies on the favorable properties of CDs have shown wide-spread research interest owing to their their practical application in the fields of cell imaging and drug delivery.[257]

Based on the ability of CDs to absorb NIR light, Wu *et al.* first conducted photoacoustic (PA) imaging of sentinel lymph nodes (SLN) *in vivo* by using CDs passivated by macromolecules. Observable signal enhancement of the SLN was exceptionally rapid within 2 min after injection of the agent. This nanoprobe exhibited strong optical absorption in the NIR region, a small size, and rapid lymphatic transport, offering valuable potential for faster resection of SLN, and may lower complications caused by using dyes or low-resolution imaging techniques.[306]

The CDs can be used for photodynamic therapy (PDT). PDT is an approved therapeutic treatment for certain types of cancers. In the presence of oxygen and light, photosensitizers (PSs) can transfer the absorbed photon energy to surrounding oxygen molecules to form reactive oxygen species (ROS) such as singlet oxygen ($^1O_2$) and free radicals, resulting in cell death and tissue destruction. Huang *et al.* designed a PS-conjugated C-dot system featuring FRET for both enhanced fluorescence imaging and PDT therapy. Chlorin e6 (Ce6) was selected as the PS, which emitted bright red fluorescence at 668 nm upon excitation at 430 nm due to the efficient FRET process with carbon dots. The feasibility of the system for fluorescence imaging-guided PDT was investigated in nude mice. After intravenous injection, the fluorescence from Ce6 became visible in tumor sites at 2–4 h post-injection and reached a plateau at 4–8 h post-injection, and thus the suitable time point to implement PDT was selected at 8 h (Fig. 35).[307]

In addition to phototherapy, CDs can be used for radiotherapy. Kleinauskas *et al.* developed PEG-CDs coated with a silver shell (C–Ag–PEG CDs) which could be used as radiosensitizers in DU145 cells.[308] When irradiated with low energy X-rays, electrons were ejected from the C–Ag–PEG CDs, which in turn generates free radicals and damages the cancer cells surrounding the CDs, reducing the damage of normal cells and increasing therapeutic selectivity.

Diagnosis of infectious diseases caused by microorganisms such as viruses, fungi, parasites or bacteria is another area of CD applications due to their photodynamic effects that induce antimicrobial photodynamic inactivation (PDI). The mechanism of action of PDI treatment is based on nonspecific oxidative damage to the cell membrane and biomolecules

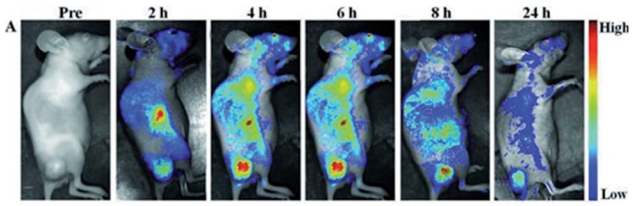

Fig. 35 Real-time *in vivo* NIR fluorescence images after intravenous injection of CDs-Ce6 in nude mice at different time points. Figure reproduced from ref. 307 with permission from Wiley, copyright 2012.

 © 2021 The Author(s). Published by the Royal Society of Chemistry

Open Access Article. Published on 08 July 2021. Downloaded on 10/31/2025 2:11:41 AM. This article is licensed under a Creative Commons Attribution-NonCommercial 3.0 Unported Licence.

(nucleic acids, proteins and lipids), decreasing resistance by target microorganisms. ROS formation in PDI treatment is through excitation of photosensitizers with an appropriate wavelength. In this context, CDs are considered excellent photosensitizers for PDI treatment by photoinduced production of ROS, which depends on the functional groups on the surface, the optical properties and the photoexcited state of CDs.[309]

Several studies have demonstrated that EDA-CDs under visible/natural light could effectively inhibit *E. coli* cells. The antibacterial activity of these CDs was attributed to the photodynamic effects of these nanoparticles.[310,311] Likewise, Li *et al.* reported that synthesized CDs by an electrochemical method with vitamin C show a broad-spectrum antibacterial activity against *Bacillus* sp, *E. coli*, ampicillin-resistant *E. coli*, *S. aureus* and *B. subtilis*. Furthermore, the authors observed that these CDs also showed an antifungal effect against *R. solani* and *P. grisea*.[312] In another reported study, Priyadarshini *et al.* demonstrated the antifungal potential of CDs and their derived conjugates against *C. albicans*.[313]

Although few studies have reported the use of CDs in antiviral treatment, Huang *et al.* found that CDs synthesized from benzoxazine (BZM-CDs) inhibited the infection of Japanese encephalitis, Zika, and dengue viruses. The results indicated that BZM-CDs could directly bind to the surface of the virion and inhibit cell-virus interaction.[314] Łoczechin *et al.* also found an antiviral effect of seven different CDs to human coronavirus HCoV-229E infection. The mechanism of action of these CDs revealed the inhibition of HCoV-229E by interactions of the functional groups of the CDs with HCoV-229E receptors. In general, these results could help replace the use of conventional antivirals with less inhibitory activity.[315]

According to previously published reports, CDs could be a useful tool for the treatment and diagnosis of diseases.

2.5. Theranostic approach in cancer treatment

In cancer treatment, chemotherapy, radiation, and surgery have certain limitations because one treatment pathway cannot address all types of cancer.[316] Tumor theranostics focuses on developing new structures that are biocompatible and biodegradable and able to perform efficient target therapy.[317] Currently, several types of theranostic nanoparticles have been developed for treating cancer, however not all are efficient and safe.[318] In this respect, carbon dots are considered potential candidates for developing tumor theranostic due to the physicochemical and optical properties described above. Indeed, compared with other existing theranostic agents such as and metal–organic framework (MOF)-based nanomedicine, lipidosomes and polyester micelles, CDs possess a series of advantages that include low cytotoxicity, biocompatibility and stable photoluminescence.[319–321] Consequently, CDs have been recognized as effective tumor theranostic agents for *in vivo* imaging and tumor therapy (Table 1).[322]

2.5.1. Photodynamic therapy (PDT) and photothermal therapy (PTT). The study and development of CDs for PDT and PTT have increased in recent years. As previously described, through PDT, CDs can destroy cancer cells by reactive oxygen species, which were produced from surrounding oxygen under the excitation of light with the corresponding wavelength.[330] In addition, PDT offers low toxicity and minimal invasiveness.[331] Therefore, this therapy has gained a lot of significance because it acts on multi-drug resistant cancers and could replace conventional chemotherapy.[332,333] In a study by Xie *et al.* the authors synthetized porphyrin-containing carbon dots which showed intrinsic photodynamic capacity upon photo-irradiation. Furthermore, the porphyrin-CDs exhibited high cellular uptake, potent cytotoxicity, good photostability and biocompatibility.[93] On the other hand, Zhou *et al.* prepared CDs from fresh tender ginger juice with good biocompatibility. The CDs showed selective cytotoxic activity towards HepG2 cells through high ROS production. However, these CDs were also cytotoxic to the normal liver cell (FL83B) and normal mammary epithelial cell (MCF-10A) lines.[334] Another study by He and *et al.* indicated that using a one-pot hydrothermal method to synthesize diketopyrrolopyrrole (DPP)-based fluorescent CDs with DPP and chitosan as precursors, the DPP-CDs could not only generate singlet oxygen ($^1O_2$) but also had excellent hydrophilic properties and biocompatibility. Moreover, the DPP-CDs inhibited tumor growth *in vitro* and *in vivo* with laser irradiation (540 nm).[92]

From a theranostic point of view, photothermal therapy (PTT) is also known as hyperthermia or thermal ablation therapy. PTT, which is used as a diagnostic and treatment strategy, uses electromagnetic radiation in the infrared (IR) region to convert the absorbed energy into heat and provides high specificity analysis and minimal invasiveness.[335,336] Carbon dots are considered attractive as photothermal agents because they contain many π electrons and behave similarly to the free electrons of metallic nanomaterials.[84] In a study by Zheng and *et al.* the researchers synthesized multifunctional theranostic CDs (named CyCD) *via* a solvothermal process. CDs exhibited an excellent PTT efficiency and the *in vitro* studies revealed that the viabilities of CT26 and HepG2 cell lines were decreased in the presence of CyCDs.[337] Another study by Nurunnabi *et al.* indicated that carboxylated photoluminescent graphene nanodots (cGDs) activated by NIR laser irradiation form electron clouds to produce heat (>50 °C) and decrease cell viability ~70% of MDA-MB 231 cancer cells by thermal ablation.[338] Bao X. *et al.* showed that after an *in vivo* injection of CDs, the PTT significantly inhibited the growth of tumor and prolonged the life of mice.[339] On the other side, some *in vitro* studies have demonstrated that chemotherapy combined with PTT is better at killing cancer cells than monotherapy.[75,340]

Although there are some advantages of PDT and PTT in cancer treatment, there are still some difficulties in their practical application. For instance, the hypoxic environment in tumors limits the therapeutic efficacy of PDT and the use of PTT damages the normal tissue around the tumor.[322,341,342] Therefore, many major challenges must be overcome.

2.5.2. Receptor-mediated therapy. Tumor-targeted CDs can specifically bind to receptors overexpressed on the cancer cell membrane.[322,343] Indeed, the receptor-mediated therapy of CDs is important for drug delivery.[322] Jianping Li *et al.* showed that hyaluronic acid (HA)-modified carbon dots (HA-CDs)

Open Access Article. Published on 08 July 2021. Downloaded on 10/31/2025 2:11:41 AM.
This article is licensed under a Creative Commons Attribution-NonCommercial 3.0 Unported Licence.

Table 1 Some theragnostic agents based on CDs[a]

Complexes-CDs	Biological activity	Ref.
CDs from HA	Preservation of the HA functionality, which has high specific affinity for CD44 receptors overexpressed on the surfaces of many cancer cells	323
FA/DOX-CDs	The system facilitates the real-time monitoring of the drug release based on the fluorescence signal	258
CDs-DOX loaded into PEG citosan nanogels	High therapeutic efficacy through the synergistic effect of combined chemophotothermal treatments	324
CDs-$MnFe_2O_4$/DOX-4 carboxyl phenylboronic acid	Acts as a cancer cell-specific targeting ligand. Effective fluorescent markers in an *in vivo* experiment. Moreover, it also showed the controlled release manner of DOX at low pH values	325
CDs-DOX/biodegradable charged polyester vectors (BCPVs)/siRNA	The heat generated enhanced the anticancer activity of the nanocomplexes which triggered the release of DOX from complexes	326
CDs-PEGFA/ZnPc or R780 iodide or Ce6	The targeting of ZnPc/CDs-PEGFA was evaluated by monitoring the blue and red fluorescence of CDs. The PDT on the HeLa cells was also demonstrated	327–329

[a] Abbreviations: HA: hyaluronic acid, FA: folic acid, ZnPc: zinc phthalocyanine.

obtained by hydrothermal treatment with branch-poly(ethylene mine) and citric acid specifically binds to CD44, which is overexpressed in several cancer cells. Furthermore, in this study the antitumor effect of HA-CDs was observed in diverse tumor models, which gives it a good application prospect for targeted cancer therapy.[323]

Although several studies are focusing on receptor-based tumor therapy, accumulating evidence suggests that this strategy has several important limitations because some receptors are present in both cancer cells and normal cells. In addition, different types of cancer cells may not be targeted using the same ligand.[322,344,345]

3. Conclusions

The unique physicochemical properties of carbon nanomaterials allow them to incorporate targeting ligands, chemotherapeutic drugs, and many other therapeutic agents making them suitable for certain imaging and therapeutic applications. This urges us to establish closer interdisciplinary connections between nanotechnology, biology, and medicine in order to develop more powerful and useful tools for biologists and clinicians. Although carbon dots are considered multifunctional and low-toxicity or non-toxic nanoparticles, there are some problems associated with their use, including synthesis methods, and control over their size and surface properties, which could cause interferences in their biological applications. Nevertheless, the strong optical absorption of carbon dots allows for photothermal and photodynamic therapies that harness the absorbed photons for selective destruction of malign microorganisms and tumors through targeted drug delivery and diagnostic imaging. With the many new avenues and opportunities offered by the unique properties of CDs, we envisage the future of such nanomaterials with an optimistic outlook. In this review paper, we have provided a comprehensive coverage of recent progress in biological imaging and nanomedicinal therapy using a variety of CDs. The CD synthesis, the resulting optical properties and the recent knowledge related to the structural–luminescence relationship have also been discussed.

Overall, there is potential for the future clinical usage of CD nanomaterials. With the multi-functionality of these materials and taking advantage of their low cost and low environmental impacts, high water solubility, biocompatibility, low toxicity, good cell permeability, excellent sensitivity of fluorescent imaging and easy conjugation with therapeutics, future developments should enable the development of versatile theranostic applications for the treatment of cancer and other diseases in the near future.

Author contributions

Samer Bayda – preparation, creation and/or presentation of the published work, specifically writing the initial draft. Emanuele Amadio – preparation, creation, data curation, and interpretation of the data. Simone Cailotto – Preparation, review – including pre- or post-publication stages. Yahima Frión-Herrera – preparation, review – including pre- or post-publication stages. Alvise Perosa – review – including pre- or post-publication stages. Flavio Rizzolio – ideas, formulation, or evolution of overarching research goals and aims, and review – including pre- or post-publication stages.

Conflicts of interest

There are no conflicts to declare.

Acknowledgements

This work was financially supported by Fondazione AIRC per la Ricerca sul Cancro (Grant AIRC IG23566) and SPIN – Supporting Principal Investigators, Ca' Foscari University of Venice, Italy.

References

1 GLOBOCAN 2018: estimated cancer incidence, mortality and prevalence worldwide in 2018, World Health Organization.

 © 2021 The Author(s). Published by the Royal Society of Chemistry

Open Access Article. Published on 08 July 2021. Downloaded on 10/31/2025 2:11:41 AM.
This article is licensed under a Creative Commons Attribution-NonCommercial 3.0 Unported Licence.

2 European Science Foundation's Forward look Nanomedicine: An EMRC Consensus Opinion.
3 D. Peer, J. M. Karp, S. Hong, O. C. Farokhzad, R. Margalit and R. Langer, Nanocarriers as an emerging platform for cancer therapy, *Nat. Nanotechnol.*, 2007, **2**, 751–760.
4 F. J. Picard and M. G. Bergeron, Rapid molecular theranostics in infectious diseases, *Drug Discovery Today*, 2002, **7**, 1092–1101.
5 N. K. Aaronson, S. Ahmedzai, B. Bergman, M. Bullinger, A. Cull, N. J. Duez, A. Filiberti, H. Flechtner, S. B. Fleishman, J. C. J. M. d. Haes, S. Kaasa, M. Klee, D. Osoba, D. Razavi, P. B. Rofe, S. Schraub, K. Sneeuw, M. Sullivan and F. Takeda, The European Organization for Research and Treatment of Cancer QLQ-C30: A Quality-of-Life Instrument for Use in International Clinical Trials in Oncology, *JNCI, J. Natl. Cancer Inst.*, 1993, **85**, 365–376.
6 C. Granchi, F. Rizzolio, V. Bordoni, I. Caligiuri, C. Manera, M. Macchia, F. Minutolo, A. Martinelli, A. Giordano and T. Tuccinardi, 4-Aryliden-2-methyloxazol-5(4H)-one as a new scaffold for selective reversible MAGL inhibitors, *J. Enzyme Inhib. Med. Chem.*, 2016, **31**, 137–146.
7 T. Tuccinardi, C. Granchi, F. Rizzolio, I. Caligiuri, V. Battistello, G. Toffoli, F. Minutolo, M. Macchia and A. Martinelli, Identification and characterization of a new reversible MAGL inhibitor, *Bioorg. Med. Chem.*, 2014, **22**, 3285–3291.
8 G. Poli, T. Tuccinardi, F. Rizzolio, I. Caligiuri, L. Botta, C. Granchi, G. Ortore, F. Minutolo, S. Schenone and A. Martinelli, Identification of New Fyn Kinase Inhibitors Using a FLAP-Based Approach, *J. Chem. Inf. Model.*, 2013, **53**, 2538–2547.
9 C. Manera, G. Saccomanni, A. M. Malfitano, S. Bertini, F. Castelli, C. Laezza, A. Ligresti, V. Lucchesi, T. Tuccinardi, F. Rizzolio, M. Bifulco, V. Di Marzo, A. Giordano, M. Macchia and A. Martinelli, Rational design, synthesis and anti-proliferative properties of new CB2 selective cannabinoid receptor ligands: an investigation of the 1,8-naphthyridin-2(1H)-one scaffold, *Eur. J. Med. Chem.*, 2012, **52**, 284–294.
10 E. L. Cooper, in *Trends in Innate Immunity. Contrib Microbiol.*, ed. A. Egesten, A. Schmidt and H. Herwald, Karger, Basel, 2008, vol. 15, pp. 1–11.
11 P. Ehrlich, Address in Pathology, ON CHEMIOTHERAPY: Delivered before the Seventeenth International Congress of Medicine, *BMJ*, 1913, **2**, 353–359.
12 H. Ringsdorf, Structure and properties of pharmacologically active polymers, *J. Polym. Sci., Polym. Symp.*, 2007, **51**, 135–153.
13 R. Duncan and J. Kopeček, Soluble synthetic polymers as potential drug carriers, *Advances in Polymer Science*, Springer Berlin Heidelberg, 1984, pp. 51–101.
14 R. Duncan and F. Spreafico, Polymer Conjugates, *Clin. Pharmacokinet.*, 1994, **27**, 290–306.
15 F. F. Davis, The origin of pegnology, *Adv. Drug Deliv. Rev.*, 2002, **54**, 457–458.
16 P. P. Speiser, Non-liposomal nanocapsules, methodology and application, *Front. Biol.*, 1979, **48**, 653–668.
17 J. Kreuter and P. P. Speiser, *In Vitro* Studies of Poly(methyl Methacrylate) Adjuvants, *J. Pharm. Sci.*, 1976, **65**, 1624–1627.
18 P. Couvreur, P. Tulkenst, M. Roland, A. Trouet and P. Speiser, Nanocapsules: A new type of lysosomotropic carrier, *FEBS Lett.*, 1977, **84**, 323–326.
19 A. D. Bangham, Lipid Bilayers and Biomembranes, *Annu. Rev. Biochem.*, 1972, **41**, 753–776.
20 G. Gregoriadis, P. D. Leathwood and B. E. Ryman, Enzyme entrapment in liposomes, *FEBS Lett.*, 1971, **14**, 95–99.
21 D. Papahadjopoulos, E. Mayhew, G. Poste, S. Smith and W. J. Vail, Incorporation of lipid vesicles by mammalian cells provides a potential method for modifying cell behaviour, *Nature*, 1974, **252**, 163–166.
22 S. Palazzolo, S. Bayda, M. Hadla, I. Caligiuri, G. Corona, G. Toffoli and F. Rizzolio, The Clinical translation of Organic Nanomaterials for Cancer Therapy: A Focus on Polymeric Nanoparticles, Micelles, Liposomes and Exosomes, *Curr. Med. Chem.*, 2018, **25**, 4224–4268.
23 S. Palazzolo, M. Hadla, C. R. Spena, S. Bayda, V. Kumar, F. Lo Re, M. Adeel, I. Caligiuri, F. Romano, G. Corona, V. Canzonieri, G. Toffoli and F. Rizzolio, Proof-of-Concept Multistage Biomimetic Liposomal DNA Origami Nanosystem for the Remote Loading of Doxorubicin, *ACS Med. Chem. Lett.*, 2019, **10**, 517–521.
24 L. Gros, H. Ringsdorf and H. Schupp, Polymeric Antitumor Agents on a Molecular and on a Cellular Level?, *Angew Chem. Int. Ed. Engl.*, 1981, **20**, 305–325.
25 M. Yokoyama, M. Miyauchi, N. Yamada, T. Okano, Y. Sakurai, K. Kataoka and S. Inoue, Characterization and anticancer activity of the micelle-forming polymeric anticancer drug adriamycin-conjugated poly(ethylene glycol)-poly(aspartic acid) block copolymer, *Cancer Res.*, 1990, **50**, 1693–1700.
26 V. I. Slepnev, L. E. Kuznetsova, A. N. Gubin, E. V Batrakova, A. VYu and A. V Kabanov, Micelles of poly(oxyethylene)-poly(oxypropylene) block copolymer (pluronic) as a tool for low-molecular compound delivery into a cell: phosphorylation of intracellular proteins with micelle incorporated [gamma-32P]ATP, *Biochem. Int.*, 1992, **26**, 587–595.
27 S. Bayda, M. Hadla, S. Palazzolo, P. Riello, G. Corona, G. Toffoli and F. Rizzolio, Inorganic Nanoparticles for Cancer Therapy: a Transition from Lab to Clinic, *Curr. Med. Chem.*, 2018, **25**, 4269–4303.
28 E. Hurwitz, R. Levy, R. Maron, M. Wilchek, R. Arnon and M. Sela, The covalent binding of daunomycin and adriamycin to antibodies, with retention of both drug and antibody activities, *Cancer Res.*, 1975, **35**, 1175–1181.
29 G. Cornu, J.-L. Michaux, G. Sokal and A. Trouet, Daunorubicin-DNA: Further clinical trials in acute non-lymphoblastic leukemia, *Eur. J. Cancer*, 1974, **10**, 695–700.
30 V. Kumar, S. Palazzolo, S. Bayda, G. Corona, G. Toffoli and F. Rizzolio, DNA Nanotechnology for Cancer Therapy, *Theranostics*, 2016, **6**, 710–725.
31 V. Kumar, S. Bayda, M. Hadla, I. Caligiuri, C. R. Spena, S. Palazzolo, S. Kempter, G. Corona, G. Toffoli and

Open Access Article. Published on 08 July 2021. Downloaded on 10/31/2025 2:11:41 AM.
This article is licensed under a Creative Commons Attribution-NonCommercial 3.0 Unported Licence.

F. Rizzolio, Enhanced Chemotherapeutic Behavior of Open-Caged DNA@Doxorubicin Nanostructures for Cancer Cells, *J. Cell. Physiol.*, 2016, **231**, 106–110.

32 A. Trouet, M. Masquelier, R. Baurain and D. Deprez-De Campeneere, A covalent linkage between daunorubicin and proteins that is stable in serum and reversible by lysosomal hydrolases, as required for a lysosomotropic drug-carrier conjugate: *in vitro* and *in vivo* studies, *Proc. Natl. Acad. Sci. U. S. A.*, 1982, **79**, 626–629.

33 L. Lerra, A. Farfalla, B. Sanz, G. Cirillo, O. Vittorio, F. Voli, M. Le Grand, M. Curcio, F. Nicoletta, A. Dubrovska, S. Hampel, F. Iemma and G. Goya, Graphene Oxide Functional Nanohybrids with Magnetic Nanoparticles for Improved Vectorization of Doxorubicin to Neuroblastoma Cells, *Pharmaceutics*, 2019, **11**, 3.

34 E. Van Cutsem, A. Cervantes, R. Adam, A. Sobrero, J. H. Van Krieken, D. Aderka, E. Aranda Aguilar, A. Bardelli, A. Benson, G. Bodoky, F. Ciardiello, A. D'Hoore, E. Diaz-Rubio, J.-Y. Douillard, M. Ducreux, A. Falcone, A. Grothey, T. Gruenberger, K. Haustermans, V. Heinemann, P. Hoff, C.-H. Köhne, R. Labianca, P. Laurent-Puig, B. Ma, T. Maughan, K. Muro, N. Normanno, P. Österlund, W. J. G. Oyen, D. Papamichael, G. Pentheroudakis, P. Pfeiffer, T. J. Price, C. Punt, J. Ricke, A. Roth, R. Salazar, W. Scheithauer, H. J. Schmoll, J. Tabernero, J. Taïeb, S. Tejpar, H. Wasan, T. Yoshino, A. Zaanan and D. Arnold, ESMO consensus guidelines for the management of patients with metastatic colorectal cancer, *Ann. Oncol.*, 2016, **27**, 1386–1422.

35 F. Rizzolio, L. Esposito, D. Muresu, R. Fratamico, R. Jaraha, G. V. Caprioli and A. Giordano, RB gene family: genome-wide ChIP approaches could open undiscovered roads, *J. Cell. Biochem.*, 2010, **109**, 839–843.

36 S. Svenson, Clinical translation of nanomedicines, *Curr. Opin. Solid State Mater. Sci.*, 2012, **16**, 287–294.

37 C. Dianzani, G. P. Zara, G. Maina, P. Pettazzoni, S. Pizzimenti, F. Rossi, C. L. Gigliotti, E. S. Ciamporcero, M. Daga and G. Barrera, Drug Delivery Nanoparticles in Skin Cancers, *BioMed Res. Int.*, 2014, **2014**, 1–13.

38 L. Y. T. Chou, K. Ming and W. C. W. Chan, Strategies for the intracellular delivery of nanoparticles, *Chem. Soc. Rev.*, 2011, **40**, 233–245.

39 Y. Li, W. Stroberg, T.-R. Lee, H. S. Kim, H. Man, D. Ho, P. Decuzzi and W. K. Liu, Multiscale modeling and uncertainty quantification in nanoparticle-mediated drug/gene delivery, *Comput. Mech.*, 2014, **53**, 511–537.

40 Y. Li, Y. Lian, L. T. Zhang, S. M. Aldousari, H. S. Hedia, S. A. Asiri and W. K. Liu, Cell and nanoparticle transport in tumour microvasculature: the role of size, shape and surface functionality of nanoparticles, *Interface Focus*, 2016, **6**, 20150086.

41 A. Albanese, P. S. Tang and W. C. W. Chan, The Effect of Nanoparticle Size, Shape, and Surface Chemistry on Biological Systems, *Annu. Rev. Biomed. Eng.*, 2012, **14**, 1–16.

42 M. L. Immordino, F. Dosio and L. Cattel, Stealth liposomes: review of the basic science, rationale, and clinical applications, existing and potential, *Int. J. Nanomed.*, 2006, **1**, 297–315.

43 G. Molineux, Pegylation: engineering improved pharmaceuticals for enhanced therapy, *Canc. Treat Rev.*, 2002, **28**, 13–16.

44 C. D. Walkey, J. B. Olsen, H. Guo, A. Emili and W. C. W. Chan, Nanoparticle Size and Surface Chemistry Determine Serum Protein Adsorption and Macrophage Uptake, *J. Am. Chem. Soc.*, 2012, **134**, 2139–2147.

45 B. Pelaz, P. del Pino, P. Maffre, R. Hartmann, M. Gallego, S. Rivera-Fernández, J. M. de la Fuente, G. U. Nienhaus and W. J. Parak, Surface Functionalization of Nanoparticles with Polyethylene Glycol: Effects on Protein Adsorption and Cellular Uptake, *ACS Nano*, 2015, **9**, 6996–7008.

46 S. D. Perrault, C. Walkey, T. Jennings, H. C. Fischer and W. C. W. Chan, Mediating Tumor Targeting Efficiency of Nanoparticles Through Design, *Nano Lett.*, 2009, **9**, 1909–1915.

47 H. Otsuka, Y. Nagasaki and K. Kataoka, PEGylated nanoparticles for biological and pharmaceutical applications, *Adv. Drug Deliv. Rev.*, 2003, **55**, 403–419.

48 J. Lipka, M. Semmler-Behnke, R. A. Sperling, A. Wenk, S. Takenaka, C. Schleh, T. Kissel, W. J. Parak and W. G. Kreyling, Biodistribution of PEG-modified gold nanoparticles following intratracheal instillation and intravenous injection, *Biomaterials*, 2010, **31**, 6574–6581.

49 Z. Liu, J. T. Robinson, S. M. Tabakman, K. Yang and H. Dai, Carbon materials for drug delivery & cancer therapy, *Mater. Today*, 2011, **14**, 316–323.

50 K. Kostarelos, A. Bianco and M. Prato, Promises, facts and challenges for carbon nanotubes in imaging and therapeutics, *Nat. Nanotechnol.*, 2009, **4**, 627–633.

51 L. Feng and Z. Liu, Graphene in biomedicine: opportunities and challenges, *Nanomedicine*, 2011, **6**, 317–324.

52 Q. Zeng, D. Shao, X. He, Z. Ren, W. Ji, C. Shan, S. Qu, J. Li, L. Chen and Q. Li, Carbon dots as a trackable drug delivery carrier for localized cancer therapy *in vivo*, *J. Mater. Chem. B*, 2016, **4**, 5119–5126.

53 S. Bayda, M. Hadla, S. Palazzolo, V. Kumar, I. Caligiuri, E. Ambrosi, E. Pontoglio, M. Agostini, T. Tuccinardi, A. Benedetti, P. Riello, V. Canzonieri, G. Corona, G. Toffoli and F. Rizzolio, Bottom-up synthesis of carbon nanoparticles with higher doxorubicin efficacy, *J. Controlled Release*, 2017, **248**, 144–152.

54 D. Maiti, X. Tong, X. Mou and K. Yang, Carbon-Based Nanomaterials for Biomedical Applications: A Recent Study, *Front. Pharmacol.*, 2019, **9**, 1401.

55 N. L. Teradal and R. Jelinek, Carbon Nanomaterials: Carbon Nanomaterials in Biological Studies and Biomedicine, *Adv. Healthcare Mater.*, 2017, **6**, 1700574.

56 M. Mohajeri, B. Behnam and A. Sahebkar, Biomedical applications of carbon nanomaterials: Drug and gene delivery potentials, *J. Cell. Physiol.*, 2019, **234**, 298–319.

57 Z. Liu, K. Yang and S.-T. Lee, Single-walled carbon nanotubes in biomedical imaging, *J. Mater. Chem.*, 2011, **21**, 586–598.

 © 2021 The Author(s). Published by the Royal Society of Chemistry

Open Access Article. Published on 08 July 2021. Downloaded on 10/31/2025 2:11:41 AM.
This article is licensed under a Creative Commons Attribution-NonCommercial 3.0 Unported Licence.

58 Y.-P. Sun, B. Zhou, Y. Lin, W. Wang, K. A. S. Fernando, P. Pathak, M. J. Meziani, B. A. Harruff, X. Wang, H. Wang, P. G. Luo, H. Yang, M. E. Kose, B. Chen, L. M. Veca and S.-Y. Xie, Quantum-Sized Carbon Dots for Bright and Colorful Photoluminescence, *J. Am. Chem. Soc.*, 2006, **128**, 7756–7757.
59 S.-J. Yu, M.-W. Kang, H.-C. Chang, K.-M. Chen and Y.-C. Yu, Bright Fluorescent Nanodiamonds: No Photobleaching and Low Cytotoxicity, *J. Am. Chem. Soc.*, 2005, **127**, 17604–17605.
60 K. P. Loh, Q. Bao, G. Eda and M. Chhowalla, Graphene oxide as a chemically tunable platform for optical applications, *Nat. Chem.*, 2010, **2**, 1015–1024.
61 W. Yang, K. R. Ratinac, S. P. Ringer, P. Thordarson, J. J. Gooding and F. Braet, Carbon Nanomaterials in Biosensors: Should You Use Nanotubes or Graphene?, *Angew. Chem. Int. Ed.*, 2010, **49**, 2114–2138.
62 N. Mohanty and V. Berry, Graphene-Based Single-Bacterium Resolution Biodevice and DNA Transistor: Interfacing Graphene Derivatives with Nanoscale and Microscale Biocomponents, *Nano Lett.*, 2008, **8**, 4469–4476.
63 S. Priyadarsini, S. Mohanty, S. Mukherjee, S. Basu and M. Mishra, Graphene and graphene oxide as nanomaterials for medicine and biology application, *J. Nanostruct. Chem.*, 2018, **8**, 123–137.
64 X. Sun, Z. Liu, K. Welsher, J. T. Robinson, A. Goodwin, S. Zaric and H. Dai, Nano-graphene oxide for cellular imaging and drug delivery, *Nano Res.*, 2008, **1**, 203–212.
65 Z. Liu, X. Sun, N. Nakayama-Ratchford and H. Dai, Supramolecular Chemistry on Water-Soluble Carbon Nanotubes for Drug Loading and Delivery, *ACS Nano*, 2007, **1**, 50–56.
66 Z. Liu, J. T. Robinson, X. Sun and H. Dai, PEGylated Nanographene Oxide for Delivery of Water-Insoluble Cancer Drugs, *J. Am. Chem. Soc.*, 2008, **130**, 10876–10877.
67 S. Syama and P. V. Mohanan, Comprehensive Application of Graphene: Emphasis on Biomedical Concerns, *Nano-Micro Lett.*, 2019, **11**, 6.
68 X.-J. Liang, H. Meng, Y. Wang, H. He, J. Meng, J. Lu, P. C. Wang, Y. Zhao, X. Gao, B. Sun, C. Chen, G. Xing, D. Shen, M. M. Gottesman, Y. Wu, J.-j. Yin and L. Jia, Metallofullerene nanoparticles circumvent tumor resistance to cisplatin by reactivating endocytosis, *Proc. Natl. Acad. Sci. U.S.A.*, 2010, **107**, 7449–7454.
69 S. Y. Hong, G. Tobias, K. T. Al-Jamal, B. Ballesteros, H. Ali-Boucetta, S. Lozano-Perez, P. D. Nellist, R. B. Sim, C. Finucane, S. J. Mather, M. L. H. Green, K. Kostarelos and B. G. Davis, Filled and glycosylated carbon nanotubes for *in vivo* radioemitter localization and imaging, *Nat. Mater.*, 2010, **9**, 485–490.
70 K. Yang, J. Wan, S. Zhang, B. Tian, Y. Zhang and Z. Liu, The influence of surface chemistry and size of nanoscale graphene oxide on photothermal therapy of cancer using ultra-low laser power, *Biomaterials*, 2012, **33**, 2206–2214.
71 K. Yang, S. Zhang, G. Zhang, X. Sun, S.-T. Lee and Z. Liu, Graphene in Mice: Ultrahigh *In Vivo* Tumor Uptake and Efficient Photothermal Therapy, *Nano Lett.*, 2010, **10**, 3318–3323.
72 X. Liu, H. Tao, K. Yang, S. Zhang, S.-T. Lee and Z. Liu, Optimization of surface chemistry on single-walled carbon nanotubes for *in vivo* photothermal ablation of tumors, *Biomaterials*, 2011, **32**, 144–151.
73 H. K. Moon, S. H. Lee and H. C. Choi, *In Vivo* Near-Infrared Mediated Tumor Destruction by Photothermal Effect of Carbon Nanotubes, *ACS Nano*, 2009, **3**, 3707–3713.
74 V. Mishra, A. Patil, S. Thakur and P. Kesharwani, Carbon dots: emerging theranostic nanoarchitectures, *Drug Discovery Today*, 2018, **23**, 1219–1232.
75 J. Du, N. Xu, J. Fan, W. Sun and X. Peng, Carbon Dots for *In Vivo* Bioimaging and Theranostics, *Small*, 2019, **15**, e1805087.
76 I. Singh, R. Arora, H. Dhiman and R. Pahwa, Carbon Quantum Dots: Synthesis, Characterization and Biomedical Applications *Turkish*, *J. Pharm. Sci.*, 2018, **15**, 219–230.
77 X. Xu, R. Ray, Y. Gu, H. J. Ploehn, L. Gearheart, K. Raker and W. A. Scrivens, Electrophoretic Analysis and Purification of Fluorescent Single-Walled Carbon Nanotube Fragments, *J. Am. Chem. Soc.*, 2004, **126**, 12736–12737.
78 Y. Wang and A. Hu, Carbon quantum dots: synthesis, properties and applications, *J. Mater. Chem. C*, 2014, **2**, 6921.
79 A. Cayuela, M. L. Soriano, C. Carrillo-Carrión and M. Valcárcel, Semiconductor and carbon-based fluorescent nanodots: the need for consistency, *Chem. Commun.*, 2016, **52**, 1311–1326.
80 Y. Yang, J. Cui, M. Zheng, C. Hu, S. Tan, Y. Xiao, Q. Yang and Y. Liu, One-step synthesis of amino-functionalized fluorescent carbon nanoparticles by hydrothermal carbonization of chitosan, *Chem. Commun.*, 2012, **48**, 380–382.
81 S.-T. Yang, L. Cao, P. G. Luo, F. Lu, X. Wang, H. Wang, M. J. Meziani, Y. Liu, G. Qi and Y.-P. Sun, Carbon Dots for Optical Imaging *in Vivo*, *J. Am. Chem. Soc.*, 2009, **131**, 11308–11309.
82 S. K. Bhunia, A. Saha, A. R. Maity, S. C. Ray and N. R. Jana, Carbon nanoparticle-based fluorescent bioimaging probes, *Sci. Rep.*, 2013, **3**, 1473.
83 B. Chen, F. Li, S. Li, W. Weng, H. Guo, T. Guo, X. Zhang, Y. Chen, T. Huang, X. Hong, S. You, Y. Lin, K. Zeng and S. Chen, Large scale synthesis of photoluminescent carbon nanodots and their application for bioimaging, *Nanoscale*, 2013, **5**, 1967.
84 K. O. Boakye-Yiadom, S. Kesse, Y. Opoku-Damoah, M. S. Filli, M. Aquib, M. M. B. Joelle, M. A. Farooq, R. Mavlyanova, F. Raza, R. Bavi and B. Wang, Carbon dots: Applications in bioimaging and theranostics, *Int. J. Pharm.*, 2019, **564**, 308–317.
85 A. Kasouni, T. Chatzimitakos and C. Stalikas, Bioimaging Applications of Carbon Nanodots: A Review, *C*, 2019, **5**, 19.
86 L. Cao, S.-T. Yang, X. Wang, P. G. Luo, J.-H. Liu, S. Sahu, Y. Liu and Y.-P. Sun, Competitive performance of carbon 'quantum' dots in optical bioimaging, *Theranostics*, 2012, **2**, 295–301.

Open Access Article. Published on 08 July 2021. Downloaded on 10/31/2025 2:11:41 AM.
This article is licensed under a Creative Commons Attribution-NonCommercial 3.0 Unported Licence.

87 S. E. Skrabalak, Ultrasound-assisted synthesis of carbon materials, *Phys. Chem. Chem. Phys.*, 2009, **11**, 4930–4942.
88 H. U. Lee, S. Y. Park, E. S. Park, B. Son, S. C. Lee, J. W. Lee, Y.-C. Lee, K. S. Kang, M. Il Kim, H. G. Park, S. Choi, Y. S. Huh, S.-Y. Lee, K.-B. Lee, Y.-K. Oh and J. Lee, Photoluminescent carbon nanotags from harmful cyanobacteria for drug delivery and imaging in cancer cells, *Sci. Rep.*, 2014, **4**, 4665.
89 D. Bechet, P. Couleaud, C. Frochot, M.-L. Viriot, F. Guillemin and M. Barberi-Heyob, Nanoparticles as vehicles for delivery of photodynamic therapy agents, *Trends Biotechnol.*, 2008, **26**, 612–621.
90 P. Juzenas, A. Kleinauskas, P. George Luo and Y.-P. Sun, Photoactivatable carbon nanodots for cancer therapy, *Appl. Phys. Lett.*, 2013, **103**, 063701.
91 C. Fowley, N. Nomikou, A. P. McHale, B. McCaughan and J. F. Callan, Extending the tissue penetration capability of conventional photosensitisers: a carbon quantum dot–protoporphyrin IX conjugate for use in two-photon excited photodynamic therapy, *Chem. Commun.*, 2013, **49**, 8934.
92 H. He, X. Zheng, S. Liu, M. Zheng, Z. Xie, Y. Wang, M. Yu and X. Shuai, Diketopyrrolopyrrole-based carbon dots for photodynamic therapy, *Nanoscale*, 2018, **10**, 10991–10998.
93 Y. Li, X. Zheng, X. Zhang, S. Liu, Q. Pei, M. Zheng and Z. Xie, Porphyrin-Based Carbon Dots for Photodynamic Therapy of Hepatoma, *Adv. Healthcare Mater.*, 2017, **6**, 1600924.
94 H. Wu, F. Zeng, H. Zhang, J. Xu, J. Qiu and S. Wu, A Nanosystem Capable of Releasing a Photosensitizer Bioprecursor under Two-Photon Irradiation for Photodynamic Therapy, *Adv. Sci.*, 2016, **3**, 1500254.
95 K. Yang, C. Wang, C. Liu, S. Ding, F. Tian and F. Li, Bioluminescence-initiated photodynamic therapy bridged on high-luminescent carbon dots-conjugated protoporphyrin IX, *J. Mater. Sci.*, 2019, **54**, 3383–3391.
96 Z. Zhang, Y. Shi, Y. Pan, X. Cheng, L. Zhang, J. Chen, M.-J. Li and C. Yi, Quinoline derivative-functionalized carbon dots as a fluorescent nanosensor for sensing and intracellular imaging of Zn 2+, *J. Mater. Chem. B*, 2014, **2**, 5020.
97 L. Zhou, Y. Lin, Z. Huang, J. Ren and X. Qu, Carbon nanodots as fluorescence probes for rapid, sensitive, and label-free detection of Hg 2+ and biothiols in complex matrices, *Chem. Commun.*, 2012, **48**, 1147–1149.
98 Q. Qu, A. Zhu, X. Shao, G. Shi and Y. Tian, Development of a carbon quantum dots-based fluorescent Cu2+ probe suitable for living cell imaging, *Chem. Commun.*, 2012, **48**, 5473.
99 Y. Jiao, B. Zhu, J. Chen and X. Duan, Fluorescent sensing of fluoride in cellular system, *Theranostics*, 2015, **5**, 173–187.
100 M. L. Liu, B. Bin Chen, C. M. Li and C. Z. Huang, Carbon dots: synthesis, formation mechanism, fluorescence origin and sensing applications, *Green Chem.*, 2019, **21**, 449–471.
101 M. Zhang, R. Su, J. Zhong, L. Fei, W. Cai, Q. Guan, W. Li, N. Li, Y. Chen, L. Cai and Q. Xu, Red/orange dual-emissive carbon dots for pH sensing and cell imaging, *Nano Res.*, 2019, **12**, 815–821.
102 S. A. Hill, D. Benito-Alifonso, S. A. Davis, D. J. Morgan, M. Berry and M. C. Galan, Practical Three-Minute Synthesis of Acid-Coated Fluorescent Carbon Dots with Tuneable Core Structure, *Sci. Rep.*, 2018, **8**, 12234.
103 S. Moonrinta, B. Kwon, I. In, S. Kladsomboon, W. Sajomsang and P. Paoprasert, Highly biocompatible yogurt-derived carbon dots as multipurpose sensors for detection of formic acid vapor and metal ions, *Opt. Mater.*, 2018, **81**, 93–101.
104 L. Tang, R. Ji, X. Cao, J. Lin, H. Jiang, X. Li, K. S. Teng, C. M. Luk, S. Zeng, J. Hao and S. P. Lau, Deep Ultraviolet Photoluminescence of Water-Soluble Self-Passivated Graphene Quantum Dots, *ACS Nano*, 2012, **6**, 5102–5110.
105 K. Dimos, Tuning Carbon Dots' Optoelectronic Properties with Polymers, *Polymers*, 2018, **10**, 1312.
106 Q. Guan, R. Su, M. Zhang, R. Zhang, W. Li, D. Wang, M. Xu, L. Fei and Q. Xu, Highly fluorescent dual-emission red carbon dots and their applications in optoelectronic devices and water detection, *New J. Chem.*, 2019, **43**, 3050–3058.
107 F. Yuan, T. Yuan, L. Sui, Z. Wang, Z. Xi, Y. Li, X. Li, L. Fan, Z. Tan, A. Chen, M. Jin and S. Yang, Engineering triangular carbon quantum dots with unprecedented narrow bandwidth emission for multicolored LEDs, *Nat. Commun.*, 2018, **9**, 2249.
108 L. Cao, S. Sahu, P. Anilkumar, C. E. Bunker, J. Xu, K. A. S. Fernando, P. Wang, E. A. Guliants, K. N. Tackett and Y.-P. Sun, Carbon nanoparticles as visible-light photocatalysts for efficient CO2 conversion and beyond, *J. Am. Chem. Soc.*, 2011, **133**, 4754–4757.
109 J. Liu, Y. Liu, N. Liu, Y. Han, X. Zhang, H. Huang, Y. Lifshitz, S.-T. Lee, J. Zhong and Z. Kang, Metal-free efficient photocatalyst for stable visible water splitting *via* a two-electron pathway, *Science*, 2015, **347**, 970–974.
110 M. Han, S. Zhu, S. Lu, Y. Song, T. Feng, S. Tao, J. Liu and B. Yang, Recent progress on the photocatalysis of carbon dots: Classification, mechanism and applications, *Nano Today*, 2018, **19**, 201–218.
111 Y. Zhou, E. M. Zahran, B. A. Quiroga, J. Perez, K. J. Mintz, Z. Peng, P. Y. Liyanage, R. R. Pandey, C. C. Chusuei and R. M. Leblanc, Size-dependent photocatalytic activity of carbon dots with surface-state determined photoluminescence, *Appl. Catal., B*, 2019, **248**, 157–166.
112 M. Pirsaheb, A. Asadi, M. Sillanpää and N. Farhadian, Application of carbon quantum dots to increase the activity of conventional photocatalysts: A systematic review, *J. Mol. Liq.*, 2018, **271**, 857–871.
113 K.-H. Ye, Z. Wang, J. Gu, S. Xiao, Y. Yuan, Y. Zhu, Y. Zhang, W. Mai and S. Yang, Carbon quantum dots as a visible light sensitizer to significantly increase the solar water splitting performance of bismuth vanadate photoanodes, *Energy Environ. Sci.*, 2017, **10**, 772–779.
114 M. K. Mahto, D. Samanta, S. Konar, H. Kalita and A. Pathak, N, S doped carbon dots—Plasmonic Au nanocomposites for visible-light photocatalytic reduction of nitroaromatics, *J. Mater. Res.*, 2018, **33**, 3906–3916.

 © 2021 The Author(s). Published by the Royal Society of Chemistry

Open Access Article. Published on 08 July 2021. Downloaded on 10/31/2025 2:11:41 AM.
This article is licensed under a Creative Commons Attribution-NonCommercial 3.0 Unported Licence.

115 Z. Zhang, H. Huang, J. Xu, N. Zhang and C. Zhang, Carbon quantum dots/BiVO4 composite with enhanced photocatalytic activity, *Sci. China Technol. Sci.*, 2019, **62**, 356–360.
116 L. Cao, X. Wang, M. J. Meziani, F. Lu, H. Wang, P. G. Luo, Y. Lin, B. A. Harruff, L. M. Veca, D. Murray, S.-Y. Xie and Y.-P. Sun, Carbon Dots for Multiphoton Bioimaging, *J. Am. Chem. Soc.*, 2007, **129**, 11318–11319.
117 H. Li, X. He, Y. Liu, H. Huang, S. Lian, S. T. Lee and Z. Kang, One-step ultrasonic synthesis of water-soluble carbon nanoparticles with excellent photoluminescent properties, *Carbon*, 2011, **49**, 605–609.
118 S. N. Baker and G. A. Baker, Luminescent carbon nanodots: emergent nanolights, *Angew. Chem., Int. Ed. Engl.*, 2010, **49**, 6726–6744.
119 J. Shen, Y. Zhu, X. Yang and C. Li, Graphene quantum dots: emergent nanolights for bioimaging, sensors, catalysis and photovoltaic devices, *Chem. Commun.*, 2012, **48**, 3686–3699.
120 S.-L. Hu, K.-Y. Niu, J. Sun, J. Yang, N.-Q. Zhao and X.-W. Du, One-step synthesis of fluorescent carbon nanoparticles by laser irradiation, *J. Mater. Chem.*, 2009, **19**, 484–488.
121 X. Wang, L. Cao, F. Lu, M. J. Meziani, H. Li, G. Qi, B. Zhou, B. A. Harruff, F. Kermarrec and Y. P. Sun, Photoinduced electron transfers with carbon dots, *Chem. Commun.*, 2009, **25**, 3774–3776.
122 S.-T. Yang, X. Wang, H. Wang, F. Lu, P. G. Luo, L. Cao, M. J. Meziani, J.-H. Liu, Y. Liu, M. Chen, Y. Huang and Y.-P. Sun, Carbon Dots as Nontoxic and High-Performance Fluorescence Imaging Agents, *J. Phys. Chem. C*, 2009, **113**, 18110–18114.
123 J. Lu, J. Yang, J. Wang, A. Lim, S. Wang and K. P. Loh, One-Pot Synthesis of Fluorescent Carbon Nanoribbons, Nanoparticles, and Graphene by the Exfoliation of Graphite in Ionic Liquids, *ACS Nano*, 2009, **3**, 2367–2375.
124 Q.-L. Zhao, Z.-L. Zhang, B.-H. Huang, J. Peng, M. Zhang and D.-W. Pang, Facile preparation of low cytotoxicity fluorescent carbon nanocrystals by electrooxidation of graphite, *Chem. Commun.*, 2008, **41**, 5116–5118.
125 L. Zheng, Y. Chi, Y. Dong, J. Lin and B. Wang, Electrochemiluminescence of Water-Soluble Carbon Nanocrystals Released Electrochemically from Graphite, *J. Am. Chem. Soc.*, 2009, **131**, 4564–4565.
126 J. Zhou, C. Booker, R. Li, X. Zhou, T.-K. Sham, X. Sun and Z. Ding, An Electrochemical Avenue to Blue Luminescent Nanocrystals from Multiwalled Carbon Nanotubes (MWCNTs), *J. Am. Chem. Soc.*, 2007, **129**, 744–745.
127 A. B. Bourlinos, A. Stassinopoulos, D. Anglos, R. Zboril, V. Georgakilas and E. P. Giannelis, Photoluminescent Carbogenic Dots, *Chem. Mater.*, 2008, **20**, 4539–4541.
128 A. B. Bourlinos, A. Stassinopoulos, D. Anglos, R. Zboril, M. Karakassides and E. P. Giannelis, Surface Functionalized Carbogenic Quantum Dots, *Small*, 2008, **4**, 455–458.
129 H. Liu, T. Ye and C. Mao, Fluorescent Carbon Nanoparticles Derived from Candle Soot, *Angew. Chem.*, 2007, **119**, 6593–6595.
130 S. C. Ray, A. Saha, N. R. Jana and R. Sarkar, Fluorescent Carbon Nanoparticles: Synthesis, Characterization, and Bioimaging Application, *J. Phys. Chem. C*, 2009, **113**, 18546–18551.
131 L. Tian, D. Ghosh, W. Chen, S. Pradhan, X. Chang and S. Chen, Nanosized Carbon Particles From Natural Gas Soot, *Chem. Mater.*, 2009, **21**, 2803–2809.
132 S. Lu, S. Guo, P. Xu, X. Li, Y. Zhao, W. Gu and M. Xue, Hydrothermal synthesis of nitrogen-doped carbon dots with real-time live-cell imaging and blood–brain barrier penetration capabilities, *Int. J. Nanomed.*, 2016, **11**, 6325–6336.
133 H. Zhu, X. Wang, Y. Li, Z. Wang, F. Yang and X. Yang, Microwave synthesis of fluorescent carbon nanoparticles with electrochemiluminescence properties, *Chem. Commun.*, 2009, 5118–5120.
134 H. Li, X. He, Y. Liu, H. Yu, Z. Kang and S. T. Lee, Synthesis of fluorescent carbon nanoparticles directly from active carbon *via* a one-step ultrasonic treatment, *Mater. Res. Bull.*, 2011, **46**, 147–151.
135 S. Kang, Y. K. Jeong, J. H. Ryu, Y. Son, W. R. Kim, B. Lee, K. H. Jung and K. M. Kim, Pulsed laser ablation based synthetic route for nitrogen-doped graphene quantum dots using graphite flakes, *Appl. Surf. Sci.*, 2020, **506**, 144998.
136 H. Li, X. He, Z. Kang, H. Huang, Y. Liu, J. Liu, S. Lian, C. H. A. Tsang, X. Yang and S. T. Lee, Water-soluble fluorescent carbon quantum dots and photocatalyst design, *Angew. Chem. Int. Ed.*, 2010, **49**, 4430–4434.
137 H. Ming, Z. Ma, Y. Liu, K. Pan, H. Yu, F. Wang and Z. Kang, Large scale electrochemical synthesis of high quality carbon nanodots and their photocatalytic property, *Dalton Trans.*, 2012, **41**, 9526.
138 L. Zeng, X. Li, S. Fan, J. Li, J. Mu, M. Qin, L. Wang, G. Gan, M. Tadé and S. Liu, The bioelectrochemical synthesis of high-quality carbon dots with strengthened electricity output and excellent catalytic performance, *Nanoscale*, 2019, **11**, 4428–4437.
139 H. Liu, T. Ye and C. Mao, Fluorescent carbon nanoparticles derived from candle soot, *Angew. Chem., Int. Ed. Engl.*, 2007, **46**, 6473–6475.
140 S. Li, L. Wang, C. C. Chusuei, V. M. Suarez, P. L. Blackwelder, M. Micic, J. Orbulescu and R. M. Leblanc, Nontoxic Carbon Dots Potently Inhibit Human Insulin Fibrillation, *Chem. Mater.*, 2015, **27**, 1764–1771.
141 Z. S. Qian, L. J. Chai, Y. Y. Huang, C. Tang, J. Jia Shen, J. R. Chen and H. Feng, A real-time fluorescent assay for the detection of alkaline phosphatase activity based on carbon quantum dots, *Biosens. Bioelectron.*, 2015, **68**, 675–680.
142 S. K. Kailasa, S. Ha, S. H. Baek, L. M. T. Phan, S. Kim, K. Kwak and T. J. Park, Tuning of carbon dots emission color for sensing of Fe3+ ion and bioimaging applications, *Mater. Sci. Eng., C*, 2019, **98**, 834–842.

Open Access Article. Published on 08 July 2021. Downloaded on 10/31/2025 2:11:41 AM. This article is licensed under a Creative Commons Attribution-NonCommercial 3.0 Unported Licence.

143 H. Li, Z. Kang, Y. Liu and S.-T. Lee, Carbon nanodots: synthesis, properties and applications, *J. Mater. Chem.*, 2012, **22**, 24230–24253.
144 A. L. Himaja, P. S. Karthik and S. P. Singh, Carbon Dots: The Newest Member of the Carbon Nanomaterials Family, *Chem. Rec.*, 2015, **15**, 595–615.
145 A. Das and P. T. Snee, Synthetic Developments of Nontoxic Quantum Dots, *ChemPhysChem*, 2016, **17**, 598–617.
146 R. Wang, K.-Q. Lu, Z.-R. Tang and Y.-J. Xu, Recent progress in carbon quantum dots: synthesis, properties and applications in photocatalysis, *J. Mater. Chem. A*, 2017, **5**, 3717–3734.
147 Y. Guo, Z. Wang, H. Shao and X. Jiang, Hydrothermal synthesis of highly fluorescent carbon nanoparticles from sodium citrate and their use for the detection of mercury ions, *Carbon*, 2013, **52**, 583–589.
148 B. C. M. Martindale, G. A. M. Hutton, C. A. Caputo, S. Prantl, R. Godin, J. R. Durrant and E. Reisner, Enhancing Light Absorption and Charge Transfer Efficiency in Carbon Dots through Graphitization and Core Nitrogen Doping, *Angew. Chem. Int. Ed.*, 2017, **56**, 6459–6463.
149 S. Zhu, X. Zhao, Y. Song, S. Lu and B. Yang, Beyond bottom-up carbon nanodots: Citric-acid derived organic molecules, *Nano Today*, 2016, **11**, 128–132.
150 Z. Bagheri, H. Ehtesabi, M. Rahmandoust, M. M. Ahadian, Z. Hallaji, F. Eskandari and E. Jokar, New Insight into the Concept of Carbonization Degree in Synthesis of Carbon Dots to Achieve Facile Smartphone Based Sensing Platform, *Sci. Rep.*, 2017, **7**, 1–11.
151 C. X. Guo, D. Zhao, Q. Zhao, P. Wang and X. Lu, Na+-functionalized carbon quantum dots: a new draw solute in forward osmosis for seawater desalination, *Chem. Commun.*, 2014, **50**, 7318–7321.
152 B. C. M. Martindale, G. A. M. Hutton, C. A. Caputo and E. Reisner, Solar Hydrogen Production Using Carbon Quantum Dots and a Molecular Nickel Catalyst, *J. Am. Chem. Soc.*, 2015, **137**, 6018–6025.
153 S. Cailotto, R. Mazzaro, F. Enrichi, A. Vomiero, M. Selva, E. Cattaruzza, D. Cristofori, E. Amadio and A. Perosa, Design of Carbon Dots for Metal-free Photoredox Catalysis, *ACS Appl. Mater. Interfaces*, 2018, **10**, 40560–40567.
154 S. Cailotto, M. Negrato, S. Daniele, R. Luque, M. Selva, E. Amadio and A. Perosa, Carbon dots as photocatalysts for organic synthesis: metal-free methylene–oxygen-bond photocleavage, *Green Chem.*, 2020, **22**, 1145–1149.
155 S. Cailotto, E. Amadio, M. Facchin, M. Selva, E. Pontoglio, F. Rizzolio, P. Riello, G. Toffoli, A. Benedetti and A. Perosa, Carbon Dots from Sugars and Ascorbic Acid: Role of the Precursors on Morphology, Properties, Toxicity, and Drug Uptake, *ACS Med. Chem. Lett.*, 2018, **9**, 832–837.
156 S. Zhu, Q. Meng, L. Wang, J. Zhang, Y. Song, H. Jin, K. Zhang, H. Sun, H. Wang and B. Yang, Highly Photoluminescent Carbon Dots for Multicolor Patterning, Sensors, and Bioimaging, *Angew. Chem.*, 2013, **125**, 4045–4049.
157 C. H. Lee, R. Rajendran, M.-S. Jeong, H. Y. Ko, J. Y. Joo, S. Cho, Y. W. Chang and S. Kim, Bioimaging of targeting cancers using aptamer-conjugated carbon nanodots, *Chem. Commun.*, 2013, **49**, 6543.
158 S. Chandra, P. Patra, S. H. Pathan, S. Roy, S. Mitra, A. Layek, R. Bhar, P. Pramanik and A. Goswami, Luminescent S-doped carbon dots: an emergent architecture for multimodal applications, *J. Mater. Chem. B*, 2013, **1**, 2375.
159 Y. Dong, H. Pang, H. Bin Yang, C. Guo, J. Shao, Y. Chi, C. M. Li and T. Yu, Carbon-based dots co-doped with nitrogen and sulfur for high quantum yield and excitation-independent emission, *Angew. Chem., Int. Ed. Engl.*, 2013, **52**, 7800–7804.
160 K. Jiang, S. Sun, L. Zhang, Y. Lu, A. Wu, C. Cai and H. Lin, Red, Green, and Blue Luminescence by Carbon Dots: Full-Color Emission Tuning and Multicolor Cellular Imaging, *Angew. Chem. Int. Ed.*, 2015, **54**, 5360–5363.
161 L. Wang, F. Ruan, T. Lv, Y. Liu, D. Deng, S. Zhao, H. Wang and S. Xu, One step synthesis of Al/N co-doped carbon nanoparticles with enhanced photoluminescence, *J. Lumin.*, 2015, **158**, 1–5.
162 C. Wang, Z. Xu, H. Cheng, H. Lin, M. G. Humphrey and C. Zhang, A hydrothermal route to water-stable luminescent carbon dots as nanosensors for pH and temperature, *Carbon*, 2015, **82**, 87–95.
163 H. K. Sadhanala, J. Khatei and K. K. Nanda, Facile hydrothermal synthesis of carbon nanoparticles and possible application as white light phosphors and catalysts for the reduction of nitrophenol, *RSC Adv.*, 2014, **4**, 11481.
164 X. Gao, Y. Lu, R. Zhang, S. He, J. Ju, M. Liu, L. Li and W. Chen, One-pot synthesis of carbon nanodots for fluorescence turn-on detection of Ag + based on the Ag + -induced enhancement of fluorescence, *J. Mater. Chem. C*, 2015, **3**, 2302–2309.
165 G. Tong, J. Wang, R. Wang, X. Guo, L. He, F. Qiu, G. Wang, B. Zhu, X. Zhu and T. Liu, Amorphous carbon dots with high two-photon fluorescence for cellular imaging passivated by hyperbranched poly(amino amine), *J. Mater. Chem. B*, 2015, **3**, 700–706.
166 L. Zhou, B. He and J. Huang, Amphibious fluorescent carbon dots: one-step green synthesis and application for light-emitting polymer nanocomposites, *Chem. Commun.*, 2013, **49**, 8078.
167 S. Pei, J. Zhang, M. Gao, D. Wu, Y. Yang and R. Liu, A facile hydrothermal approach towards photoluminescent carbon dots from amino acids, *J. Colloid Interface Sci.*, 2015, **439**, 129–133.
168 C.-L. Li, C.-C. Huang, A. P. Periasamy, P. Roy, W.-C. Wu, C.-L. Hsu and H.-T. Chang, Synthesis of photoluminescent carbon dots for the detection of cobalt ions, *RSC Adv.*, 2015, **5**, 2285–2291.
169 Z. Zhang, W. Sun and P. Wu, Highly Photoluminescent Carbon Dots Derived from Egg White: Facile and Green

 © 2021 The Author(s). Published by the Royal Society of Chemistry

Open Access Article. Published on 08 July 2021. Downloaded on 10/31/2025 2:11:41 AM. This article is licensed under a Creative Commons Attribution-NonCommercial 3.0 Unported Licence.

Synthesis, Photoluminescence Properties, and Multiple Applications, *ACS Sustain. Chem. Eng.*, 2015, **3**, 1412–1418.
170 Z. L. Wu, P. Zhang, M. X. Gao, C. F. Liu, W. Wang, F. Leng and C. Z. Huang, One-pot hydrothermal synthesis of highly luminescent nitrogen-doped amphoteric carbon dots for bioimaging from Bombyx mori silk – natural proteins, *J. Mater. Chem. B*, 2013, **1**, 2868.
171 V. N. Mehta, S. Jha, H. Basu, R. K. Singhal and S. K. Kailasa, One-step hydrothermal approach to fabricate carbon dots from apple juice for imaging of mycobacterium and fungal cells, *Sens. Actuators, B*, 2015, **213**, 434–443.
172 M. Xue, M. Zou, J. Zhao, Z. Zhan and S. Zhao, Green preparation of fluorescent carbon dots from lychee seeds and their application for the selective detection of methylene blue and imaging in living cells, *J. Mater. Chem. B*, 2015, **3**, 6783–6789.
173 S. Liu, J. Tian, L. Wang, Y. Zhang, X. Qin, Y. Luo, A. M. Asiri, A. O. Al-Youbi and X. Sun, Hydrothermal Treatment of Grass: A Low-Cost, Green Route to Nitrogen-Doped, Carbon-Rich, Photoluminescent Polymer Nanodots as an Effective Fluorescent Sensing Platform for Label-Free Detection of Cu(II) Ions, *Adv. Mater.*, 2012, **24**, 2037–2041.
174 L. Wu, M. Luderer, X. Yang, C. Swain, H. Zhang, K. Nelson, A. J. Stacy, B. Shen, G. M. Lanza and D. Pan, Surface passivation of carbon nanoparticles with branched macromolecules influences near infrared bioimaging, *Theranostics*, 2013, **3**, 677–686.
175 S. Y. Park, H. U. Lee, E. S. Park, S. C. Lee, J.-W. Lee, S. W. Jeong, C. H. Kim, Y.-C. Lee, Y. S. Huh and J. Lee, Photoluminescent green carbon nanodots from food-waste-derived sources: large-scale synthesis, properties, and biomedical applications, *ACS Appl. Mater. Interfaces*, 2014, **6**, 3365–3370.
176 D. Sun, R. Ban, P.-H. Zhang, G.-H. Wu, J.-R. Zhang and J.-J. Zhu, Hair fiber as a precursor for synthesizing of sulfur- and nitrogen-co-doped carbon dots with tunable luminescence properties, *Carbon*, 2013, **64**, 424–434.
177 A. Prasannan and T. Imae, One-Pot Synthesis of Fluorescent Carbon Dots from Orange Waste Peels, *Ind. Eng. Chem. Res.*, 2013, **52**, 15673–15678.
178 H. Qi, M. Teng, M. Liu, S. Liu, J. Li, H. Yu, C. Teng, Z. Huang, H. Liu, Q. Shao, A. Umar, T. Ding, Q. Gao and Z. Guo, Biomass-derived nitrogen-doped carbon quantum dots: highly selective fluorescent probe for detecting Fe3+ ions and tetracyclines, *J. Colloid Interface Sci.*, 2019, **539**, 332–341.
179 J. Zhang, W. Shen, D. Pan, Z. Zhang, Y. Fang and M. Wu, Controlled synthesis of green and blue luminescent carbon nanoparticles with high yields by the carbonization of sucrose, *New J. Chem.*, 2010, **34**, 591.
180 X. He, H. Li, Y. Liu, H. Huang, Z. Kang and S.-T. Lee, Water soluble carbon nanoparticles: hydrothermal synthesis and excellent photoluminescence properties, *Colloids Surf., B*, 2011, **87**, 326–332.
181 B. Zhang, C. Liu and Y. Liu, A Novel One-Step Approach to Synthesize Fluorescent Carbon Nanoparticles, *Eur. J. Inorg. Chem.*, 2010, **2010**, 4411–4414.
182 D. Pan, L. Guo, J. Zhang, C. Xi, Q. Xue, H. Huang, J. Li, Z. Zhang, W. Yu, Z. Chen, Z. Li and M. Wu, Cutting sp2 clusters in graphene sheets into colloidal graphene quantum dots with strong green fluorescence, *J. Mater. Chem.*, 2012, **22**, 3314.
183 J. Zhou, Z. Sheng, H. Han, M. Zou and C. Li, Facile synthesis of fluorescent carbon dots using watermelon peel as a carbon source, *Mater. Lett.*, 2012, **66**, 222–224.
184 C. Ding, A. Zhu and Y. Tian, Functional surface engineering of C-dots for fluorescent biosensing and *in vivo* bioimaging, *Acc. Chem. Res.*, 2014, **47**, 20–30.
185 S. Sahu, B. Behera, T. K. Maiti and S. Mohapatra, Simple one-step synthesis of highly luminescent carbon dots from orange juice: application as excellent bio-imaging agents, *Chem. Commun.*, 2012, **48**, 8835–8837.
186 N. Puvvada, B. N. P. Kumar, S. Konar, H. Kalita, M. Mandal and A. Pathak, Synthesis of biocompatible multicolor luminescent carbon dots for bioimaging applications, *Sci. Technol. Adv. Mater.*, 2012, **13**, 045008.
187 W. Wang, Y. Li, L. Cheng, Z. Cao and W. Liu, Water-soluble and phosphorus-containing carbon dots with strong green fluorescence for cell labeling, *J. Mater. Chem. B*, 2014, **2**, 46–48.
188 X. Wang, K. Qu, B. Xu, J. Ren and X. Qu, Microwave assisted one-step green synthesis of cell-permeable multicolor photoluminescent carbon dots without surface passivation reagents, *J. Mater. Chem.*, 2011, **21**, 2445.
189 C. Ding, Z. Deng, J. Chen and Y. Jin, One-step microwave synthesis of N,S co-doped carbon dots from 1,6-hexanediamine dihydrochloride for cell imaging and ion detection, *Colloids Surf., B*, 2020, **189**, 110838.
190 A. Jaiswal, S. S. Ghosh and A. Chattopadhyay, One step synthesis of C-dots by microwave mediated caramelization of poly(ethylene glycol), *Chem. Commun.*, 2012, **48**, 407–409.
191 E. Budak, S. Aykut, M. E. Paşaoğlu and C. Ünlü, Microwave assisted synthesis of boron and nitrogen rich graphitic quantum dots to enhance fluorescence of photosynthetic pigments, *Mater. Today Commun.*, 2020, **24**, 100975.
192 F. Rigodanza, L. Đorđević, F. Arcudi and M. Prato, Customizing the Electrochemical Properties of Carbon Nanodots by Using Quinones in Bottom-Up Synthesis, *Angew. Chem. Int. Ed.*, 2018, **57**, 5062–5067.
193 L. Đorđević, F. Arcudi, A. D'Urso, M. Cacioppo, N. Micali, T. Bürgi, R. Purrello and M. Prato, Design principles of chiral carbon nanodots help convey chirality from molecular to nanoscale level, *Nat. Commun.*, 2018, **9**, 3442.
194 C.-W. Lai, Y.-H. Hsiao, Y.-K. Peng and P.-T. Chou, Facile synthesis of highly emissive carbon dots from pyrolysis of glycerol; gram scale production of carbon dots/mSiO2 for cell imaging and drug release, *J. Mater. Chem.*, 2012, **22**, 14403.
195 W. Wei, C. Xu, L. Wu, J. Wang, J. Ren and X. Qu, Non-enzymatic-browning-reaction: a versatile route for production of nitrogen-doped carbon dots with tunable multicolor luminescent display, *Sci. Rep.*, 2014, **4**, 3564.

Open Access Article. Published on 08 July 2021. Downloaded on 10/31/2025 2:11:41 AM. This article is licensed under a Creative Commons Attribution-NonCommercial 3.0 Unported Licence.

196 Z. Qian, J. Ma, X. Shan, H. Feng, L. Shao and J. Chen, Highly Luminescent N-Doped Carbon Quantum Dots as an Effective Multifunctional Fluorescence Sensing Platform, *Chem. - Eur. J.*, 2014, **20**, 2254–2263.

197 Y. Xu, M. Wu, Y. Liu, X.-Z. Feng, X.-B. Yin, X.-W. He and Y.-K. Zhang, Nitrogen-Doped Carbon Dots: A Facile and General Preparation Method, Photoluminescence Investigation, and Imaging Applications, *Chem. - Eur. J.*, 2013, **19**, 2276–2283.

198 Z.-Q. Xu, L.-Y. Yang, X.-Y. Fan, J.-C. Jin, J. Mei, W. Peng, F.-L. Jiang, Q. Xiao and Y. Liu, Low temperature synthesis of highly stable phosphate functionalized two color carbon nanodots and their application in cell imaging, *Carbon*, 2014, **66**, 351–360.

199 S. Chandra, P. Das, S. Bag, D. Laha and P. Pramanik, Synthesis, functionalization and bioimaging applications of highly fluorescent carbon nanoparticles, *Nanoscale*, 2011, **3**, 1533–1540.

200 S. Jahan, F. Mansoor, S. Naz, J. Lei and S. Kanwal, Oxidative synthesis of highly fluorescent boron/nitrogen co-doped carbon nanodots enabling detection of photosensitizer and carcinogenic dye, *Anal. Chem.*, 2013, **85**, 10232–10239.

201 S. Hu, R. Tian, Y. Dong, J. Yang, J. Liu and Q. Chang, Modulation and effects of surface groups on photoluminescence and photocatalytic activity of carbon dots, *Nanoscale*, 2013, **5**, 11665.

202 A. P. Demchenko and M. O. Dekaliuk, Novel fluorescent carbonic nanomaterials for sensing and imaging, *Methods Appl. Fluoresc.*, 2013, **1**, 042001.

203 L. Deng, X. Wang, Y. Kuang, C. Wang, L. Luo, F. Wang and X. Sun, Development of hydrophilicity gradient ultracentrifugation method for photoluminescence investigation of separated non-sedimental carbon dots, *Nano Res.*, 2015, **8**, 2810–2821.

204 Y. Song, S. Zhu, S. Zhang, Y. Fu, L. Wang, X. Zhao and B. Yang, Investigation from chemical structure to photoluminescent mechanism: a type of carbon dots from the pyrolysis of citric acid and an amine, *J. Mater. Chem. C*, 2015, **3**, 5976–5984.

205 L. Shi, J. H. Yang, H. B. Zeng, Y. M. Chen, S. C. Yang, C. Wu, H. Zeng, O. Yoshihito and Q. Zhang, Carbon dots with high fluorescence quantum yield: the fluorescence originates from organic fluorophores, *Nanoscale*, 2016, **8**, 14374–14378.

206 J. Schneider, C. J. Reckmeier, Y. Xiong, M. von Seckendorff, A. S. Susha, P. Kasák and A. L. Rogach, Molecular Fluorescence in Citric Acid-Based Carbon Dots, *J. Phys. Chem. C*, 2017, **121**, 2014–2022.

207 Q. Fang, Y. Dong, Y. Chen, C.-H. Lu, Y. Chi, H.-H. Yang and T. Yu, Luminescence origin of carbon based dots obtained from citric acid and amino group-containing molecules, *Carbon*, 2017, **118**, 319–326.

208 M. Fu, F. Ehrat, Y. Wang, K. Z. Milowska, C. Reckmeier, A. L. Rogach, J. K. Stolarczyk, A. S. Urban and J. Feldmann, Carbon Dots: A Unique Fluorescent Cocktail of Polycyclic Aromatic Hydrocarbons, *Nano Lett.*, 2015, **15**, 6030–6035.

209 Y. Dong, J. Shao, C. Chen, H. Li, R. Wang, Y. Chi, X. Lin and G. Chen, Blue luminescent graphene quantum dots and graphene oxide prepared by tuning the carbonization degree of citric acid, *Carbon*, 2012, **50**, 4738–4743.

210 S. Wang, Z.-G. Chen, I. Cole and Q. Li, Structural evolution of graphene quantum dots during thermal decomposition of citric acid and the corresponding photoluminescence, *Carbon*, 2015, **82**, 304–313.

211 M. J. Krysmann, A. Kelarakis, P. Dallas and E. P. Giannelis, Formation Mechanism of Carbogenic Nanoparticles with Dual Photoluminescence Emission, *J. Am. Chem. Soc.*, 2012, **134**, 747–750.

212 C. Hu, C. Yu, M. Li, X. Wang, J. Yang, Z. Zhao, A. Eychmüller, Y.-P. Sun and J. Qiu, Chemically Tailoring Coal to Fluorescent Carbon Dots with Tuned Size and Their Capacity for Cu(II) Detection, *Small*, 2014, **10**, 4926–4933.

213 H. Peng and J. Travas-Sejdic, Simple Aqueous Solution Route to Luminescent Carbogenic Dots from Carbohydrates, *Chem. Mater.*, 2009, **21**, 5563–5565.

214 F. Zhang, F. Liu, C. Wang, X. Xin, J. Liu, S. Guo and J. Zhang, Effect of Lateral Size of Graphene Quantum Dots on Their Properties and Application, *ACS Appl. Mater. Interfaces*, 2016, **8**, 2104–2110.

215 S. Zhu, Y. Song, J. Wang, H. Wan, Y. Zhang, Y. Ning and B. Yang, Photoluminescence mechanism in graphene quantum dots: Quantum confinement effect and surface/edge state, *Nano Today*, 2017, **13**, 10–14.

216 J. Shen, Y. Zhu, C. Chen, X. Yang and C. Li, Facile preparation and upconversion luminescence of graphene quantum dots, *Chem. Commun.*, 2011, **47**, 2580–2582.

217 H. Ding, S.-B. Yu, J.-S. Wei and H.-M. Xiong, Full-Color Light-Emitting Carbon Dots with a Surface-State-Controlled Luminescence Mechanism, *ACS Nano*, 2016, **10**, 484–491.

218 S. Qu, H. Chen, X. Zheng, J. Cao and X. Liu, Ratiometric fluorescent nanosensor based on water soluble carbon nanodots with multiple sensing capacities, *Nanoscale*, 2013, **5**, 5514.

219 X. Jia, J. Li and E. Wang, One-pot green synthesis of optically pH-sensitive carbon dots with upconversion luminescence, *Nanoscale*, 2012, **4**, 5572.

220 X. Jia, X. Yang, J. Li, D. Li and E. Wang, Stable Cu nanoclusters: from an aggregation-induced emission mechanism to biosensing and catalytic applications, *Chem. Commun.*, 2014, **50**, 237–239.

221 H. Chen, Y. Xie, A. M. Kirillov, L. Liu, M. Yu, W. Liu and Y. Tang, A ratiometric fluorescent nanoprobe based on terbium functionalized carbon dots for highly sensitive detection of an anthrax biomarker, *Chem. Commun.*, 2015, **51**, 5036–5039.

222 V. Hinterberger, C. Damm, P. Haines, D. M. Guldi and W. Peukert, Purification and structural elucidation of carbon dots by column chromatography, *Nanoscale*, 2019, **11**, 8464–8474.

223 J. Ge, Q. Jia, W. Liu, L. Guo, Q. Liu, M. Lan, H. Zhang, X. Meng and P. Wang, Red-Emissive Carbon Dots for

 © 2021 The Author(s). Published by the Royal Society of Chemistry

Open Access Article. Published on 08 July 2021. Downloaded on 10/31/2025 2:11:41 AM. This article is licensed under a Creative Commons Attribution-NonCommercial 3.0 Unported Licence.

Fluorescent, Photoacoustic, and Thermal Theranostics in Living Mice, *Adv. Mater.*, 2015, **27**, 4169–4177.
224 S. Y. Lim, W. Shen and Z. Gao, Carbon quantum dots and their applications, *Chem. Soc. Rev.*, 2014, **44**, 362–381.
225 X. Wang, L. Cao, S.-T. Yang, F. Lu, M. J. Meziani, L. Tian, K. W. Sun, M. a Bloodgood and Y.-P. Sun, Band gap-like strong fluorescence in functionalized carbon nanoparticles, *Angew. Chem., Int. Ed. Engl.*, 2010, **49**, 5310–5314.
226 H. Zheng, Q. Wang, Y. Long, H. Zhang, X. Huang and R. Zhu, *Chem. Commun.*, 2011, **47**, 10650.
227 J. Wang, S. Su, J. Wei, R. Bahgi, L. Hope-Weeks, J. Qiu and S. Wang, Ratio-metric sensor to detect riboflavin *via* fluorescence resonance energy transfer with ultrahigh sensitivity, *Phys. E*, 2015, **72**, 17–24.
228 H. Zhang, Y. Chen, M. Liang, L. Xu, S. Qi, H. Chen and X. Chen, Solid-Phase Synthesis of Highly Fluorescent Nitrogen-Doped Carbon Dots for Sensitive and Selective Probing Ferric Ions in Living Cells, *Anal. Chem.*, 2014, **86**, 9846–9852.
229 J. Jiang, Y. He, S. Li and H. Cui, Amino acids as the source for producing carbon nanodots: microwave assisted one-step synthesis, intrinsic photoluminescence property and intense chemiluminescence enhancement, *Chem. Commun.*, 2012, **48**, 9634.
230 Q. Xu, P. Pu, J. Zhao, C. Dong, C. Gao, Y. Chen, J. Chen, Y. Liu and H. Zhou, Preparation of highly photoluminescent sulfur-doped carbon dots for Fe(III) detection, *J. Mater. Chem. A*, 2015, **3**, 542–546.
231 Y. Sun, X. Wang, F. Lu, L. Cao, M. J. Meziani, P. G. Luo, L. Gu and L. M. Veca, Doped Carbon Nanoparticles as a New Platform for Highly Photoluminescent Dots, *J. Phys. Chem. C*, 2008, **112**, 18295–18298.
232 C. S. Stan, C. Albu, A. Coroaba, M. Popa and D. Sutiman, One step synthesis of fluorescent carbon dots through pyrolysis of N-hydroxysuccinimide, *J. Mater. Chem. C*, 2015, **3**, 789–795.
233 J. Shen, Y. Zhu, X. Yang, J. Zong, J. Zhang and C. Li, One-pot hydrothermal synthesis of graphenequantum dots surface-passivated by polyethylene glycol and their photoelectric conversion under near-infrared light, *New J. Chem.*, 2012, **36**, 97–101.
234 Z. Lin, W. Xue, H. Chen and J.-M. Lin, Classical oxidant induced chemiluminescence of fluorescent carbon dots, *Chem. Commun.*, 2012, **48**, 1051–1053.
235 P. Teng, J. Xie, Y. Long, X. Huang, R. Zhu, X. Wang, L. Liang, Y. Huang and H. Zheng, Chemiluminescence behavior of the carbon dots and the reduced state carbon dots, *J. Lumin.*, 2014, **146**, 464–469.
236 Y. Li and S. Han, Carbon dots-enhanced chemiluminescence method for the sensitive determination of iodide, *Microchem. J.*, 2020, **154**, 104638.
237 L. Zhao, F. Di, D. Wang, L.-H. Guo, Y. Yang, B. Wan and H. Zhang, Chemiluminescence of carbon dots under strong alkaline solutions: a novel insight into carbon dot optical properties, *Nanoscale*, 2013, **5**, 2655.
238 C. Venkateswara Raju, G. Kalaiyarasan, S. Paramasivam, J. Joseph and S. Senthil Kumar, Phosphorous doped carbon quantum dots as an efficient solid state electrochemiluminescence platform for highly sensitive turn-on detection of Cu2+ ions, *Electrochim. Acta*, 2020, **331**, 135391.
239 T. A. Tabish, C. J. Scotton, D. C. J Ferguson, L. Lin, A. Van Der Veen, S. Lowry, M. Ali, F. Jabeen, P. G. Winyard and S. Zhang, Biocompatibility and toxicity of graphene quantum dots for potential application in photodynamic therapy, *Nanomedicine*, 2018, **13**, 1923–1937.
240 M. A. Jhonsi, D. A. Ananth, G. Nambirajan, T. Sivasudha, R. Yamini, S. Bera and A. Kathiravan, Antimicrobial activity, cytotoxicity and DNA binding studies of carbon dots, *Spectrochim. Acta, Part A*, 2018, **196**, 295–302.
241 H. Yao, J. Li, Y. Song, H. Zhao, Z. Wei, X. Li, Y. Jin, B. Yang and J. Jiang, Synthesis of ginsenoside Re-based carbon dots applied for bioimaging and effective inhibition of cancer cells, *Int. J. Nanomed.*, 2018, **13**, 6249–6264.
242 Y. Wang, P. Anilkumar, L. Cao, J.-H. Liu, P. G. Luo, K. N. Tackett, S. Sahu, P. Wang, X. Wang and Y.-P. Sun, Carbon dots of different composition and surface functionalization: cytotoxicity issues relevant to fluorescence cell imaging, *Exp. Biol. Med.*, 2011, **236**, 1231–1238.
243 J. Yan, S. Hou, Y. Yu, Y. Qiao, T. Xiao, Y. Mei, Z. Zhang, B. Wang, C. C. Huang, C. H. Lin and G. Suo, The effect of surface charge on the cytotoxicity and uptake of carbon quantum dots in human umbilical cord derived mesenchymal stem cells, *Colloids Surf., B*, 2018, **171**, 241–249.
244 D. Shukla, M. Das, D. Kasade, M. Pandey, A. K. Dubey, S. K. Yadav and A. S. Parmar, Sandalwood-derived carbon quantum dots as bioimaging tools to investigate the toxicological effects of malachite green in model organisms, *Chemosphere*, 2020, **248**, 125998.
245 S. Jha, P. Mathur, S. Ramteke and N. K. Jain, Pharmaceutical potential of quantum dots, *Artif. Cells, Nanomed., Biotechnol.*, 2018, **46**, 57–65.
246 K. Wang, Z. Gao, G. Gao, Y. Wo, Y. Wang, G. Shen and D. Cui, Systematic safety evaluation on photoluminescent carbon dots, *Nanoscale Res. Lett.*, 2013, **8**, 1–9.
247 H. Tao, K. Yang, Z. Ma, J. Wan, Y. Zhang, Z. Kang and Z. Liu, *In vivo* NIR fluorescence imaging, biodistribution, and toxicology of photoluminescent carbon dots produced from carbon nanotubes and graphite, *Small*, 2012, **8**, 281–290.
248 U. J. Pyati, A. T. Look and M. Hammerschmidt, Zebrafish as a powerful vertebrate model system for *in vivo* studies of cell death, *Semin. Cancer Biol.*, 2007, **17**, 154–165.
249 Y. Wang, J. L. Seebald, D. P. Szeto and J. Irudayaraj, Biocompatibility and biodistribution of surface-enhanced raman scattering nanoprobes in zebrafish embryos: *In vivo* and multiplex imaging, *ACS Nano*, 2010, **4**, 4039–4053.
250 K. Howe, M. D. Clark, C. F. Torroja, J. Torrance, C. Berthelot, M. Muffato, J. E. Collins, S. Humphray, K. McLaren, D. L. Stemple, *et al.*, The zebrafish reference

Open Access Article. Published on 08 July 2021. Downloaded on 10/31/2025 2:11:41 AM.
This article is licensed under a Creative Commons Attribution-NonCommercial 3.0 Unported Licence.

genome sequence and its relationship to the human genome, *Nature*, 2013, **496**, 498–503.

251 T. Pal, S. Mohiyuddin and G. Packirisamy, Facile and Green Synthesis of Multicolor Fluorescence Carbon Dots from Curcumin: *In Vitro* and *in Vivo* Bioimaging and Other Applications, *ACS Omega*, 2018, **3**, 831–843.

252 C. Dias, N. Vasimalai, M. P. Sárria, I. Pinheiro, V. Vilas-Boas, J. Peixoto and B. Espiña, Biocompatibility and bioimaging potential of fruit-based carbon dots, *Nanomaterials*, 2019, **9**, 199.

253 Z. Fatahi, N. Esfandiari, H. Ehtesabi, Z. Bagheri, H. Tavana, Z. Ranjbar and H. Latifi, Physicochemical and cytotoxicity analysis of green synthesis carbon dots for cell imaging, *EXCLI J.*, 2019, **18**, 454–466.

254 S. Li, Z. Guo, R. Feng, Y. Zhang, W. Xue and Z. Liu, Hyperbranched polyglycerol conjugated fluorescent carbon dots with improved: *In vitro* toxicity and red blood cell compatibility for bioimaging, *RSC Adv.*, 2017, **7**, 4975–4982.

255 M. J. Molaei, A review on nanostructured carbon quantum dots and their applications in biotechnology, sensors, and chemiluminescence, *Talanta*, 2019, **196**, 456–478.

256 V. N. Mehta, S. Jha, R. K. Singhal and S. K. Kailasa, Preparation of multicolor emitting carbon dots for HeLa cell imaging, *New J. Chem.*, 2014, **38**, 6152–6160.

257 M. Tuerhong, Y. XU and X. B. YIN, Review on Carbon Dots and Their Applications, *Chin. J. Anal. Chem.*, 2017, **45**, 139–150.

258 J. Tang, B. Kong, H. Wu, M. Xu, Y. Wang, Y. Wang, D. Zhao and G. Zheng, Carbon Nanodots Featuring Efficient FRET for Real-Time Monitoring of Drug Delivery and Two-Photon Imaging, *Adv. Mater.*, 2013, **25**, 6569–6574.

259 D. Zhao, X. Liu, Z. Zhang, R. Zhang, L. Liao, X. Xiao and H. Cheng, Synthesis of multicolor carbon dots based on solvent control and its application in the detection of crystal violet, *Nanomaterials*, 2019, **9**, 1556.

260 H. Ding, J. S. Wei, P. Zhang, Z. Y. Zhou, Q. Y. Gao and H. M. Xiong, Solvent-Controlled Synthesis of Highly Luminescent Carbon Dots with a Wide Color Gamut and Narrowed Emission Peak Widths, *Small*, 2018, **14**, 1800612.

261 C. Liu, P. Zhang, X. Zhai, F. Tian, W. Li, J. Yang, Y. Liu, H. Wang, W. Wang and W. Liu, Nano-carrier for gene delivery and bioimaging based on carbon dots with PEI-passivation enhanced fluorescence, *Biomaterials*, 2012, **33**, 3604–3613.

262 J. Liu, S. Lu, Q. Tang, K. Zhang, W. Yu, H. Sun and B. Yang, One-step hydrothermal synthesis of photoluminescent carbon nanodots with selective antibacterial activity against Porphyromonas gingivalis, *Nanoscale*, 2017, **9**, 7135–7142.

263 J. J. Liu, D. Li, K. Zhang, M. Yang, H. Sun and B. Yang, One-Step Hydrothermal Synthesis of Nitrogen-Doped Conjugated Carbonized Polymer Dots with 31% Efficient Red Emission for *In Vivo* Imaging, *Small*, 2018, **12**, 1703919.

264 D. Li, P. Jing, L. Sun, Y. An, X. Shan, X. Lu, D. Zhou, D. Han, D. Shen, Y. Zhai, S. Qu, R. Zbořil and A. L. Rogach, Near-Infrared Excitation/Emission and Multiphoton-Induced Fluorescence of Carbon Dots, *Adv. Mater.*, 2018, **30**, 1705913.

265 J. Shao, S. Zhu, H. Liu, Y. Song, S. Tao and B. Yang, Full-Color Emission Polymer Carbon Dots with Quench-Resistant Solid-State Fluorescence, *Adv. Sci.*, 2017, **4**, 1700395.

266 S. Khan, A. Sharma, S. Ghoshal, S. Jain, M. K. Hazra and C. K. Nandi, Small molecular organic nanocrystals resemble carbon nanodots in terms of their properties, *Chem. Sci.*, 2017, **9**, 175–180.

267 Y. Li, G. Bai, S. Zeng and J. Hao, Theranostic Carbon Dots with Innovative NIR-II Emission for *in Vivo* Renal-Excreted Optical Imaging and Photothermal Therapy, *ACS Appl. Mater. Interfaces*, 2019, **11**, 4737–4744.

268 Y. F. Kang, Y. H. Li, Y. W. Fang, Y. Xu, X. M. Wei and X. B. Yin, Carbon Quantum Dots for Zebrafish Fluorescence Imaging, *Sci. Rep.*, 2015, **5**, 11835.

269 H. Li, Y. Zhang, L. Wang, J. Tian and X. Sun, Nucleic acid detection using carbon nanoparticles as a fluorescent sensing platform, *Chem. Commun.*, 2011, **47**, 961–963.

270 H. X. Zhao, L. Q. Liu, Z. De Liu, Y. Wang, X. J. Zhao and C. Z. Huang, Highly selective detection of phosphate in very complicated matrixes with an off–on fluorescent probe of europium-adjusted carbon dots, *Chem. Commun.*, 2011, **47**, 2604.

271 J. Liu, J. Li, Y. Jiang, S. Yang, W. Tan and R. Yang, Combination of π–π stacking and electrostatic repulsion between carboxylic carbon nanoparticles and fluorescent oligonucleotides for rapid and sensitive detection of thrombin, *Chem. Commun.*, 2011, **47**, 11321.

272 Z. Lin, W. Xue, H. Chen and J.-M. Lin, Peroxynitrous-Acid-Induced Chemiluminescence of Fluorescent Carbon Dots for Nitrite Sensing, *Anal. Chem.*, 2011, **83**, 8245–8251.

273 W. Shi, Q. Wang, Y. Long, Z. Cheng, S. Chen, H. Zheng and Y. Huang, Carbon nanodots as peroxidase mimetics and their applications to glucose detection, *Chem. Commun.*, 2011, **47**, 6695.

274 L. Liu, Y. Li, L. Zhan, Y. Liu and C. Huang, One-step synthesis of fluorescent hydroxyls-coated carbon dots with hydrothermal reaction and its application to optical sensing of metal ions, *Sci. China Chem.*, 2011, **54**, 1342–1347.

275 P. Karfa, E. Roy, S. Patra, S. Kumar, A. Tarafdar, R. Madhuri and P. K. Sharma, Amino acid derived highly luminescent, heteroatom-doped carbon dots for label-free detection of Cd2+/Fe3+ , cell imaging and enhanced antibacterial activity, *RSC Adv.*, 2015, **5**, 58141–58153.

276 H. Li, J. Zhai and X. Sun, Sensitive and Selective Detection of Silver(I) Ion in Aqueous Solution Using Carbon Nanoparticles as a Cheap, Effective Fluorescent Sensing Platform, *Langmuir*, 2011, **27**, 4305–4308.

277 H. Li, J. Zhai, J. Tian, Y. Luo and X. Sun, Carbon nanoparticle for highly sensitive and selective fluorescent detection of mercury(II) ion in aqueous solution, *Biosens. Bioelectron.*, 2011, **26**, 4656–4660.

278 Y. Hou, Q. Lu, J. Deng, H. Li and Y. Zhang, One-pot electrochemical synthesis of functionalized fluorescent

 © 2021 The Author(s). Published by the Royal Society of Chemistry

Open Access Article. Published on 08 July 2021. Downloaded on 10/31/2025 2:11:41 AM. This article is licensed under a Creative Commons Attribution-NonCommercial 3.0 Unported Licence.

carbon dots and their selective sensing for mercury ion, *Anal. Chim. Acta*, 2015, **866**, 69–74.

279 B. Kong, A. Zhu, C. Ding, X. Zhao, B. Li and Y. Tian, Carbon Dot-Based Inorganic-Organic Nanosystem for Two-Photon Imaging and Biosensing of pH Variation in Living Cells and Tissues, *Adv. Mater.*, 2012, **24**, 5844–5848.

280 Y. Dong, R. Wang, G. Li, C. Chen, Y. Chi and G. Chen, Polyamine-Functionalized Carbon Quantum Dots as Fluorescent Probes for Selective and Sensitive Detection of Copper Ions, *Anal. Chem.*, 2012, **84**, 6220–6224.

281 W. Shi, X. Li and H. Ma, A Tunable Ratiometric pH Sensor Based on Carbon Nanodots for the Quantitative Measurement of the Intracellular pH of Whole Cells, *Angew. Chem. Int. Ed.*, 2012, **51**, 6432–6435.

282 F. Yan, Y. Zou, M. Wang, X. Mu, N. Yang and L. Chen, Highly photoluminescent carbon dots-based fluorescent chemosensors for sensitive and selective detection of mercury ions and application of imaging in living cells, *Sens. Actuators, B*, 2014, **192**, 488–495.

283 K. Qu, J. Wang, J. Ren and X. Qu, Carbon Dots Prepared by Hydrothermal Treatment of Dopamine as an Effective Fluorescent Sensing Platform for the Label-Free Detection of Iron(III) Ions and Dopamine, *Chem.–Eur. J.*, 2013, **19**(22), 7243–7249.

284 L. Wu, J. Wang, J. Ren, W. Li and X. Qu, Highly sensitive electrochemiluminescent cytosensing using carbon nanodot@Ag hybrid material and graphene for dual signal amplification, *Chem. Commun.*, 2013, **49**, 5675.

285 M. Zulfajri, H. N. Abdelhamid, S. Sudewi, S. Dayalan, A. Rasool, A. Habib and G. G. Huang, Plant Part-Derived Carbon Dots for Biosensing, *Biosensors*, 2020, **10**, 68.

286 V. Roshni, S. Misra, M. K. Santra and D. Ottoor, One pot green synthesis of C-dots from groundnuts and its application as Cr(VI) sensor and *in vitro* bioimaging agent, *J. Photochem. Photobiol., A*, 2019, **373**, 28–36.

287 M. Jaishankar, T. Tseten, N. Anbalagan, B. B. Mathew and K. N. Beeregowda, Toxicity, mechanism and health effects of some heavy metals, *Interdiscip. Toxicol.*, 2014, **7**, 60–72.

288 S. S. Monte-Filho, S. I. E. Andrade, M. B. Lima and M. C. U. Araujo, Synthesis of highly fluorescent carbon dots from lemon and onion juices for determination of riboflavin in multivitamin/mineral supplements, *J. Pharm. Anal.*, 2019, **9**, 209–216.

289 S. Ahmadian-Fard-Fini, M. Salavati-Niasari and D. Ghanbari, Hydrothermal green synthesis of magnetic Fe3O4-carbon dots by lemon and grape fruit extracts and as a photoluminescence sensor for detecting of E. coli bacteria, *Spectrochim. Acta, Part A*, 2018, **203**, 481–493.

290 J. Zuo, T. Jiang, X. Zhao, X. Xiong, S. Xiao and Z. Zhu, Preparation and Application of Fluorescent Carbon Dots, *J. Nanomater.*, 2015, **2015**, 1–13.

291 A. M. Alkilany and C. J. Murphy, Toxicity and cellular uptake of gold nanoparticles: what we have learned so far?, *J. Nanopart. Res.*, 2010, **12**, 2313–2333.

292 V. Kumar, G. Toffoli and F. Rizzolio, Fluorescent carbon nanoparticles in medicine for cancer therapy, *ACS Med. Chem. Lett.*, 2013, **4**, 1012–1013.

293 M. Zheng, S. Liu, J. Li, D. Qu, H. Zhao, X. Guan, X. Hu, Z. Xie, X. Jing and Z. Sun, Integrating oxaliplatin with highly luminescent carbon dots: an unprecedented theranostic agent for personalized medicine, *Adv. Mater.*, 2014, **26**, 3554–3560.

294 A. Mewada, S. Pandey, M. Thakur, D. Jadhav and M. Sharon, Swarming carbon dots for folic acid mediated delivery of doxorubicin and biological imaging, *J. Mater. Chem. B*, 2014, **2**, 698–705.

295 Z. Wang, H. Liao, H. Wu, B. Wang, H. Zhao and M. Tan, Fluorescent carbon dots from beer for breast cancer cell imaging and drug delivery, *Anal. Methods*, 2015, **7**, 8911–8917.

296 E. Dulkeith, A. C. Morteani, T. Niedereichholz, T. A. Klar, J. Feldmann, S. A. Levi, F. C. J. M. van Veggel, D. N. Reinhoudt, M. Möller and D. I. Gittins, Fluorescence Quenching of Dye Molecules near Gold Nanoparticles: Radiative and Nonradiative Effects, *Phys. Rev. Lett.*, 2002, **89**, 203002.

297 R. Mohammadinejad, A. Dadashzadeh, S. Moghassemi, M. Ashrafizadeh, A. Dehshahri, A. Pardakhty, H. Sassan, S. M. Sohrevardi and A. Mandegary, Shedding light on gene therapy: Carbon dots for the minimally invasive image-guided delivery of plasmids and noncoding RNAs - A review, *J. Adv. Res.*, 2019, **18**, 81–93.

298 A. Sharma and J. Das, Small molecules derived carbon dots: synthesis and applications in sensing, catalysis, imaging, and biomedicine, *Nanobiotechnology*, 2019, **17**(1), 92–115.

299 J. Kim, J. Park, H. Kim, K. Singha and W. J. Kim, Transfection and intracellular trafficking properties of carbon dot-gold nanoparticle molecular assembly conjugated with PEI-pDNA, *Biomaterials*, 2013, **34**, 7168–7180.

300 M. Zhang, X. Zhao, Z. Fang, Y. Niu, J. Lou, Y. Wu, S. Zou, S. Xia, M. Sun and F. Du, Fabrication of HA/PEI-functionalized carbon dots for tumor targeting, intracellular imaging and gene delivery, *RSC Adv.*, 2017, **7**, 3369–3375.

301 J. Chen, Q. Wang, J. Zhou, W. Deng, Q. Yu, X. Cao, J. Wang, F. Shao, Y. Li, P. Ma, M. Spector, J. Yu and X. Xu, Porphyra polysaccharide-derived carbon dots for non-viral co-delivery of different gene combinations and neuronal differentiation of ectodermal mesenchymal stem cells, *Nanoscale*, 2017, **9**, 10820–10831.

302 S. M. Ghafary, M. Nikkhah, S. Hatamie and S. Hosseinkhani, Simultaneous Gene Delivery and Tracking through Preparation of Photo-Luminescent Nanoparticles Based on Graphene Quantum Dots and Chimeric Peptides, *Sci. Rep.*, 2017, **7**, 9552.

303 S. Kim, Y. Choi, G. Park, C. Won, Y. J. Park, Y. Lee, B. S. Kim and D. H. Min, Highly efficient gene silencing and bioimaging based on fluorescent carbon dots *in vitro* and *in vivo*, *Nano Res.*, 2017, **10**, 503–519.

304 H. Dong, W. Dai, H. Ju, H. Lu, S. Wang, L. Xu, S.-F. Zhou, Y. Zhang and X. Zhang, Multifunctional Poly(l-lactide)–Polyethylene Glycol-Grafted Graphene Quantum Dots for Intracellular MicroRNA Imaging and Combined Specific-

Open Access Article. Published on 08 July 2021. Downloaded on 10/31/2025 2:11:41 AM. This article is licensed under a Creative Commons Attribution-NonCommercial 3.0 Unported Licence.

Gene-Targeting Agents Delivery for Improved Therapeutics, *ACS Appl. Mater. Interfaces*, 2015, **7**, 11015–11023.

305 Y. F. Wu, H. C. Wu, C. H. Kuan, C. J. Lin, L. W. Wang, C. W. Chang and T. W. Wang, Multi-functionalized carbon dots as theranostic nanoagent for gene delivery in lung cancer therapy, *Sci. Rep.*, 2016, **6**, 21170.

306 L. Wu, X. Cai, K. Nelson, W. Xing, J. Xia, R. Zhang, A. J. Stacy, M. Luderer, G. M. Lanza, L. V Wang, B. Shen and D. Pan, A Green Synthesis of Carbon Nanoparticle from Honey for Real-Time Photoacoustic Imaging, *Nano Res.*, 2013, **6**, 312–325.

307 P. Huang, J. Lin, X. Wang, Z. Wang, C. Zhang, M. He, K. Wang, F. Chen, Z. Li, G. Shen, D. Cui and X. Chen, Light-Triggered Theranostics Based on Photosensitizer-Conjugated Carbon Dots for Simultaneous Enhanced-Fluorescence Imaging and Photodynamic Therapy, *Adv. Mater.*, 2012, **24**, 5104–5110.

308 A. Kleinauskas, S. Rocha, S. Sahu, Y.-P. Sun and P. Juzenas, Carbon-core silver-shell nanodots as sensitizers for phototherapy and radiotherapy, *Nanotechnology*, 2013, **24**(32), 325103.

309 X. Dong, W. Liang, M. J. Meziani, Y. P. Sun and L. Yang, Carbon Dots as Potent Antimicrobial Agents, *Theranostics*, 2020, **10**, 671–686.

310 M. J. Meziani, X. Dong, L. Zhu, L. P. Jones, G. E. Lecroy, F. Yang, S. Wang, P. Wang, Y. Zhao, L. Yang, R. A. Tripp and Y. P. Sun, Visible-Light-Activated Bactericidal Functions of Carbon 'quantum' Dots, *ACS Appl. Mater. Interfaces*, 2016, **8**, 10761–10766.

311 D. I. Abu Rabe, M. M. Al Awak, F. Yang, P. A. Okonjo, X. Dong, L. R. Teisl, P. Wang, Y. Tang, N. Pan, Y. P. Sun and L. Yang, The dominant role of surface functionalization in carbon dots' photo-activated antibacterial activity, *Int. J. Nanomed.*, 2019, **14**, 2655–2665.

312 H. Li, J. Huang, Y. Song, M. Zhang, H. Wang, F. Lu, H. Huang, Y. Liu, X. Dai, Z. Gu, Z. Yang, R. Zhou and Z. Kang, Degradable Carbon Dots with Broad-Spectrum Antibacterial Activity, *ACS Appl. Mater. Interfaces*, 2018, **10**, 26936–26946.

313 E. Priyadarshini, K. Rawat, T. Prasad and H. B. Bohidar, Antifungal efficacy of Au@ carbon dots nanoconjugates against opportunistic fungal pathogen, Candida albicans, *Colloids Surf., B*, 2018, **163**, 355–361.

314 S. Huang, J. Gu, J. Ye, B. Fang, S. Wan, C. Wang, U. Ashraf, Q. Li, X. Wang, L. Shao, Y. Song, X. Zheng, F. Cao and S. Cao, Benzoxazine monomer derived carbon dots as a broad-spectrum agent to block viral infectivity, *J. Colloid Interface Sci.*, 2019, **542**, 198–206.

315 A. Łoczechin, K. Séron, A. Barras, E. Giovanelli, S. Belouzard, Y. T. Chen, N. Metzler-Nolte, R. Boukherroub, J. Dubuisson and S. Szunerits, Functional Carbon Quantum Dots as Medical Countermeasures to Human Coronavirus, *ACS Appl. Mater. Interfaces*, 2019, **11**, 42964–42974.

316 Z. Abbas and S. Rehman, *An Overview of Cancer Treatment Modalities, Neoplasm*, InTech, 2018.

317 P. P. Shanbhag, S. V. Jog, M. M. Chogale and S. S. Gaikwad, Theranostics for Cancer Therapy, *Curr. Drug Delivery*, 2013, **10**, 357–362.

318 F. Chen, E. B. Ehlerding and W. Cai, Theranostic Nanoparticles, *J. Nucl. Med.*, 2014, **55**, 1919–1922.

319 Y. Yi, G. Lin, S. Chen, J. Liu, H. Zhang and P. Mi, Polyester micelles for drug delivery and cancer theranostics: Current achievements, progresses and future perspectives, *Mater. Sci. Eng., C*, 2018, **83**, 218–232.

320 B. S. Pattni, V. V. Chupin and V. P. Torchilin, New Developments in Liposomal Drug Delivery, *Chem. Rev.*, 2015, **115**, 10938–10966.

321 W. Cai, C. C. Chu, G. Liu and Y. X. J. Wáng, Metal-Organic Framework-Based Nanomedicine Platforms for Drug Delivery and Molecular Imaging, *Small*, 2015, **11**, 4806–4822.

322 H. Wu, W. Su, H. Xu, Y. Zhang, Y. Li, X. Li and L. Fan, Applications of carbon dots on tumour theranostics, *View*, 2021, **2**, 20200061.

323 J. Li, M. Li, L. Tian, Y. Qiu, Q. Yu, X. Wang, R. Guo and Q. He, Facile strategy by hyaluronic acid functional carbon dot-doxorubicin nanoparticles for CD44 targeted drug delivery and enhanced breast cancer therapy, *Int. J. Pharm.*, 2020, **578**, 119122.

324 H. Wang, J. Di, Y. Sun, J. Fu, Z. Wei, H. Matsui, A. del C. Alonso and S. Zhou, Biocompatible PEG-Chitosan@Carbon Dots Hybrid Nanogels for Two-Photon Fluorescence Imaging, Near-Infrared Light/pH Dual-Responsive Drug Carrier, and Synergistic Therapy, *Adv. Funct. Mater.*, 2015, **25**, 5537–5547.

325 M. Z. Fahmi, J. K. Chen, C. C. Huang, Y. C. Ling and J. Y. Chang, Phenylboronic acid-modified magnetic nanoparticles as a platform for carbon dot conjugation and doxorubicin delivery, *J. Mater. Chem. B*, 2015, **3**, 5532–5543.

326 C. Yang, K. K. Chan, G. Xu, M. Yin, G. Lin, X. Wang, W. J. Lin, M. D. Birowosuto, S. Zeng, T. Ogi, K. Okuyama, F. A. Permatasari, F. Iskandar, C. K. Chen and K. T. Yong, Biodegradable Polymer-Coated Multifunctional Graphene Quantum Dots for Light-Triggered Synergetic Therapy of Pancreatic Cancer, *ACS Appl. Mater. Interfaces*, 2019, **11**, 2768–2781.

327 Y. Choi, S. Kim, M.-H. Choi, S.-R. Ryoo, J. Park, D.-H. Min and B.-S. Kim, Highly Biocompatible Carbon Nanodots for Simultaneous Bioimaging and Targeted Photodynamic Therapy *In Vitro* and *In Vivo*, *Adv. Funct. Mater.*, 2014, **24**, 5781–5789.

328 S. Li, S. Zhou, Y. Li, X. Li, J. Zhu, L. Fan and S. Yang, Exceptionally High Payload of the IR780 Iodide on Folic Acid-Functionalized Graphene Quantum Dots for Targeted Photothermal Therapy, *ACS Appl. Mater. Interfaces*, 2017, **9**, 22332–22341.

329 M. Xue, J. Zhao, Z. Zhan, S. Zhao, C. Lan, F. Ye and H. Liang, Dual functionalized natural biomass carbon dots from lychee exocarp for cancer cell targetable near-infrared fluorescence imaging and photodynamic therapy, *Nanoscale*, 2018, **10**, 18124–18130.

 © 2021 The Author(s). Published by the Royal Society of Chemistry

Open Access Article. Published on 08 July 2021. Downloaded on 10/31/2025 2:11:41 AM. This article is licensed under a Creative Commons Attribution-NonCommercial 3.0 Unported Licence.

330 Q. Li, Y. Li, T. Min, J. Gong, L. Du, D. L. Phillips, J. Liu, J. W. Y. Lam, H. H. Y. Sung, I. D. Williams, R. T. K. Kwok, C. L. Ho, K. Li, J. Wang and B. Z. Tang, Time-Dependent Photodynamic Therapy for Multiple Targets: A Highly Efficient AIE-Active Photosensitizer for Selective Bacterial Elimination and Cancer Cell Ablation, *Angew. Chem. Int. Ed.*, 2020, **59**, 9470–9477.

331 J. Chen, L. Keltner, J. Christophersen, F. Zheng, M. Krouse, A. Singhal and S. Wang, New Technology for Deep Light Distribution in Tissue for Phototherapy, *Cancer J.*, 2002, **8**, 154–163.

332 Y. Sun, J. Campisi, C. Higano, T. M. Beer, P. Porter, I. Coleman, L. True and P. S. Nelson, Treatment-induced damage to the tumor microenvironment promotes prostate cancer therapy resistance through WNT16B, *Nat. Med.*, 2012, **18**, 1359–1368.

333 A. Onaciu, A. Jurj, C. Moldovan and I. Berindan-Neagoe, in *Engineered Nanomaterials - Health and Safety*, IntechOpen, 2020.

334 C. L. Li, C. M. Ou, C. C. Huang, W. C. Wu, Y. P. Chen, T. E. Lin, L. C. Ho, C. W. Wang, C. C. Shih, H. C. Zhou, Y. C. Lee, W. F. Tzeng, T. J. Chiou, S. T. Chu, J. Cang and H. T. Chang, Carbon dots prepared from ginger exhibiting efficient inhibition of human hepatocellular carcinoma cells, *J. Mater. Chem. B*, 2014, **2**, 4564–4571.

335 L. Zou, H. Wang, B. He, L. Zeng, T. Tan, H. Cao, X. He, Z. Zhang, S. Guo and Y. Li, Current Approaches of Photothermal Therapy in Treating Cancer Metastasis with Nanotherapeutics, *Theranostics*, 2016, **6**, 762–772.

336 V. Shanmugam, S. Selvakumar and C. S. Yeh, Near-infrared light-responsive nanomaterials in cancer therapeutics, *Chem. Soc. Rev.*, 2014, **43**, 6254–6287.

337 M. Zheng, Y. Li, S. Liu, W. Wang, Z. Xie and X. Jing, One-Pot to Synthesize Multifunctional Carbon Dots for Near Infrared Fluorescence Imaging and Photothermal Cancer Therapy, *ACS Appl. Mater. Interfaces*, 2016, **8**, 23533–23541.

338 M. Nurunnabi, Z. Khatun, G. R. Reeck, D. Y. Lee and Y. K. Lee, Photoluminescent graphene nanoparticles for cancer phototherapy and imaging, *ACS Appl. Mater. Interfaces*, 2014, **6**, 12413–12421.

339 X. Bao, Y. Yuan, J. Chen, B. Zhang, D. Li, D. Zhou, P. Jing, G. Xu, Y. Wang, K. Holá, D. Shen, C. Wu, L. Song, C. Liu, R. Zbořil and S. Qu, *In vivo* theranostics with near-infrared-emitting carbon dots—highly efficient photothermal therapy based on passive targeting after intravenous administration, *Light Sci. Appl.*, 2018, **7**, 2047–7538.

340 H. Wang, S. Mukherjee, J. Yi, P. Banerjee, Q. Chen and S. Zhou, Biocompatible Chitosan-Carbon Dot Hybrid Nanogels for NIR-Imaging-Guided Synergistic Photothermal-Chemo Therapy, *ACS Appl. Mater. Interfaces*, 2017, **9**, 18639–18649.

341 Q. Jia, Z. Zhao, K. Liang, F. Nan, Y. Li, J. Wang, J. Ge and P. Wang, Recent advances and prospects of carbon dots in cancer nanotheranostics, *Mater. Chem. Front.*, 2020, **4**, 449–471.

342 W. Fan, P. Huang and X. Chen, Overcoming the Achilles' heel of photodynamic therapy, *Chem. Soc. Rev.*, 2016, **45**, 6488–6519.

343 A. G. Arranja, V. Pathak, T. Lammers and Y. Shi, Tumor-targeted nanomedicines for cancer theranostics, *Pharmacol. Res.*, 2017, **115**, 87–95.

344 Y. H. Bae and K. Park, Targeted drug delivery to tumors: myths, reality and possibility, *J. Controlled Release*, 2011, **153**, 198–205.

345 L. Belfiore, D. N. Saunders, M. Ranson, K. J. Thurecht, G. Storm and K. L. Vine, *J. Controlled Release*, 2018, **277**, 1–13.